



universität  
wien

# DISSERTATION

Titel der Dissertation

Proliferation control in *Drosophila* stem cell lineages

angestrebter akademischer Grad

Doktor der Naturwissenschaften (Dr. rer.nat.)

Verfasserin / Verfasser: Mag. Ralph Alexander Neumüller

Matrikel-Nummer: 9908177

Dissertationsgebiet (lt. Studienblatt): A 091 442 (Anthropologie)

Betreuerin / Betreuer: Dr. Jürgen Knoblich

Wien, am , 06. April. 2009

---

# Table of Contents

Summary.....	3
Zusammenfassung.....	5
I. Introduction.....	7
1. Stem cells and asymmetric cell division.....	7
2. Drosophila as a model system to study stem cell proliferation.....	8
2.1 Drosophila Neural Precursor Cells.....	9
2.1.1 Establishment of polarity and determinant localization.....	10
2.1.2. Spindle orientation.....	12
2.2 The ovarian stem cell lineage.....	14
3. Trim- NHL domain proteins and proliferation control.....	17
II. Results.....	21
1. Part I: The Drosophila NuMA homologue Mud regulates spindle orientation in asymmetric cell division.....	21
1.1. Mud is the Drosophila homologue of NuMA.....	21
1.2. Mud is part of a conserved heterotrimeric complex.....	22
1.3. Mud interacts with microtubules.....	23
1.4. Mud regulates spindle orientation in larval neuroblasts.....	24
1.5. Mud localizes to spindle poles and the apical cell cortex of neuroblasts.....	25
1.6. mud mutant brains overproliferate due to an increased neuroblast pool.....	26
1.8. Methods.....	30
Figure1: Evolutionary conservation of NuMA.....	33
Figure 2: Mud is in a complex with Pins and G $\alpha$ i.....	35
Figure 3: Mud associates with microtubules.....	37
Figure 4: Spindle orientation defects in mud mutant neuroblasts.....	39
Figure 5: Mud localization in neuroblasts.....	41
Figure 6: Overproliferation in mud mutant brains.....	43
Figure 7: A model for Mud function in asymmetric cell division.....	45
Figure 8: Multiple Sequence Alignment of the Conserved N- and C- Terminal Segments of the Homologous NuMA, Mud and Lin-5 Proteins.....	47
Figure 9: Western Blots Showing Protein Expression in Wild-Type and mud Mutant Brain Extracts. ....	48
Figure 10: pins Interacts genetically with mud.....	49
2. Part II: Mei-P26 regulates micro RNAs and cell growth in the Drosophila ovarian stem cell lineage.....	50
2.1. Materials and Methods.....	56
Figure 1: Differentiation and cell cycle defects in mei-P26 mutant ovaries.....	59
Figure 2: Cystocytes overproliferate in mei-P26 mutants.....	61

Figure 3: Mei-P26 regulates cell and nucleolar size.....	63
Figure 4: mei-P26 regulates growth. ....	65
Figure 5: Bam requires the Ago1 binding protein Mei-P26 to induce proper cystocyte differentiation.....	67
Figure 6: mei-P26 is expressed in the larval brain.....	69
Figure 7: Trim-NHL proteins interact with Ago1.....	71
Figure 8: Ago1 is required for germline stem cell maintenance.....	73
Figure 9: Mei-P26 regulates miRNAs. ....	75
Figure 10: microRNAs are deregulated in germline tumors.....	77
Figure 11: loquacious is required mei-P26 loss of function associated tumor growth. ....	79
III. Discussion.....	81
1. Spindle orientation and neurogenesis.....	81
2. The role of the Trim-NHL protein in the ovarian stem cell lineage.....	87
2.1. Mei-P26 and growth control.....	87
2.2. Mei-P26 and microRNAs.....	88
3. Concluding remarks.....	91
IV. References.....	93
V. Contributions.....	101
VI. Acknowledgments.....	102
VII. Publications.....	103
VIII. CURRICULUM VITAE.....	104

## Summary

Stem cells possess the remarkable ability to generate another stem cell and a differentiating cell upon division. While one cell will self-renew and thus retain stem cell identity, its sibling will be committed to further differentiate. These different cell fates can either be generated by the establishment of a cellular polarity and the subsequent segregation of cell fate determinants into only one of the two daughter cells or by the unequal exposure of the two cells to an extracellular, instructive signal. *Drosophila* neural and germline stem cells provide the unique opportunity to study these different division modes in genetic accessible model systems.

I will provide evidence that the *Drosophila* NuMA homolog *mushroom body defect (mud)* is required in mitotic spindle orientation, a process which constitutes a prerequisite for correct cell fate determinant segregation. In *mud* mutant neuroblasts the mitotic spindle is not aligned with the axis of cellular polarity and thus stem cells can divide in a symmetric manner. As a consequence the stem cell pool increases significantly due to the inheritance of cell fate determinants in both daughter cells. Besides its centrosomal localization the Mud protein accumulates at the apical cortex in dividing neuroblasts and links the mitotic spindle to this cortical domain. Thereby Mud ensures alignment of the axis of cell division with the axis of cellular polarity.

Further I will discuss the function of the Trim-NHL protein Mei-P26 in the context of the *Drosophila* female germline stem cell lineage. *mei-P26* shows similarities to a segregating cell fate determinant, called *brat* in the central nervous system. Surprisingly the paralogs *mei-P26* and *brat* fulfill similar functions in neural and germline stem cell lineages respectively and both act as tumor suppressors. *mei-P26* is strongly expressed in stem cell daughter cells, is required to inhibit mitotic proliferation and slows down cellular growth in these cells. In *mei-P26* mutants stem cell daughter cells continue to proliferate mitotically leading to the formation of an ovarian tumor. On the molecular level both Mei-P26 and Brat interact with Ago-1 and regulate

microRNAs. These data suggest that Trim-NHL proteins are regulators of growth and proliferation in stem cell lineages and their evolutionary conservation renders the possibility that these proteins fulfill analogous functions in vertebrates.

## Zusammenfassung

Stammzellen besitzen die Fähigkeit, zwei unterschiedliche Zelltypen nach der Zellteilung zu generieren. Während eine Zelle sich selbst erneuert und somit Stammzellcharakter beibehält, aktiviert die zweite Tochterzelle ein Differenzierungsprogramm. Diese unterschiedlichen Zellschicksale können auf zweierlei Art generiert werden. Entweder durch die Etablierung einer zellintrinsischen Polarität und der daraus resultierenden ungleichen Verteilung von Zellschicksalsdeterminanten oder der asymmetrischen Exposition der beiden Tochterzellen gegenüber extrazellulärer, zellschicksalsbestimmender Signale. *Drosophila* neuronale- und Keimbahnstammzellen bieten die Möglichkeit, diese beiden Modi der Stammzellteilung in einem genetisch zugänglichen Modellorganismus zu studieren.

Im Weiteren werde ich die Rolle des *Drosophila* NuMA Homologs *mushroom body defect (mud)* bei der Orientierung der mitotischen Spindel, einer fundamentalen Voraussetzung für die korrekte Zellschicksalsdeterminatensegregation, diskutieren. In *mud* Mutanten neuronalen Stammzellen ist die mitotische Spindel nicht mit der Achse der zellulären Polarität gekoppelt und aufgrund dessen können sich diese Stammzellen statt asymmetrisch auch symmetrisch teilen. Daraus resultierend kommt es zu einer signifikanten Expansion der Stammzellpopulation. Neben der zentrosomalen Lokalisierung von Mud akkumuliert das Protein am apikalen Kortex in den sich teilenden Neuroblasten und verbindet die mitotische Spindel mit dieser kortikalen Domäne. Dies garantiert die Ausrichtung der Zellteilungsebene mit der Achse der Zellpolarität.

Darüberhinaus werde ich die Funktion des Trim-NHL Proteins *mei-P26* in dem Kontext der *Drosophila* Keimbahnstammzelllinie diskutieren. Mei-P26 besitzt auf Domänenebene augenscheinliche Ähnlichkeit mit der in Neuroblasten asymmetrisch segregierenden Zellschicksalsdeterminante *brain tumor (brat)*. *mei-P26* und *brat* besitzen eine ähnliche Funktion in diesen beiden unterschiedlichen Stammzelllinien: Beide Proteine regulieren Wachstums- und Proliferationsprozesse. Mei-P26 akkumuliert in den Tochterzellen der Stamzellen und

unterdrückt in diesen das Zellwachstum und die mitotische Teilungsaktivität. Fehlt Mei-P26 kommt es zu unkontrollierter Proliferation und folglich Tumorwachstum. Sowohl Brat als auch Mei-P26 interagieren mit Ago1, ein Befund welcher eine Regulation von microRNAs durch Mei-P26 und Brat nahelegt. Aufgrund ihrer evolutionären Konservierung könnten Trim-NHL Proteine in Vertebraten ähnliche Funktionen in Stammzelllinien ausüben.

# I. Introduction

## 1. Stem cells and asymmetric cell division

Stem cells are characterized by two criteria: A) Stem cells are undifferentiated cells that can give rise to fully differentiated cells (*potency*) and B) stem cells can go through multiple rounds of mitotic divisions while retaining their undifferentiated state (*self-renewal*). These characteristics account for the fundamental importance that stem cells possess throughout the lifetime of a multicellular organism. During organogenesis and maintenance of tissues, but also during regenerative processes as tissue repair following injury, stem cells deliver the building blocks of all organs through repeated rounds of asymmetric cell division. These asymmetric divisions ensure that the ability to self-renew as well as the ability to differentiate are 'segregated' into the stem cell and differentiating progeny cell respectively. This asymmetry can in theory be twofold: A) An external, instructive signal supports stem cell identity in only one of the two daughter cells upon stem cell division (*niche mechanism*). B) A cell intrinsic asymmetry results in the unequal distribution of cell fate determinants between the two daughter cells (*intrinsic asymmetric division*). Conceptually it is also possible that these two mechanisms (unequal exposure to an extracellular instructive signal and asymmetric distribution of cell fate determinants) cooperate in stem cell lineages (for reviews see<sup>1,2</sup> and references therein).

Besides their role during morphogenesis and tissue homeostasis, stem cells have also been implicated in pathophysiological processes as cancer formation and progression<sup>3</sup>. Several tumors<sup>4-7</sup> have recently been shown to contain a small population of slow cycling cells that possess stem cell characteristics (*cancer stem cells*). Whereas the majority of cells in a tumor are thought to be non- tumorigenic, cancer stem cells seem to drive tumor formation because of their



ability to self renew and generate the multiple different cells present in a tumor. Thus the cancer stem cell hypothesis could provide a potential explanation why tumors reappear after extensive treatment: Due to their slow cycling rates and the presence of pumps that confer multi drug resistance<sup>8</sup>, cancer stem cells could escape conventional cancer treatment and thus drive relapse.

It is therefore essential to understand which molecular mechanisms safeguard stem cell division and which pathophysiological mechanisms cause neoplastic transformation. These insights into stem cell biology will hopefully entail new strategies in cancer therapy.

## **2. *Drosophila* as a model system to study stem cell proliferation**

Due to the available genetic tools and the 'relative' simple tissue architecture *Drosophila* has long been a favorable model organism in genetic research. Also for stem cell research, *Drosophila* has made fundamental contributions as for example the first identification of a stem cell niche<sup>9</sup>.

*Drosophila* possesses two stem cell types (Illustration 1) that gained notable attention in *Drosophila* stem cell research since they are particularly useful to unravel basic mechanisms underlying stem cell biology: A) Neural precursor cells (***neuroblasts***, ***Nb***) and B) germline stem cells (***GSC***) in the ovary and testes. Neuroblasts provide an excellent model system to study the molecular mechanisms that regulate intrinsic asymmetric cell divisions whereas germline stem cells are regulated by a stem cell niche<sup>1,2</sup>.

### *Niche mechanism*

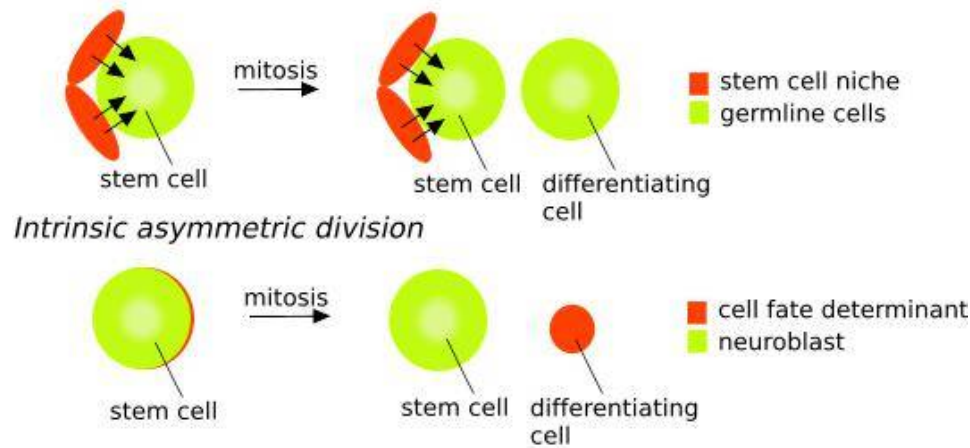


**Illustration 1**

## **2.1 Drosophila Neural Precursor Cells**

Neuroblasts are the neural stem cells of the fly and produce all the neurons and glia of the brain through repeated rounds of asymmetric divisions<sup>1,2</sup>. Neuroblasts are specified within an embryonic epithelial mono layer by the action of proneural genes and differential Notch signaling and subsequently delaminate from this epithelium. Once located subepithelially, neuroblasts start to divide asymmetrically to produce the neurons and glia of the respective lineages. The spatial/temporal identity of a neuroblast not only determines the number of neurons and glia it produces but also determines the proliferation pattern during development. Most neuroblast lineages follow a highly stereotyped proliferation pattern throughout neurogenesis: During embryonic phases neuroblasts divide asymmetrically to produce another neuroblast and a smaller ganglion mother cell (GMC) that terminally divides once more to produce neurons or/and glia. After embryogenesis neuroblasts enter a short phase of quiescence and reenter mitotic proliferation

during first instar larval stages to continue asymmetric cell divisions and hence neurogenesis until early pupal stages<sup>10</sup>. Two neuroblast populations have however been found that follow a different proliferation pattern: A) The 4 Mushroom Body (MB) neuroblasts which generate the Mushroom Body (a brain structure required for associative learning) do not enter a phase of quiescence and proliferate longer during pupal stages<sup>10</sup>. B) The Posterior- Asense- Negative (PAN) neuroblast lineages (also called Type II and DM lineages) contain transit amplifying secondary neuroblasts and thus generate more neurons in a given time frame than regular neuroblast lineages<sup>11-13</sup>.

Importantly however all neuroblasts studied so far use the same molecular machinery to divide asymmetrically (see <sup>14</sup> for embryonic neuroblasts; <sup>11-13</sup> for PAN (DM/ TypeII) lineages and results section for MB neuroblasts). The process of asymmetric cell division can conceptually be divided into three distinct phases: A) Establishment of polarity, B) alignment of the mitotic spindle with the axis of polarity and C) unequal segregation of cell fate determinants (and hence establishment of different cell fates and subsequent maintenance of different cell fates).

Even though substantial progress has been made in understanding these phases of asymmetric cell division, multiple gaps remain in describing asymmetric cell division on the molecular level (see below). (Since the data on *mushroom body defect*, presented below, base on concepts of polarity establishment and spindle orientation, I will review these topics in the introductory section. Issues of cell fate specification will be addressed in the Discussion.)

### **2.1.1 Establishment of polarity and determinant localization**

A genetic screen set up to identify genes involved in the first asymmetric division of the *C. elegans* zygote led to the identification of the *par* (partitioning defective) genes<sup>15</sup>. With exception of *par-2*, all members of the partitioning defective genes (*par-1* through *par-6* and *pkc-3*) are conserved during evolution but only *par-3*, *par-6* and *atypical protein kinase C* (*aPKC*) have a

conserved role during asymmetric cell division<sup>14</sup>. In *Drosophila* neuroblasts the Par proteins (Par6, Par3 and aPKC) localize to the apical cortex and are required for proper localization of the cell fate determinants; namely Numb, Prospero and Brat and their adapter proteins Partner of numb (Pon) and Miranda to the basal cortex<sup>14,16-19</sup>. An important substrate of the Par complex during asymmetric cell division is the cytoskeletal protein Lethal giant larvae (Lgl)<sup>20</sup>. Lgl is phosphorylated by aPKC and this phosphorylation induces the apical to basal cortical release of Lgl during mitosis<sup>21</sup>. The temporal coupling of this phosphorylation event to mitosis is triggered by the phosphorylation of Par-6 at Ser 34 by AuroraA. This phosphorylation is associated with a release of aPKC from Par-6 mediated inhibition and the consequent phosphorylation of Lgl by activated aPKC. Lgl phosphorylation is accompanied by an disassembly of the Lgl/ Par-6/ aPKC complex inasmuch as Lgl is replaced by Par-3 which competes with Lgl for entry into the Par complex. This complex remodeling is associated with a new substrate specificity of aPKC which now phosphorylates Numb that is subsequently released from the cortex<sup>21,22</sup>. The binding of the aPKC specificity factor Par-3 to the Par complex and the consequential spatial restricted/ polarized localization allows Numb phosphorylation on only one side of the cortex, ensuring its accumulation on the basal cortex of the cell. While this model can potentially explain the localization of Numb during neuroblast division, it is unclear if the adapter protein Miranda and its cargo Brat and Prospero are localized by direct aPKC phosphorylation as well. Recent data suggest that Miranda might follow a different molecular route of basal localization<sup>23</sup>. APC5 mutant neuroblasts have defects in Miranda (and Miranda cargo protein) localization whereas Numb and Pon localize correctly to the basal cortex<sup>24</sup>. Similarly live imaging studies using GFP tagged Pon and Miranda suggest that these two proteins indeed use a different spatial route through the cell during basal localization and additionally are affected differently in mutant situations of *Myosin VI* but are both miss- localized upon *Myosin II* loss of function achieved by injection of the Rho inhibitor Y-27632<sup>23</sup>. It is yet also unclear how nonmuscle Myosin II contributes to the basal localization of PON/ Numb and Miranda<sup>25</sup>.

Overall biochemical approaches and forward genetic screens have led to the realization that the apical cortex of a neuroblast harbors a complex network of proteins that regulates and functions

during asymmetric cell division. Multiple interconnected molecular pathways and networks ensure correct cell fate determinant localization and it will be a challenging task in the future to assemble these pathways into a comprehensive model of cell fate determinant localization and asymmetric cell division.

### 2.1.2. Spindle orientation

Besides its role in promoting basal localization of cell fate determinants, the Par complex and associated proteins provide attachment sites for astral microtubules to anchor the mitotic spindle in an apical-basal orientation. Faulty aligned mitotic spindles can result in equal inheritance of cell fate determinants and consequently symmetric divisions<sup>26</sup>.

On the molecular level spindle orientation in *Drosophila* is best understood in neuroblasts<sup>26,27</sup>. Several proteins have been identified that regulate spindle orientation (Illustration 2). *inscuteable*<sup>28</sup> (*insc*) and its binding partner *partner of inscuteable*<sup>29</sup> (*pins*) which localize to the apical cortex in neuroblasts are required for proper spindle alignment. Inscuteable has been shown to bind Par3 and this binding is required for its apical recruitment<sup>19</sup>. The Insc binding protein Pins gets localized in an Insc dependent manner and is required for maintaining Insc at the apical cortex and for proper cell fate determinant localization<sup>29</sup>. Pins contains three GoLoco motifs which interact with the  $\alpha$  subunit of heterotrimeric G proteins. Pins can catalyze the dissociation of the  $\alpha$  and  $\beta\gamma$  subunits in a receptor independent manner and is required for orientation of the mitotic spindle. It is however unclear how the the protein network of the apical cell cortex contacts the mitotic spindle and maintains its position parallel to the axis of cell polarity.

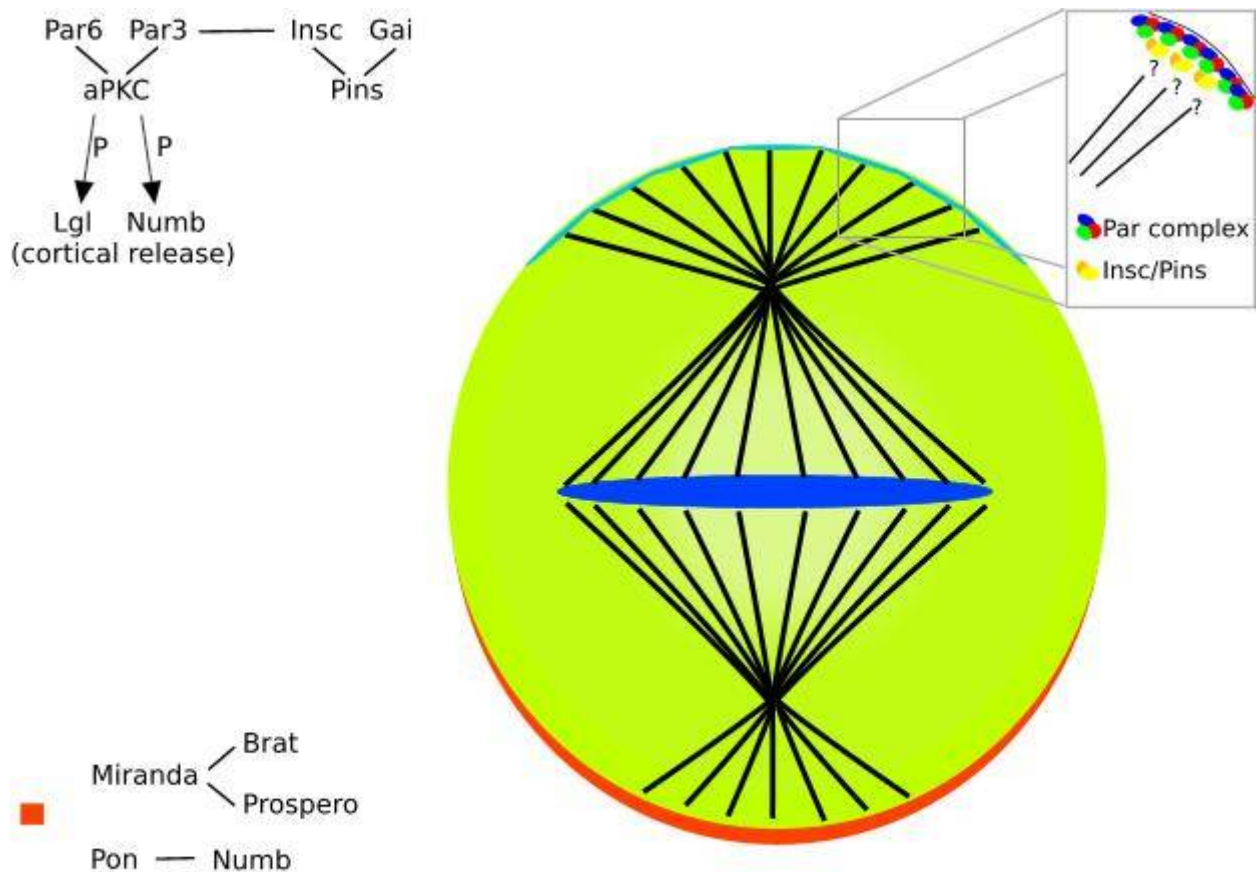


**Illustration 2**

Importantly studies in vertebrates have led to the identification of NuMA (nuclear mitotic apparatus protein), a protein that could potentially bridge this gap and mediate the interaction of cell cortex proteins and the astral microtubules<sup>30</sup>. NuMA is a large coiled- coil domain protein that possesses a LGN (the mammalian Pins homolog) binding domain in its C- terminus. Importantly NuMA has also been demonstrated to bind microtubules via its C- terminus. Interestingly the LGN and microtubules binding domains overlap by ten amino acids which makes the binding to LGN and microtubules mutually exclusive. It has been demonstrated that overexpression of LGN and its binding partner G $\alpha$ i induce spindle oscillations and rotations in MDCK cells that can either be inhibited by low doses of nocodazole or by simultaneously expressing the LGN binding partner NuMA<sup>30</sup>. These data suggest that NuMA participates with LGN and G $\alpha$ i to regulate these spindle movements.

During interphase, the NuMA protein is localized to the nucleus. Upon mitosis (nuclear

envelope breakdown) NuMA is released from the nucleus and is subsequently able to bind LGN. Consistently a fraction of NuMA, which predominately localizes to the spindle pole region during mitosis, can also be detected at the cell cortex<sup>30</sup>. The binding of LGN to NuMA induces a conformational switch which abrogates the 'inactive state'/ closed conformation of LGN. The binding of NuMA to LGN seems to be a prerequisite for efficient binding of LGN to the myristoylated and thus cortically anchored G $\alpha$ i. Subsequently a trimeric complex, consisting of LGN, G $\alpha$ i and NuMA forms which is required to interact with the spindle. Although NuMA can bind microtubules it is unlikely that this binding is necessary during this step, since LGN can inhibit this interaction. Alternatively NuMA could mediate spindle positioning via its interaction with dynein/dynactin (reviewed in<sup>31</sup>).

Given this appealing model in vertebrates it is however unclear how the mitotic spindle is oriented in invertebrates, since a NuMA homolog has not yet been identified. Furthermore the relative contribution of the different apical components to spindle orientation and the molecular link that connects the apical domain in neuroblasts to the spindle are not known in *Drosophila*. The dependency of individual members of the apical proteins on each other during initiation and maintenance of apical localization has so far made it impossible to work out a molecular flowchart of the processes that link the mitotic spindle with the axis of cellular polarity in *Drosophila*. In vertebrates, however it has similarly been difficult to convincingly demonstrate a requirement of NuMA in spindle orientation due to its pleiotropic cellular effects. Thus identifying a protein in *Drosophila* that shares the ability of NuMA to bind members of the apical complex and the mitotic spindle simultaneously could provide important insights into spindle orientation on the molecular and phenotypic level.

## **2.2 The ovarian stem cell lineage**

*Drosophila* ovarian germline stem cells reside in a specialized structure called the germarium which is the most anterior structure of an ovariole. An ovariole consists of an linear array of one

germarium and subsequent egg chambers at increasing differentiation stages. Of all germline cells within the germarium, the stem cells are the most anterior cells directly contacting the more anterior somatic CAP cells. The CAP cells (and terminal filament cells, which are not in contact with the GSCs and reside anterior to the CAP cells) constitute the germline stem cell niche<sup>9</sup> which is required for proper stem cell maintenance. Decapentaplegic (Dpp), secreted from CAP and terminal filament cells, instructs germline stem cells to retain their fate and thus self-renewal potential<sup>32</sup>. Dpp has been shown to act by repressing the expression of the *bag of marbles* (*bam*) gene in the niche contacting cell (GSC)<sup>33</sup>. Consistent with its instructive role in GSC fate maintenance, artificially expanding the Dpp signalling range by either overexpressing Dpp in a broader range of somatic cells in the germarium or by overexpressing thickveins (the Dpp receptor) in the germline, is accompanied with the formation of ectopic stem cells (reviewed in<sup>34</sup>). Consistent with the role of Dpp none of these ectopic stem cells express *bam*.

After stem cell division one of the two daughter cells is not in contact with the stem cell niche, does not receive the instructive niche signal and consequently upregulates the *bag of marbles* gene<sup>33,35</sup>. Bam and Benign cell neoplasm (Bcgn)<sup>36,37</sup> consequently counteract Pumilio/Nanos in this niche detached daughter cell (the so called cystoblast)<sup>38,39</sup>. Pumilio and Nanos have been suggested to repress the translation of 'differentiation mRNAs' in the stem cell<sup>40-43</sup> and this repression is relieved by Bam/Bcgn in the cystoblast. In *bam* mutants the transition from stem cell to cystoblast is impaired and consequently stem cells overproliferate at the expense of differentiated cells leading to the formation of an ovarian stem cell tumor<sup>44,45</sup>. If *pumilio* is removed in a *bam* mutant background signs of further differentiation are detectable, suggesting that *pumilio* acts downstream or in parallel to *bam*<sup>38,39</sup>. Besides Pumilio/ Nanos and Bam/ Bcgn, additional pathways act in the stem cells to promote their maintenance. Importantly the microRNA pathway is required and sufficient for germline stem cell fate<sup>46-49</sup>. Loss of function of either *dicer*, *loquacious* or *argonaute1* (*ago1*) results in stem cell loss whereas overexpression of *ago1* leads to the formation of ectopic stem cells and even tumorous germaria at a low frequency<sup>48</sup>. This suggests that Ago1 is a limiting factor in cystoblasts and increasing Ago1 levels is sufficient to increase miRNA signaling. Since *ago1*, *bam* double mutants show signs of further



differentiation miRNAs seem to act parallel to Nanos and Pumilio to ensure GSC maintenance and differentiation<sup>48</sup>.

Once committed to further differentiate, the cystoblast will undergo four transit- amplifying divisions with incomplete cytokinesis to generate 2-, 4-, 8- and finally 16- interconnected cystocytes. The cells are connected through cytoplasmic bridges by the so called fusome, a membranous organelle. The fusome originates from the spectroosome which is present in the stem cell and the cystoblast<sup>50,51</sup> <sup>i</sup>. Amongst these 16 cystocyte cells, one cell is selected to become to future oocyte whereas the remaining cells will differentiate into nurse/ support cells. These 16 cells are then ensheathed by somatic cells and leave the germarium to form individual egg chambers.

Up to now, cyst completion is a poorly understood process. It is unclear how the precise 4 transit amplifying divisions are 'counted' and what drives the cystocytes out of mitotic proliferation and into meiosis (oocyte) and endoreplication (nurse cells) respectively. Interestingly Cyclin E has been shown to be sufficient to promote an additional round of cystocyte division when overexpressed from a heat shock inducible promoter, yielding cysts with 32 interconnected cells<sup>52</sup>. Additionally several mutants are known in which cystocytes proliferate indefinitely leading to the formation of germline cyst tumors. Loss of function of *bruno* (a RRM containing RNA binding protein) lead to cystocyte tumors that proliferate mitotically<sup>53,54</sup>. It has further been demonstrated that *bruno* downregulates *sex lethal (sxl)* via 'bruno responsive elements' (BREs) in the *sxl* 3'UTR and that this downregulation is required for proper cyst differentiation. Overexpression of *sex lethal Δ BRE* in the germline induces severe overproliferation of cysts<sup>55</sup>. Similarly mutations in genes as *fused*<sup>56</sup> (a Serine- Threonine kinase implicated in Hedgehog (Hh) signalling) and *rbp9*<sup>57</sup> (a Drosophila Hu homolog) cause overproliferation suggesting (together with mutants as *bam* and *bcgn*) that all cells in the early germline stem cell lineage (until the 16 cell stage) can be the source of tumorous proliferation.

---

i Since this structure is segregated asymmetrically upon stem cell division into the stem cell, it is newly synthesized by the cystoblast. Thus the spectroosome constitutes an intrinsic asymmetric component in GSC division; however it is unlikely that the spectroosome has an instructive role in cell fate decisions.

Importantly it has recently been demonstrated that 16 cell cysts, can disassemble and de-differentiate into functional stem cells, highlighting their plasticity in terms of cell fate<sup>58</sup>. This ability of differentiating cells to respond to niche derived instructive cues is of fundamental importance during germline tissue homeostasis, because stem cells are lost even in the wild type situation and have to be replaced by either symmetric divisions of other stem cells or de-differentiation of nearby germline cells.

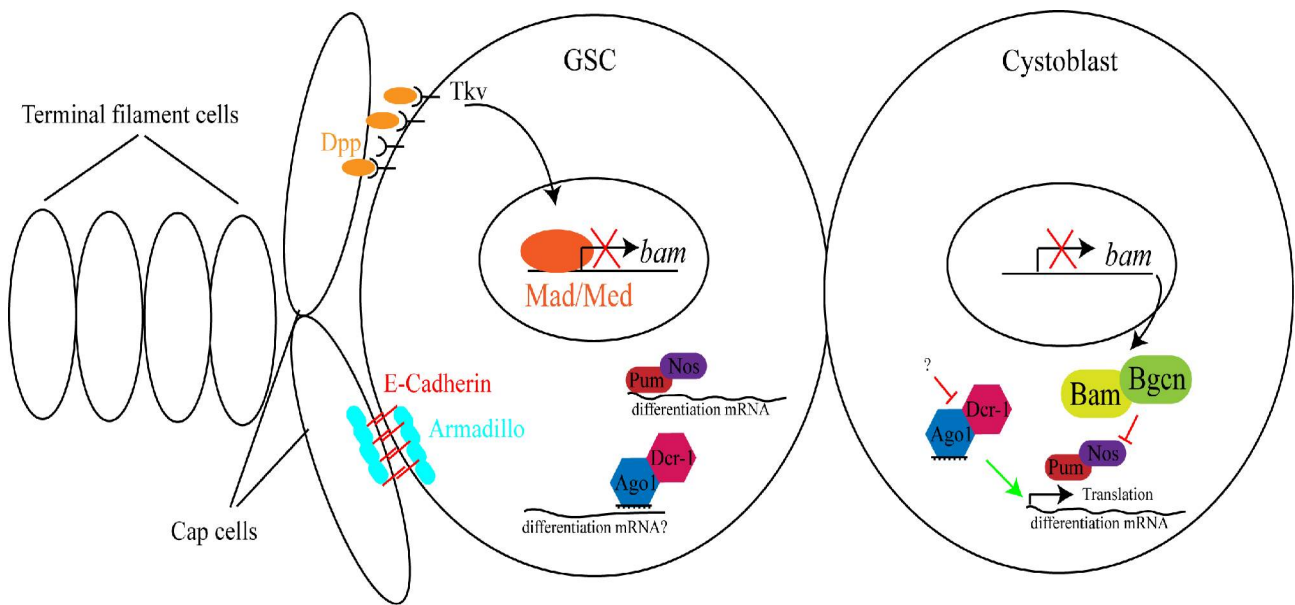


**Illustration 3**

The recent implication of the Trim protein Brat in the regulation of asymmetric neural stem cell divisions and the observation that mutations in *mei-P26*, another member of this protein family, causes ovarian tumors, raises the interesting possibility that intrinsic and extrinsic stem cell divisions might be regulated by members of the same protein family.

### 3. Trim- NHL domain proteins and proliferation control

Members of the RBCC/Trim protein super- family are characterized by the presence of a RING ('really interesting new gene') domain, a B-box and a coiled-coil motif. The completion of the genome sequence of multiple organisms has led to the identification of an ever increasing number of Trim proteins. Analysis of the human genome revealed the existence of 68 Trim proteins of which only a few have been studied on a functional/ molecular level. Similar genomics analyses in other species led to the realization the Trim proteins are well conserved during evolution from nematodes to vertebrates. The conserved tripartite domain architecture is followed by a C-terminal domain which is variable between members of this protein family. Besides WD40, SPRY, Filamin, BROMO and AFR domains, multiple NHL repeats can constitute this C-terminal part of the protein. (For reviews on the Trim protein superfamily see <sup>59-61</sup>.)

The presence of an NHL domain defines a subfamily of Trim proteins which further on will be referred to as Trim-NHL domain proteins. The NHL repeat was identified by amino acid sequence similarities among *ncl-1*, HT2A and *lin-41*<sup>62</sup>. Trim-NHL proteins are well conserved during evolution<sup>62</sup> and some members have been studied on the phenotypic and molecular level in worms (*lin-41*, *ncl-1*, *nhl-1*, *nhl-2*, *nhl-3*)<sup>63,64</sup>, flies (*brat*, *mei-P26*, *dappled/wech* and *abba*)<sup>65-78</sup> and mice (*trim32*)<sup>79,80</sup>. Loss and gain of function studies in these model organisms implicate Trim-NHL domain proteins in a plethora of biological processes as: asymmetric cell division (*ncl-1*, *nhl-2*, *nhl-3*, *nhl-1*, *lin-41*, *brat*, *dpld/wech*, *trim32*), embryonic patterning (*brat*), muscle development and function (*dpld/wech*, *trim32*), meiosis (*mei-P26*), growth inhibition (*ncl-1*, *brat*) and cancer (*trim32*).

In flies three of the four Trim-NHL domain proteins have been implicated in proliferation control. *brat* was identified in a genetic screen to cause overproliferation<sup>81</sup> (reviewed in <sup>82</sup>) in the developing central nervous system of the fly, loss of *mei-P26* has been reported to induce tumorous proliferation in the ovaries<sup>77</sup> and *dappled* mutations result in melanotic tumor formation<sup>74</sup>. Recently however the role of *dappled* as a tumor suppressor has been challenged

since Löer et al.<sup>71</sup> report that newly identified mutations in CG1624 do not correspond to *dappled* which they rename *wech*. Thus further studies are required to address the question if *dappled* and the fourth Drosophila Trim-NHL protein Abba are involved in proliferation control and tumor suppression as their paralogs *brat* and *mei-P26*.

The so far best studied Drosophila Trim-NHL protein is Brat. Recessive mutations in the *brat* gene lead to tumor like, neoplastic growth in the larval brain which ultimately kills the animal<sup>65,70,82</sup>. Further on *brat* mutant brain tissue can be transplanted and propagated over multiple generations of host animals<sup>83</sup>. Analysis of point mutants revealed that mutations in the NHL domain are sufficient to induce the tumor phenotype<sup>65</sup>. Although the neoplastic phenotype of neuroblast over proliferation was known for decades only recently have substantial insights into the tumor suppressor activity of *brat* been made. Especially two lines of experimental data have provided an intellectual framework of how *brat* might suppress neoplastic growth in the larval CNS: A). It has recently been demonstrated that the Brat protein segregates asymmetrically in neuroblasts upon mitosis and is preferentially inherited by the future ganglion mother cell<sup>67,72</sup>. B) *brat* as its *C. elegans* homolog *ncl-1* have been implicated in nucleolar size and thus cellular growth regulation<sup>64,68</sup>. From these data *brat* was proposed to restrict self-renewal capacity to the neural stem cell only, since the segregation and subsequent cell growth inhibition of Brat in the ganglion mother cell prevents further proliferation. It is however unclear if sole growth inhibition is sufficient to restrict self renewal. It might thus be possible that *brat* either activates 'differentiation genes' or represses 'self renewal genes' in the ganglion mother cell. The inhibition of cell growth of *brat* however seems to be independent of cell differentiation, since *brat* mutant wing disc cells are larger and have excess rRNA<sup>68</sup>. Brat has interestingly been suggested to inhibit dMyc at the post-transcriptional level in the larval CNS<sup>67</sup> which could potentially explain the increased rRNA abundance in *brat* mutant cells. In vertebrates a recent study further investigated a possible regulation of *myc* by the *brat* homolog *trim32*<sup>84</sup>. Surprisingly this study revealed that the RING finger is involved in c-Myc ubiquitination and subsequent degradation; a domain that is absent in *brat*. This suggests that the downregulation of dMyc in ganglion mother cells might be an indirect consequence of neuronal

differentiation. This is further supported by the fact that cells with high levels of Brat exist in the PAN neuroblast lineages that simultaneously express high levels of dMyc<sup>13</sup>. Further studies are therefore required to reveal by which molecular mechanism *brat* regulates cellular growth.

On the molecular level Brat has further been suggested to be a translational regulator required for the repression of *hunchback* in the posterior part of the *Drosophila* embryo<sup>75</sup>. Using a yeast four hybrid and an *in vitro* binding assay, Sonoda and Wharton could demonstrate that Brat forms a quaternary complex with Pumilio, Nanos and the *hunchback* RNA. The interaction seems to be specific for *hunchback*, since the *cyclinB* mRNA, which (like *hunchback*) contains 'nanos responsive elements' (NREs) and therefore can assemble into a ternary complex with Nanos and Pumilio, does not recruit Brat. Thus *brat* may function as a translational regulator, in the restriction of self- renewal.

The other Trim-NHL protein which has convincingly demonstrated to function as a tumor suppressor in flies is *mei-P26*.

*mei-P26* has been identified in a genetic screen to be required for meiosis in the female germline<sup>78</sup>. It could further be demonstrated that stronger alleles of *mei-P26* result in an ovarian tumor phenotype<sup>77</sup>. This phenotype was so far only analyzed at the level of DNA stainings which do not allow to decide if *mei-P26* loss of function results in stem cell lineage defects. Since *brat* loss of function causes defects in the neural stem cell lineage, it is however tempting to speculate that *mei-P26* tumors might also arise from stem cells or early stem cell progeny.

## II. Results

### 1. Part I: The *Drosophila* NuMA homologue Mud regulates spindle orientation in asymmetric cell division

#### 1.1. Mud is the *Drosophila* homologue of NuMA

Pins and G $\alpha$ i are functionally conserved from *C. elegans* to vertebrates. In vertebrates, they seem to connect to the mitotic spindle via the microtubule binding protein NuMA, but so far no NuMA ortholog has been identified in invertebrate organisms. To search for NuMA orthologs outside the vertebrate family, we used a bioinformatics approach. NuMA is a tripartite molecule containing an N-terminal CH (calponin homology) domain, a long coiled-coil, and a C-terminal region that binds Pins and microtubules (Fig. 1A). Searching protein databases with the non-coiled N- and C-terminal regions identified clear homologs of NuMA in deuterostomia, including the vertebrates mouse, zebrafish, chicken, and frog, as well as lower chordates and sea urchin (Fig. 1B). Notably, analysis of the multiple sequence alignment using Plotcon and Gblocks determined that the region of highest conservation corresponds to the Pins and microtubule binding sites in human NuMA.

To find more distant homologs, Hidden Markov Models (HMMs) were derived from the N- and C-terminal segments and applied independently in searches against protostomian proteomes, including worm and fly. From the *C. elegans* proteome, the C-terminal HMM recovered F01G10.05 and LIN-5. These proteins feature NuMA-like domain architecture (Fig. 1A), and their high similarity suggests they are paralogs. F01G10.5 is uncharacterized, but LIN-5 binds

GoLoco motif proteins and regulates spindle positioning during *C. elegans* embryogenesis . In *Drosophila*, independent searches with the N- and C-terminal HMMs recovered Mud (Mushroom Body Defect) as the only protein with significant similarity to NuMA. Like in NuMA, the N- and C-terminal regions of Mud are separated by a long coiled-coil (Fig. 1A) . In addition, Mud has a 500 amino acid C-terminal extension, a feature not present in the homologous proteins in *Anopheles*, *C. elegans*, or vertebrates. The *Drosophila mud* gene also codes for two shorter isoforms lacking the putative Pins and microtubule binding regions, but current EST data provide no evidence for such alternative splicing of *NuMA* in mice or humans (M.N., unpublished observations). While the sequence similarity between Mud and human NuMA in the N-terminus is low (17% identical, 35% similar), this region of Mud is predicted to adopt a similar CH-like fold . The sequence conservation in the C-terminus is higher (27% identical, 41% similar), with the highest similarity in the region where Pins and microtubules bind to human NuMA. We conclude from this data that F01G10.5, LIN-5, and Mud are the sequence homologs of NuMA in *C. elegans* and *Drosophila*.

## 1.2. Mud is part of a conserved heterotrimeric complex

To test whether the sequence similarity results in conserved protein interactions, we checked if Mud, like NuMA, is part of a ternary complex with Pins and G $\alpha$ i. Similar to previous studies, we used C-terminal truncations of Mud (Mud-C) containing the putative Pins and microtubule binding regions (Fig. 1A). G $\alpha$ i complexes were immunoprecipitated from S2 cells transfected with myc-tagged Mud-C. In untransfected cells, G $\alpha$ i can coprecipitate Pins. Upon transfection of myc-Mud-C, immunoprecipitation of G $\alpha$ i co-precipitates Pins and myc-Mud-C (Fig. 2A). This suggests that Mud-C is in a complex with Pins and G $\alpha$ i. To determine whether Mud-C binds directly to Pins, we tested these proteins in an *in vitro* binding assay. *In vitro* translated Mud-C can bind to bacterially produced GST-Pins, but not GST alone (Fig. 2B), indicating that a Pins/Mud-C complex can form *in vitro* without additional cofactors. Consistent with this, Mud

co-immunoprecipitates with Pins from wild-type embryo extracts (Fig. 2C). We conclude that Mud binds to Pins using a C-terminal region and is part of a ternary complex with G $\alpha$ i.

Because NuMA binds to the N-terminal TPR repeats of mammalian Pins, we investigated whether Mud behaves similarly in *Drosophila*. For this, the N-terminal TPR and C-terminal GoLoco repeats of *Drosophila* Pins were GFP-tagged and expressed in S2 cells with Myc-Mud-C. Immunoprecipitation of GFP shows that Myc-Mud-C binds to Pins-TPR-GFP, but not GFP-Pins-GoLoco (Fig. 2D), indicating that Pins binds to Mud using the TPR repeats. G $\alpha$ i does not bind to Mud-C *in vitro* (data not shown), but earlier work shows that G $\alpha$ i directly binds to the C-terminal GoLoco repeats of mammalian and *Drosophila* Pins . Because Mud, like NuMA, binds to the N-terminus of Pins, this suggests that the geometry of the heterotrimeric NuMA-Pins-G $\alpha$ i complex is conserved in *Drosophila*.

The conserved C-terminal fragment of human NuMA can interact with the TPR repeats of *Drosophila* Pins , so we tested whether Mud could bind to human Pins. For this, His-HsPins-TPR and GST-Mud-C fusion proteins were produced in bacteria and used in an *in vitro* binding assay. His-HsPins-TPR binds to GST-Mud-C but not GST alone (Fig. 2E). The binding of human Pins to *Drosophila* Mud argues for the evolutionary conservation of this interaction. Taken together, these results demonstrate that Mud is part of a heterotrimeric complex that is highly conserved from insects to vertebrates.

### **1.3. Mud interacts with microtubules**

NuMA binds to microtubules and can stimulate their polymerization. To find out if Mud has similar biochemical qualities, we tested whether Mud binds microtubules in a microtubule sedimentation assay. In this experiment, a soluble protein extract was created from S2 cells transfected with myc-Mud-C. Polymerization of microtubules with GTP and taxol followed by high speed centrifugation separated microtubules and microtubule binding proteins from the supernatant. As expected,  $\alpha$ -tubulin and the microtubule binding protein Ebf1 remain soluble in



the absence of GTP and taxol (Fig. 3A). When microtubules are stabilized, however, these proteins can be found in the microtubule pellet along with Pins and Myc-Mud-C (Fig. 3A). We conclude that Mud and Pins can associate with microtubules. To test whether Mud, like NuMA, can stimulate microtubule polymerization, we performed a solution microtubule formation assay. Tubulin subunits labeled with rhodamine were incubated in an energy-regenerating system with GST, with GST-Mud-C fusion protein, or in buffer alone. After fixation of this preparation to coverslips, the number of microtubules generated were counted in 10 random fields. The average number of microtubules per field formed with GST or buffer alone is less than 20 ( $18.5 \pm 1.0$  and  $8.6 \pm 0.6$ , respectively), but when Tubulin is incubated with GST-Mud-C, the average number of microtubules formed increases to over 100 per field ( $104.2 \pm 3.2$ , Fig. 3B, 3C). This shows that the interaction of Mud-C with Tubulin is direct, and, like NuMA-C, Mud-C can stimulate microtubule formation *in vitro*. The interaction of Mud with microtubules together with its membership in a ternary complex with Pins and G $\alpha$ i strongly suggest that Mud is the functional homolog of NuMA in *Drosophila*.

#### **1.4. Mud regulates spindle orientation in larval neuroblasts**

A Pins/G $\alpha$ i interacting protein that also binds microtubules is a good candidate for a regulator of spindle orientation in asymmetric cell division. To find out if Mud controls spindle orientation, we analyzed larval neuroblast divisions in animals homozygous for *mud*<sup>4</sup>, a presumptive null allele affecting all Mud isoforms. For this, we immunostained third instar larval brains for Miranda and Centrosomin. Neuroblasts were defined as Miranda-expressing cells greater than 10 microns in diameter (see supplementary methods for details). In wild type neuroblasts, Miranda forms a crescent in metaphase, and segregates into a single daughter cell at telophase (Fig. 4A-C). In *mud* zygotic mutants, the Miranda crescent can be bisected by the cleavage plane and inherited by both daughter cells (Fig. 4D-F) (see below). Mis-segregation of Miranda could be due either to defective spindle orientation or be a secondary consequence of a

general loss of polarity. Alternatively, Mud could regulate mitotic spindle morphology or formation. All *mud* mutant neuroblasts form crescents of aPKC (n=40, Fig. 4J, 4K) and opposing crescents of Insc and Miranda (n=40, Fig. 4H, 4I). Furthermore, spindles in *mud* mutant neuroblasts appear bipolar with no gross morphological differences from wild type (Fig. 4N, 4O). From this data, we conclude that *mud* mutants form functional spindles and the neuroblasts are correctly polarized. Consistent with this, Brat (Fig. 4L, 4M) and Numb (data not shown) form crescents in *mud* mutant neuroblasts, but the spindle is not aligned with them. Therefore, the spindle orientation defect is a direct consequence of Mud loss of function. To quantify this defect, we measured the angle between a line connecting the two centrosomes and a line bisecting the crescent of Miranda in metaphase neuroblasts (Fig. 4G). A small angle indicates tight coupling of the mitotic spindle with the polarity axis. In wild type, the measured angle is almost always less than 10° (90% of neuroblasts, n=50). In *mud* mutants, the majority of spindles show more oblique orientations (63%, n=89), and only a minority of spindles have measured angles 10° or less (37%, n=89, Fig. 4P). We conclude that Mud is required for coordinating the mitotic spindle with the axis of polarity. Together, these observations demonstrate that *mud* mutant neuroblasts polarize correctly, but in the absence of Mud, the polarized cortical domains can not direct the orientation of the mitotic spindle. As a result, cell fate determinants can fail to segregate asymmetrically.

### **1.5. Mud localizes to spindle poles and the apical cell cortex of neuroblasts**

To analyze Mud localization in asymmetric cell division, we stained Mud in embryonic neuroblasts using an anti-Mud antibody. At neuroblast delamination, Mud colocalizes with Pins on the apical cell cortex (Fig. 5A). This cortical localization is maintained through interphase (Fig. 5B), when alternative methods of fixation also reveal a pool of Mud on the nuclear rim (data not shown). At metaphase, when the spindle aligns with the apical crescents of Mud and Pins (Fig. 5C), Mud can also be observed on spindle poles. At telophase, Mud preferentially

segregates into the neuroblast (Fig. 5D). This localization is consistent with recent work showing that Mud decorates mitotic and meiotic spindle poles and is required for positioning spindles in meiosis II . Although Mud is expressed in larval brains (Fig. 9), fixation conditions could not be found for analyzing Mud localization in larval tissue. We conclude that Mud co-localizes with Pins on the cortex of asymmetrically dividing neuroblasts.

To test if the localization of Mud depends on its binding partner Pins, we examined *pins*  $\Delta 50$  maternal and zygotic mutant embryos. The apical enrichment of Mud is lost in *pins* mutant metaphase neuroblasts and the cortical association is weaker, but Mud remains associated with spindle poles (Fig. 5E, 5F). To test whether Pins is sufficient for directing apical localization of Mud, we used transgenic *inscuteable* under the control of the *hsp70* promoter to express Inscuteable in epithelial cells. Epithelial cells normally divide parallel to the plane of the epithelium (Fig. 5G). Introduction of ectopic Inscuteable recruits Pins and G $\alpha$ i from the basolateral to the apical cortex, inducing a spindle reorientation . Mud is also recruited apically and colocalizes with Pins (Fig. 5H). This suggests that Pins recruits Mud to the apical cortex of epithelial cells in the presence of Inscuteable, and by extension, Pins recruits Mud apically in neuroblasts. We conclude from these experiments that Pins is required and sufficient for the apical recruitment of Mud, but the spindle pole localization of Mud is independent of Pins. Both the apical localization of Mud and its association with microtubules are consistent with a role in spindle orientation.

## **1.6. *mud* mutant brains overproliferate due to an increased neuroblast pool**

Mud gets its name from defective formation of the mushroom body, an adult brain structure required for olfactory learning and memory . The neurons forming the mushroom body, called Kenyon cells, are generated by four mushroom body neuroblasts which divide repeatedly throughout embryonic, larval, and pupal development . Mushroom body neuroblasts, like all neuroblasts in *Drosophila*, divide asymmetrically to yield a ganglion mother cell that produces

two neurons and a self-renewing neuroblast . Notably, wild type mushroom body neuroblasts form crescents of Miranda, which segregate into a single small cell (Fig. 4A-C). This shows that neuroblasts of this lineage segregate cell fate determinants asymmetrically. In *mud* mutants, Miranda also forms a crescent, but spindle misorientation leads to mis-segregation of Miranda in approximately 4% of mushroom body neuroblasts (n=80 telophase neuroblasts) (Fig. 4D-F). We propose that the remaining neuroblasts divide asymmetrically by repositioning the either spindle or the cell polarity axis during telophase. A similar rescue of defects during asymmetric cell division at late stages of mitosis has been described for other mutants, where it is called telophase rescue. Although the vast majority of *mud* mutant neuroblasts still divide asymmetrically, in those cells that inherit equal amounts of Miranda, and presumably equal amounts of the apical complex members known to regulate cell size asymmetry , the daughter cell size is equal (Fig. 4F). We conclude that mushroom body neuroblasts segregate Miranda and therefore its binding partners Brat and Prospero asymmetrically, but faulty spindle orientation leads to occasional mis-segregation in *mud* mutants.

Mis-segregation of cell fate determinants can result in the transformation of GMCs to neuroblasts . We therefore investigated whether symmetric segregation of Miranda resulted in increased numbers of mushroom body neuroblasts in *mud* mutants. For this, we used the mushroom body-specific GAL4 line OK107 and UAS CD8-GFP to label mushroom body neuroblasts and their progeny , and immunostained for Miranda, which is present in neuroblasts but rapidly degraded in GMCs. While the number of mushroom body neuroblasts in wild type late third instar brains is always four ( $4.0 \pm 0.0$ , n=6 mushroom bodies), the average number of mushroom body neuroblasts in *mud* mutants is nearly 14 ( $13.6 \pm 1.5$ , n=9 mushroom bodies, Fig. 6A-C). Neuroblast number increases over time, as we observed an average of around 8 mushroom body neuroblasts in the early third instar brains of *mud* mutants (R.A.N unpublished observations). From these experiments, we conclude that *mud* mutants generate excess mushroom body neuroblasts, a conclusion consistent with an earlier study . We also observed increased numbers of neuroblasts in the posterior half of the larval brain hemisphere (wild type  $23.5 \pm 0.4$ , n=6; *mud*  $61.1 \pm 7.7$ , n=9, Fig. 6D-F), ventral nerve cord, and the anterior brain regions

of *mud* mutants (data not shown). Ectopic neuroblasts in *mud* mutants express the neuroblast marker Deadpan (Fig. 6G, 6H), and incorporate BrdU (Fig. 6I, 6J), showing that they are correctly specified and mitotically active.

In *brat* mutants, transformation of GMCs to neuroblasts leads to a decrease in the number of neurons. To see if this is true for *mud* mutants, we analyzed Kenyon cells in late third instar larval brains using OK107-GAL4 driven CD8-GFP to mark the progeny of the mushroom body neuroblasts. Wild type larval brains contain around 500 Kenyon cells ( $521.3 \pm 35.1$ ,  $n=3$  mushroom bodies), but in *mud* mutants the average number of Kenyon cells increases ( $818.5 \pm 57.7$ ,  $n=3$  mushroom bodies, Fig. 6K). This suggests that unlike in *brat* mutants, the ectopic neuroblasts in *mud* mutants produce ectopic progeny cells. We propose that the penetrant symmetric division phenotype in *brat* mutants makes neuroblasts nearly incapable of producing GMCs, while the frequent asymmetric divisions in *mud* mutants can still give rise to differentiated progeny.

To test whether the ectopic neuroblasts and progeny cells develop normally, we investigated the morphology of the mushroom body in *mud* mutant adults. During development, repeated divisions of mushroom body neuroblasts sequentially generate three types of morphologically distinct Kenyon cells. These neurons project axons that form the characteristic lobed structure of the adult mushroom body. Kenyon cells born from late embryogenesis to the early third instar project their axons into the  $\gamma$  lobe, Kenyon cells born between early third instar and puparium formation project branched axons into the  $\alpha'$  and  $\beta'$  lobes, and finally, Kenyon cells born after puparium formation project their branched axons into the  $\alpha$  and  $\beta$  lobes. Like larval brains, *mud* mutant adult brains contain an increased number of Kenyon cells (wild type  $1225 \pm 12$ ,  $n=3$  mushroom bodies; *mud*  $4362 \pm 176$ ,  $n=3$  mushroom bodies, Fig. 6N; . The number of wild type Kenyon cells is lower than expected, but OK107 may not detectably label every Kenyon cell. Interestingly, while a small  $\gamma$  lobe is present in *mud* mutants, the ectopic Kenyon cells are unable to project axons into the  $\alpha \beta$  or  $\alpha\beta$  lobes (Fig. 6L, 6M). The absence of these lobes could indicate a role for Mud in axon guidance. Alternatively, the presence of the  $\gamma$  lobe suggests that

Kenyon cells born early in development, when the maternal supply of Mud is sufficient, are correctly specified. Consistent with this, the *mud* mutant  $\gamma$  lobe expresses low levels of Fasciclin-II, as in wild type  $\gamma$  lobes (data not shown, . At later stages, the reduced levels of Mud may result in misspecification of the  $\alpha\beta$  and  $\alpha\beta$  neurons, resulting in an absence of projections. Taken together, these observations suggest that in *mud* mutants, the occasional transformation of a GMC into a neuroblast causes overproliferation and cell fate misspecification.

To ask if *pins* and *mud* act in the same genetic pathway, we removed *pins* in a *mud* mutant background. Compared with the single mutant, *pins*, *mud* double mutant brains were filled with deadpan positive neuroblasts (Figure 10). These data with our biochemical analysis suggest that Pins and Mud act in a genetic pathway to control proliferation in *Drosophila* neural stem cell lineages.

## 1.8. Methods

### Flies and Immunohistochemistry

The allele of *mud* used in this study is *mud*<sup>4</sup>, a presumptive null with a nonsense mutation creating an early stop after the 5<sup>th</sup> amino acid. *mud*<sup>4</sup> hemizygotes and homozygotes were identified by selecting against an FM7-Krüppel-GFP balancer chromosome (Barry Dickson). UAS-CD8-GFP (Bloomington Stock Center) was expressed in the mushroom body using OK107-GAL4. The *pins*  $\Delta 50$  allele and the *hsp70-Insc* flies are described elsewhere. For immunofluorescence, third instar wandering larvae were dissected in PBS, and brains with attached ventral nerve cords (or adult brains) were fixed for 20 min in 5% PFA, 0.2% Triton X-100, then processed as described. Embryos were fixed in 8% PFA and processed as described (ibid). Samples were mounted in Vectashield with DAPI (Vector Laboratories). The secondary antibodies used in immunofluorescence were coupled to Alexa 488 (Molecular Probes), Cy3, or Cy5 (Jackson Immunofluorescence). Images were recorded on a Zeiss LSM510 confocal equipped with a blue diode laser to visualize DAPI for DNA. See supplementary methods for BrdU incorporation and additional imaging details.

### Antibodies and constructs

Antibodies used in this study were mouse anti-Pins (1:500; , rabbit anti-Pins (1:500; , 9E10 anti-myc (1:1000; 2 mg/mL stock), rabbit anti- G $\alpha$ i (1:100; , rabbit anti-GFP (1:1000; Abcam), mouse anti-His6 (1:1000; Qiagen), mouse anti- $\alpha$ -tubulin (1:1000; Sigma), mouse anti-Eb1 (1:500; , rabbit anti-Miranda (1:100; , mouse anti-Prospero (1:10, Developmental Studies Hybridoma Bank), rabbit anti-Centrosomin (1:200, , mouse anti-Inscuteable (1:200; , rat anti-Brat (1:100; , mouse anti-phospho Histone 3 (1:1000, Cell Signaling Technology), rabbit anti-PKC $\zeta$ /aPKC (1:200, Santa Cruz) rabbit anti-Mud (1:500; , mouse anti-BrdU (1:100, Sigma),

guinea pig anti-Deadpan (1:1000, Jim Skeath, unpublished), and mouse anti-Elav (1:30, Developmental Studies Hybridoma Bank). Mud-C transgenes were generated by PCR from mixed stage cDNA using primers containing attB recombination sites and including nucleotides 5551-6174 of the mud-RB coding sequence. Pins transgenes were generated by PCR from EST LD35569 using primers containing attB recombination sites and including nucleotides 1-1977 (full length), 1-1230 (Pins-TPR), and 1123-1977 (Pins-GoLoco) of the Pins-RA coding sequence. PCR products were recombined into pDONR-221 (Invitrogen) and subsequently recombined into the following fusion protein vectors containing attR recombination sites: pUAST-6x-myc (N-terminal; ), pUAST-EGFP (N- or C-terminal; Frederik Wirtz-Peitz and Alfonso Martinez Arias, unpublished), pDEST-15 (N-terminal GST, Invitrogen) pDEST-17 (N-terminal His6, Invitrogen). His-HsLGN-TPR (1-373) is described elsewhere .

### **Transfection, Immunoprecipitation, and In vitro Binding Assays**

S2 cells were propagated in Schneider's medium (Gibco) with 10% fetal calf serum, 50 U ml<sup>-1</sup> penicillin and 50 mg ml<sup>-1</sup> streptomycin. UAS constructs were expressed by cotransfection with actin-Gal4 (a gift from Talia Volk) using Cellfectin (Invitrogen). Cells were collected in lysis buffer (25 mM HEPES [pH 7.5], 150 mM NaCl, 0.5 or 1% Triton X-100, 0.5 mM EDTA, 5 mM MgCl<sub>2</sub>, 1 mM DTT, 1mM PMSF, and Complete EDTA-free protease inhibitors [Roche]). Immunoprecipitations were carried out for 1 or 2 hours at 4°C using protein A sepharose (Amersham). For IP from embryo extract, embryos 0-7 hours old were homogenized in lysis buffer and processed as above. GST, GST-Pins (full length), and GST-Mud-C were expressed at 37°C in BL-21 cells by induction with 1mM IPTG and purified using glutathione sepharose (Amersham). <sup>35</sup>S-Mud-C was produced by using an in vitro transcription and translation kit (Promega). Binding assays were performed using glutathione sepharose (Amersham) in binding buffer (50 mM HEPES [pH 7.5], 150 mM NaCl, 5 mM MgCl<sub>2</sub>, 1 mM DTT, and 0.1 or 0.01% Tween-20) with incubation for 1 hour at 4°C.



### **Microtubule assays**

Microtubule sedimentation assays were performed essentially as described with some modifications. S2 cells transfected with pUAST myc-Mud-C were lysed in extraction buffer (1X PEM, 2.5 mM MgSO<sub>4</sub>, 1 mM PMSF, 1 mM DTT, and Complete EDTA-free protease inhibitors [Roche]). The lysate was incubated on ice for 10 min, spun at 20 000 g at 4°C for 30 min to remove cell debris, and then spun at 140 000 g at 4°C for 30 min to yield a supernatant of soluble proteins. A final concentration of 20 µM of taxol (Paclitaxel, Sigma) and 1mM GTP was added before incubation at room temperature for 30 min to polymerize microtubules. The microtubules and associated proteins were pelleted by room temperature centrifugation at 80 000 g for 30 min, through a 30% sucrose cushion in extraction buffer supplemented with 20 µM taxol and 1 mM GTP. The microtubule fraction was collected in 1/10<sup>th</sup> the volume of the cushion and soluble protein fractions. Solution microtubule assays were performed as described .

**Figure1: Evolutionary conservation of NuMA.**

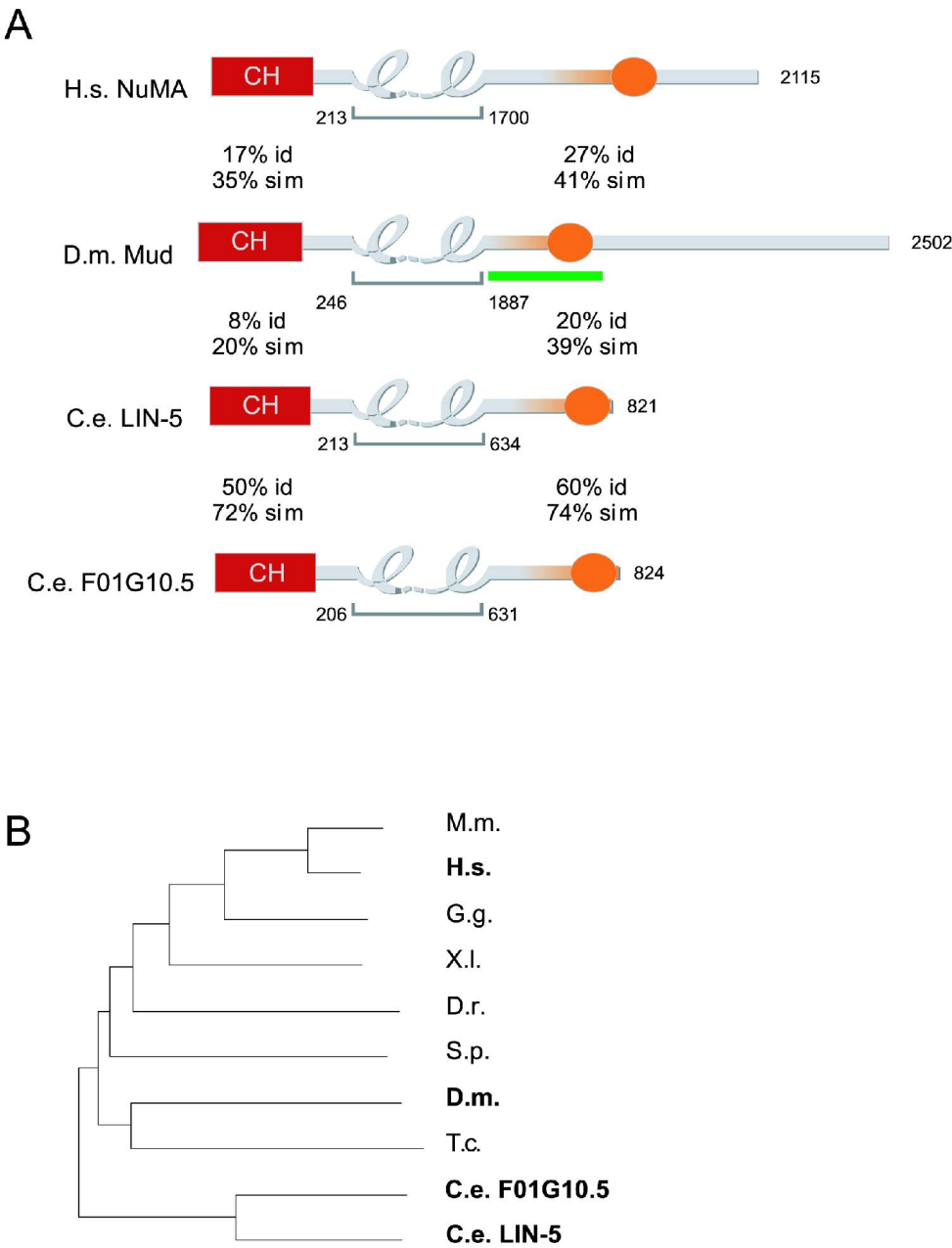


### **Figure 1: Evolutionary conservation of NuMA.**

(A) The molecular architecture of the NuMA sequence homologs in human (H.s.), fly (D.m.) and worm (C.e.). Red boxes: CH domain. Loops: coiled-coil segment, with length indicated by numbers near the underlying brackets. Orange ellipses: highly conserved C-terminal motif involved in Pins and microtubule binding. Shaded orange: graded similarity extending from ellipse region. Green bar: fragment of Mud cloned for Mud-C constructs. Percentage of sequence identity (% id) as well as sequence similarity (% sim) are indicated for the N-terminal CH domain and the C-terminal conserved motif. (B) Phylogenetic analysis of NuMA homologs. Neighbor joining tree based on a multiple sequence alignment of the N-terminal CH domain of the two worm (C.e.) paralogs LIN-5 and F01G10.05, and the candidate NuMA orthologs in human (H.s.), mouse (M.m.), chicken (G.g.), frog (X.l.), zebrafish (D.r.), sea urchin (S.p.), fly (D.m.) and beetle (T.c.). Analysis performed using PHYLIP.

**Figure 2: Mud is in a complex with Pins and G $\alpha$ i.**

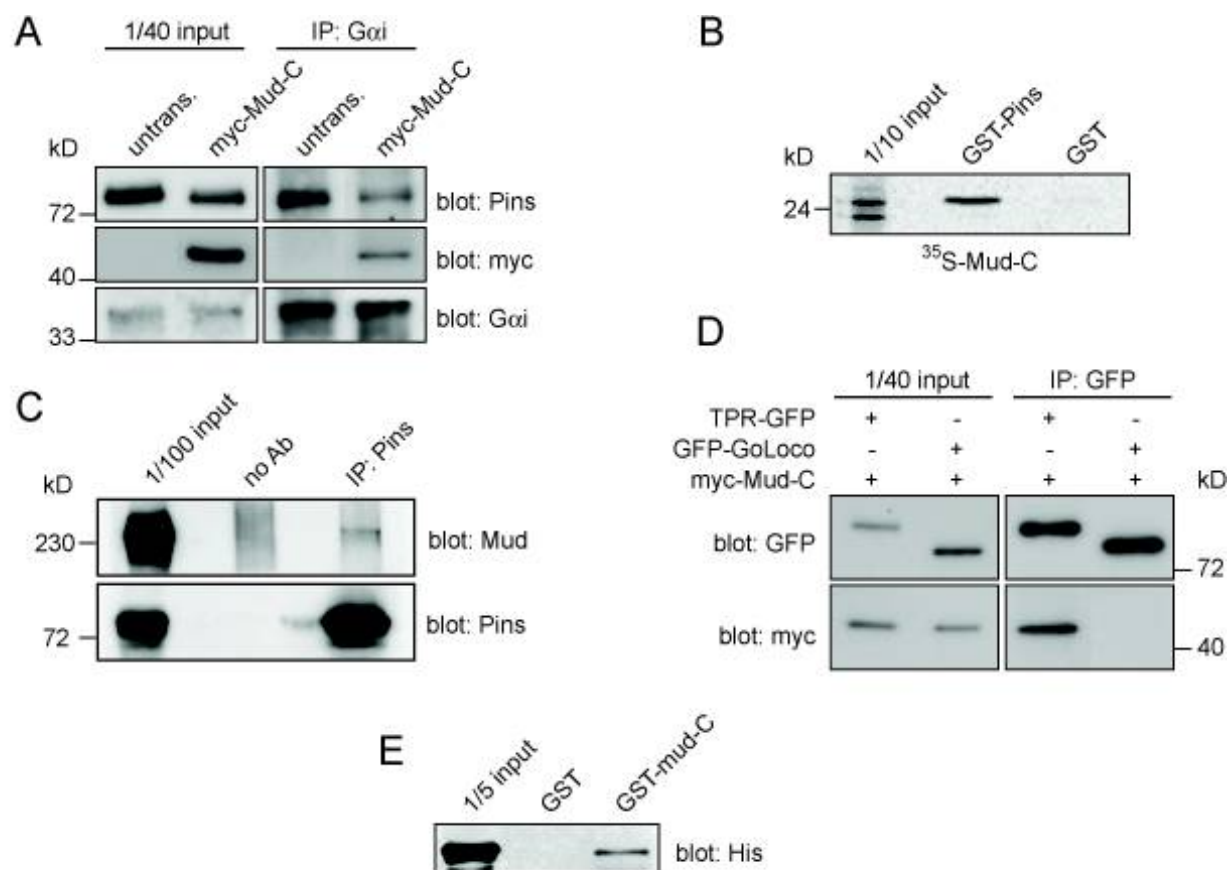


**Figure 2: Mud is in a complex with Pins and G $\alpha$ i.**

(A) Protein extracts (input) and immunoprecipitations (IPs) using anti G $\alpha$ i antibody from untransfected *Drosophila* S2 cells or cells transfected with Myc-Mud-C. Myc-Mud-C and Pins co-precipitate with G $\alpha$ i. (B) GST-Pins coupled to glutathione sepharose beads can co-precipitate Mud-C, which was in vitro translated in the presence of <sup>35</sup>S-methionine. (C) IP using anti Pins antibody from embryo extract. Mud co-precipitates with Pins. (D) IPs using anti GFP antibody from S2 cells transfected with Myc-Mud-C and either Pins-TPR-GFP or GFP-Pins-GoLoco. Myc-Mud-C coprecipitates with Pins-TPR-GFP, but not GFP-Pins-GoLoco. (E) GST-Mud-C coupled to glutathione sepharose beads co-precipitates His-tagged human Pins-TPR.

**Figure 3: Mud associates with microtubules.**

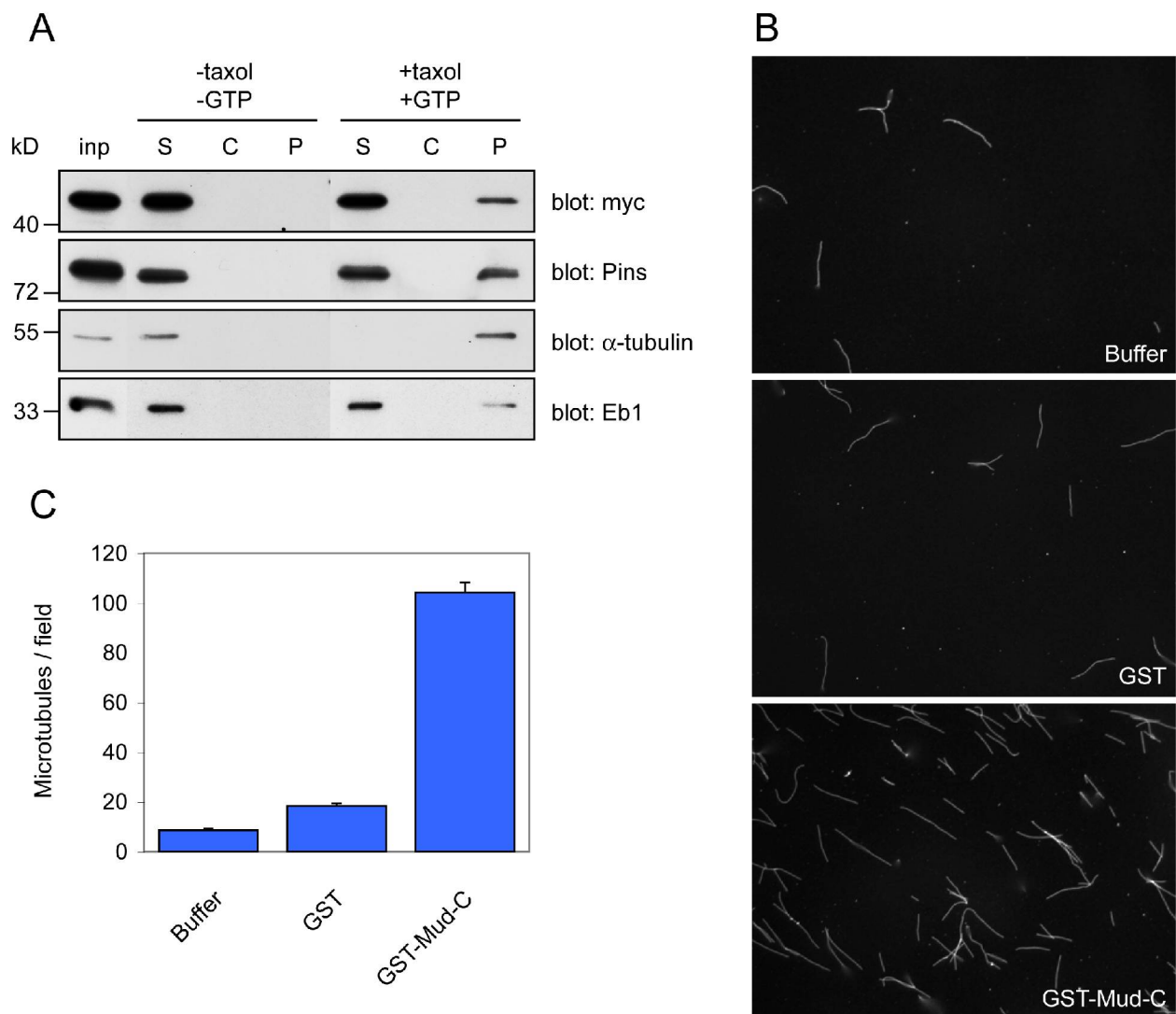


**Figure 3: Mud associates with microtubules.**

(A) Microtubule sedimentation assay. Immunoblots of fractions from supernatant, S, cushion, C, and pellet, P. S2 cells were transfected with Myc-Mud-C, lysed, and incubated on ice to depolymerize microtubules. High speed supernatant from the lysate (input) was incubated in the presence or absence of taxol and GTP, then subjected to centrifugation through a sucrose cushion. With addition of taxol and GTP, microtubules and associated proteins separate into a pellet. The pellet contains  $\alpha$ -tubulin, Eb1, Pins, and Myc-Mud-C. (B) Representative fields from a solution microtubule formation assay. (C) Quantification of solution microtubule formation assays. Microtubules in ten microscope fields were counted, and the average number of microtubules per field is plotted. Error bar is standard error of the mean.

**Figure 4: Spindle orientation defects in *mud* mutant neuroblasts.**

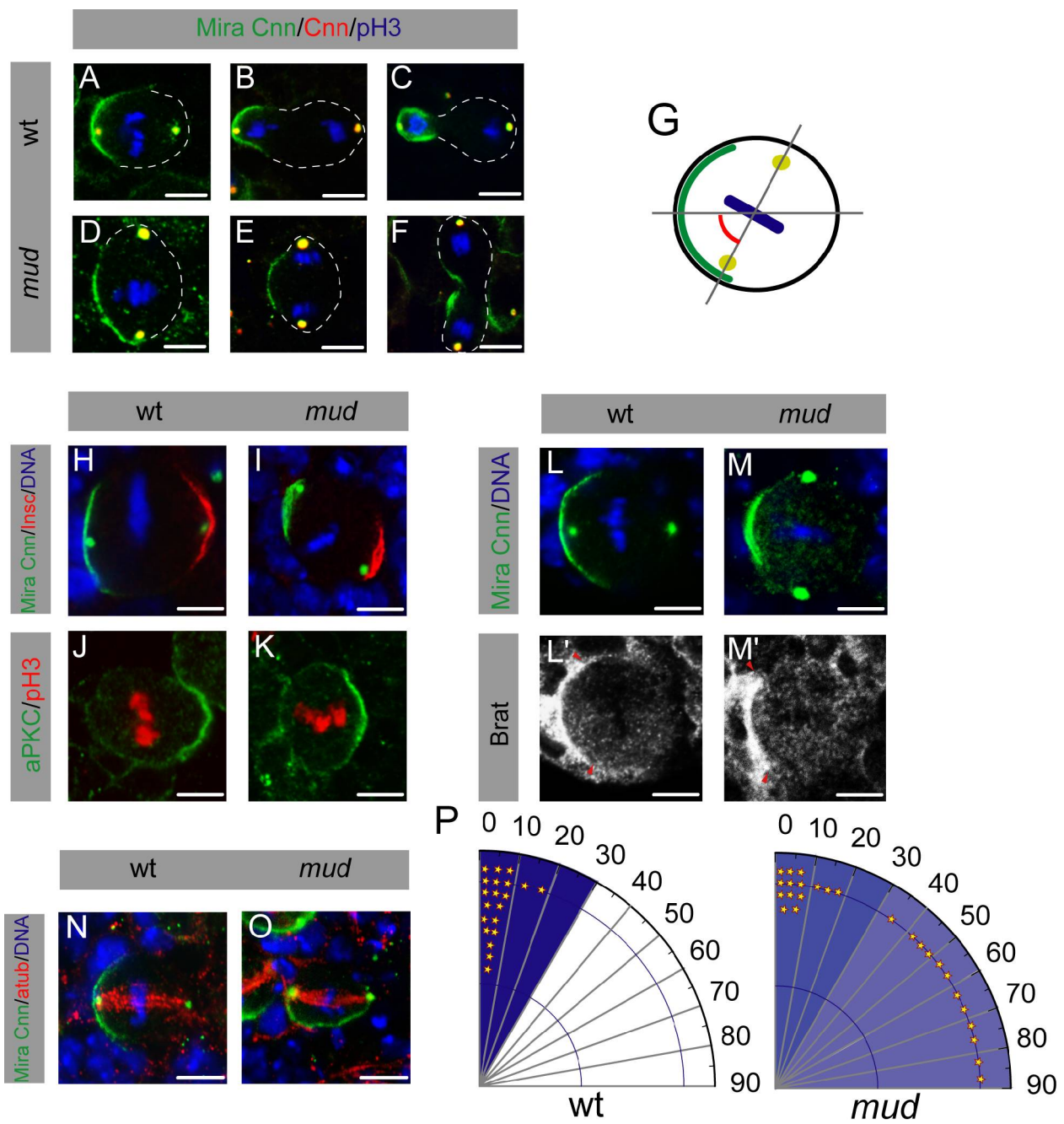




**Figure 4: Spindle orientation defects in *mud* mutant neuroblasts.**

(A-C) Wild type third instar mushroom body neuroblasts, stained with Miranda (green), Centrosomin (red), and phospho-Histone 3 (blue) have Miranda crescents tightly aligned with centrosomes at metaphase (A). From anaphase (B) through telophase (C), Miranda segregates into a single small daughter cell. (D-F) Miranda crescents in *mud* mutant neuroblasts are mispositioned relative to the centrosomes at metaphase (D). Symmetric distribution of Miranda begins starting in anaphase (E) and occurs in 4% of the observed telophase neuroblasts. Note the equal size of these daughter cells (F). Mushroom body neuroblasts were identified using OK107-GAL4-driven expression of CD8-GFP. (G) Schematic for measurement of spindle orientation. (H-K) Apico-basal neuroblast polarity is unaffected in *mud* mutants. Like wild type neuroblasts (H, J), *mud* mutant neuroblasts generate opposing crescents of Inscuteable (red) and Miranda (green) (I), as well as crescents of aPKC (green) in metaphase (K). (L, M) The cell fate determinant Brat forms crescents that are not coordinated with the spindle in *mud* mutants. (N, O) Mitotic spindles show no gross morphological defects in *mud* mutant neuroblasts. (P) Quantification of spindle orientation. Plot generated from a random sample of angles from wild type or *mud* mutant neuroblasts measured as depicted in G. Scale bars: 5 microns (A-O).

**Figure 5: Mud localization in neuroblasts.**

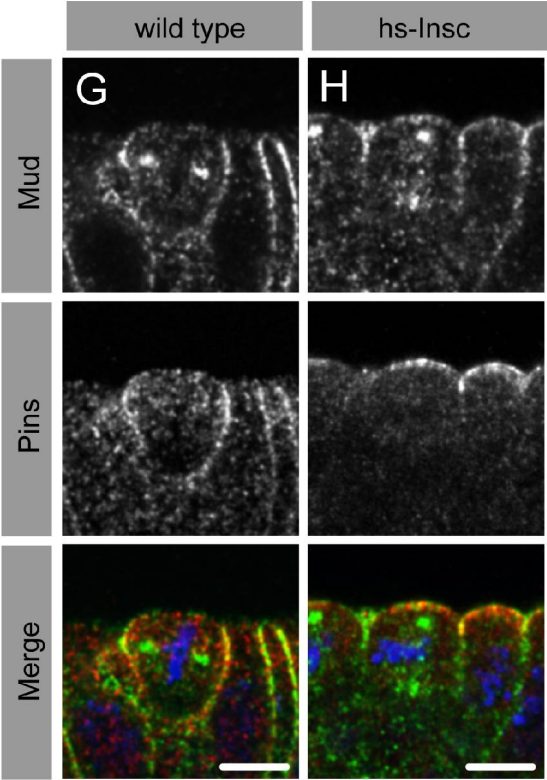
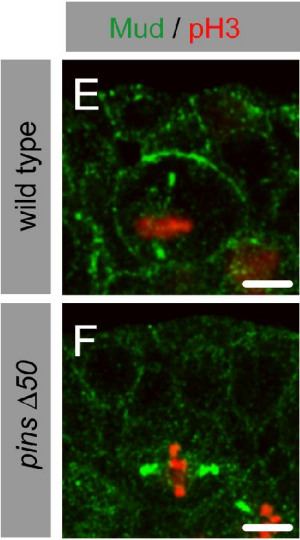
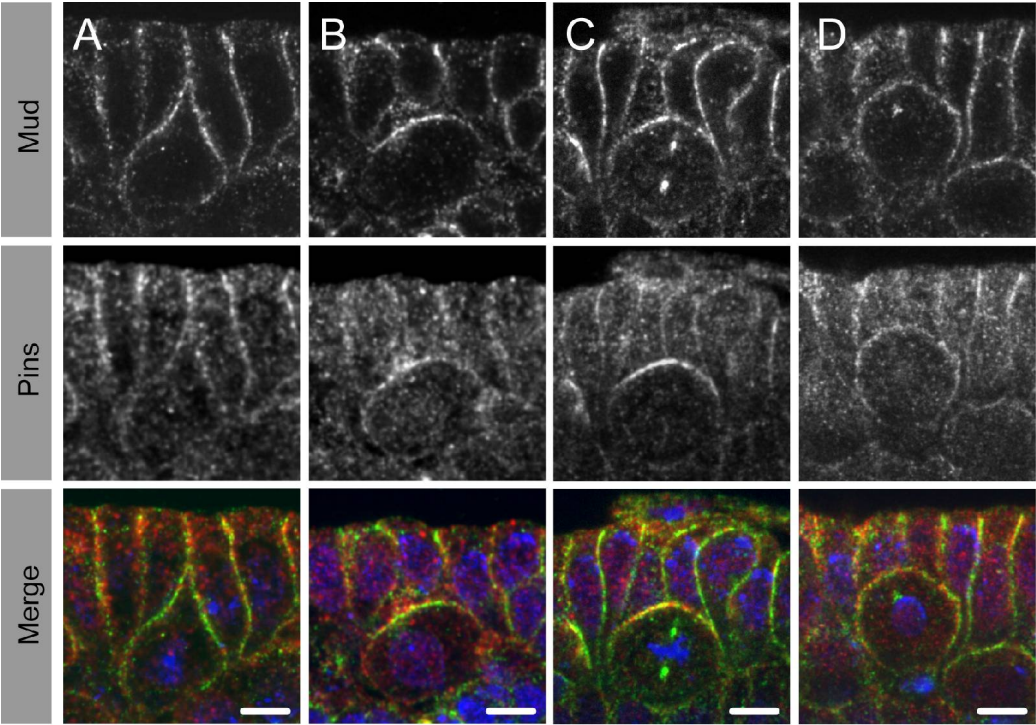


**Figure 5: Mud localization in neuroblasts.**

(A-D) Embryonic neuroblasts stained for Mud (green) and Pins (red). Mud and Pins concentrate apically beginning at delamination (A). Colocalization and apical enrichment is maintained through interphase (B) and metaphase (C), when Mud decorates the spindle poles. Mud is inherited by the neuroblast in telophase (D). (E, F) The enrichment of Mud on the apical cortex of wild type neuroblasts (E) is lost in *pins* mutants (F). (G, H) Mud (green) and Pins (red) localize basolaterally in wild type epithelial cells (G). In the presence of Inscuteable, Pins and Mud relocate apically (H). Scale bars: 5 microns (A-H).

Figure 6: Overproliferation in *mud* mutant brains.

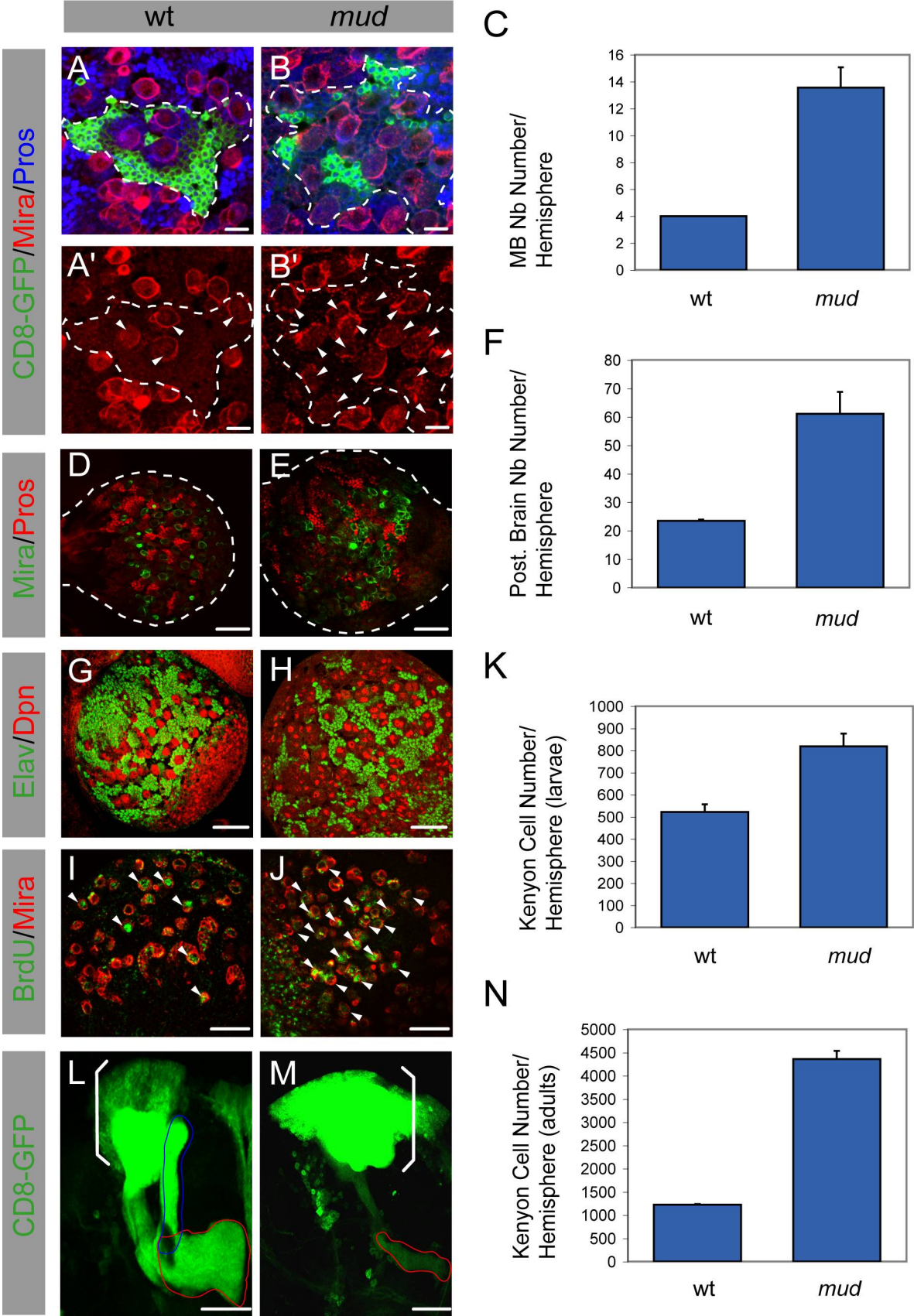


**Figure 6: Overproliferation in *mud* mutant brains.**

(A, B) Excess mushroom body neuroblasts in *mud* mutants. OK107-GAL4-dependent CD8-GFP expression marks the mushroom body lineage (outline). In wild type, four large mushroom body neuroblasts (arrowheads in A), that express Miranda (red), weakly express CD8 GFP (green), and do not express Prospero (blue) are in a cluster of Kenyon cells that express high levels of CD8-GFP. *mud* mutant Kenyon cells (B) do not cluster on the surface as in wild type (A). The number of mushroom body neuroblasts >10 microns in diameter is increased in *mud* mutant larvae. (C) Quantification of mean mushroom body neuroblast number. (D, E) Excess neuroblasts in posterior brain hemisphere of *mud* mutants. Miranda (green) positive, Prospero (red) negative neuroblasts >10 microns in diameter are overrepresented in *mud* mutant brains (E) compared to wild type control (D). Note strong overall Miranda expression and increased brain size in *mud* mutants. (F) Quantification of mean neuroblast number in the posterior brain hemisphere of third instar larvae. (G, H) Excess neuroblasts in *mud* mutants express the neuroblast marker Deadpan. (I, J) The number of neuroblasts incorporating BrdU is increased in *mud* mutant brains. (L, M) Mushroom body morphology in adult *mud* mutant escapers is defective. Green: OK107-GAL4-driven CD8-GFP. The Kenyon cell and calyx region (bracket), dorsal axonal projections ( $\beta$  and  $\beta$  lobes, blue outline) and medial axonal projections ( $\alpha$ ,  $\alpha$ , and  $\gamma$  lobes, red outline) are visible in wild type brains (L). In *mud* mutants (M), the Kenyon cell and calyx region is larger (bracket), and only the medially projecting  $\gamma$  lobe (red outline) is present. (N) Quantification of mean Kenyon cell number in adult brains. Error bars are standard error of the mean. Scale bars are 10 microns (A, B) or 50 microns (D, E, G, H, I, J, L, M).

**Figure 7: A model for Mud function in asymmetric cell division.**

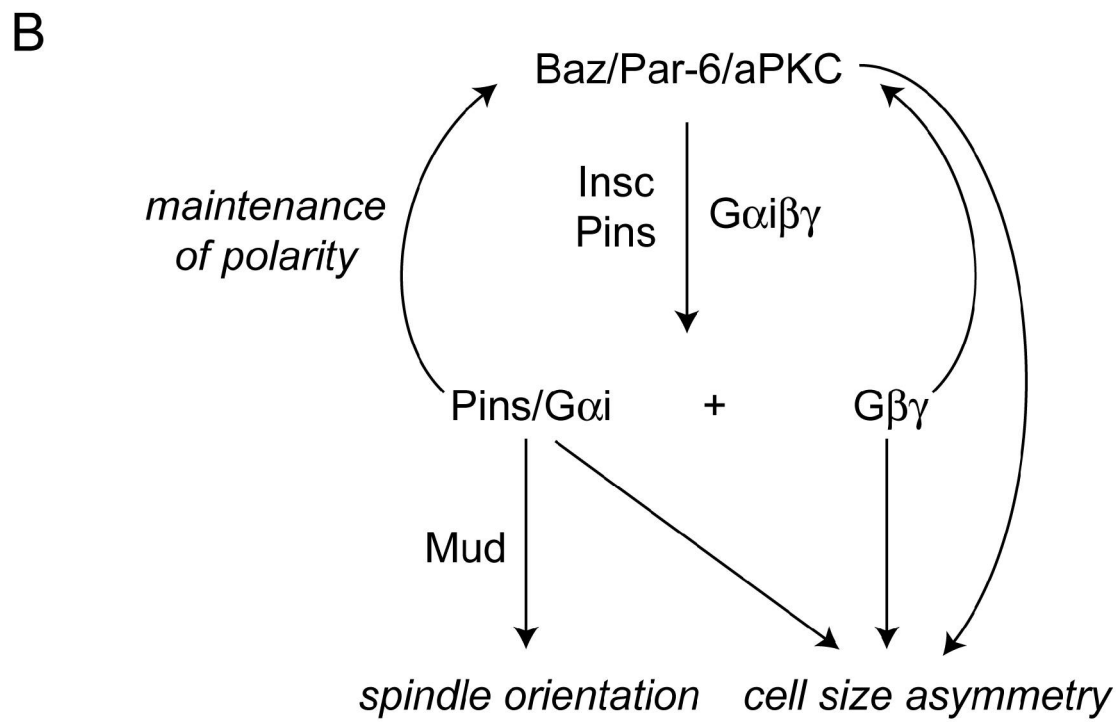
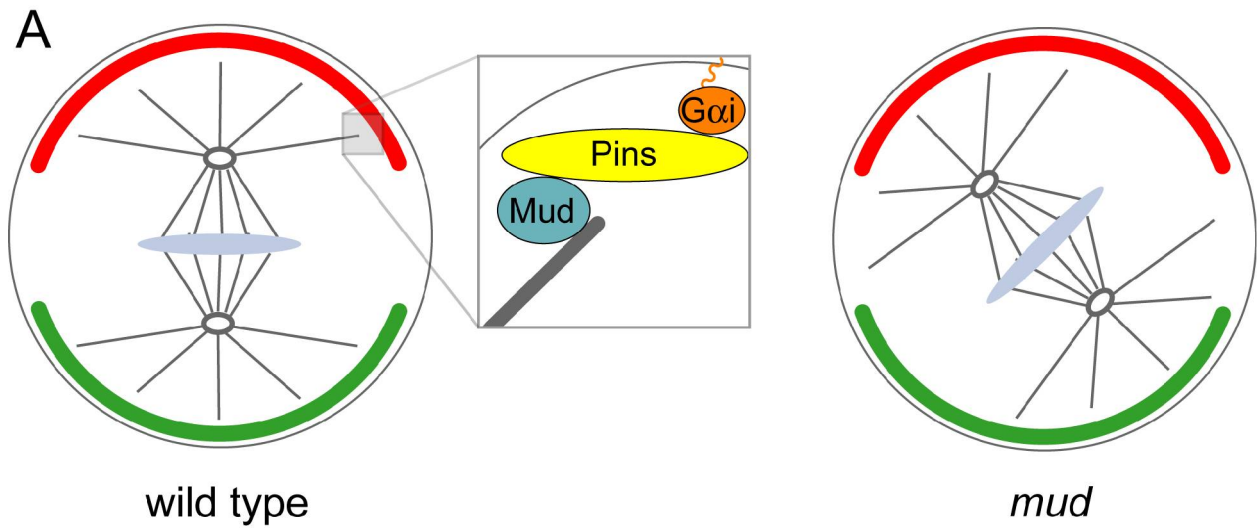


**Figure 7: A model for Mud function in asymmetric cell division.**

(A) Mud (blue) links Pins (yellow) and G $\alpha$ i (orange) to the astral microtubules of the mitotic spindle. The spindle is misoriented in *mud* mutants, but the polarity of Inscuteable (red) and Miranda (green) is unaffected. (B) Pins and heterotrimeric G proteins regulate spindle orientation, cell size asymmetry, and the apical localization of Inscuteable and the Par complex. Mud is required for spindle orientation but not for the other functions.



**Figure 8: Multiple Sequence Alignment of the Conserved N- and C- Terminal Segments of the Homologous NuMA, Mud and Lin-5 Proteins.**

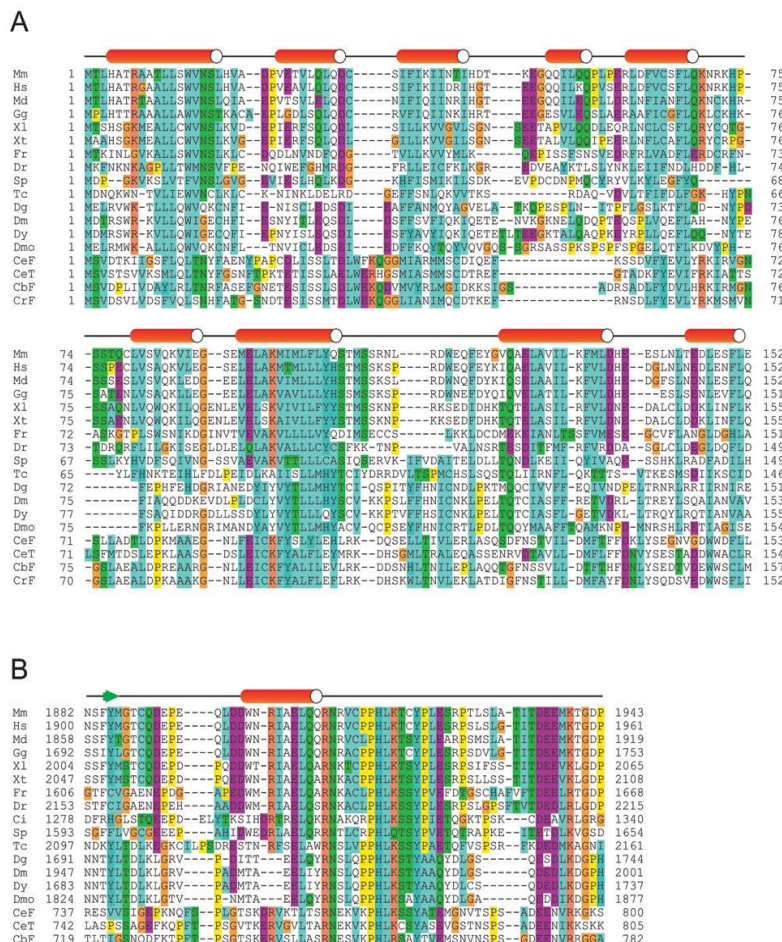


**Figure 8: Multiple Sequence Alignment of the Conserved N- and C- Terminal Segments of the Homologous NuMA, Mud and Lin-5 Proteins.**



**Figure 9: Western Blots Showing Protein Expression in Wild-Type and *mud* Mutant Brain Extracts.**

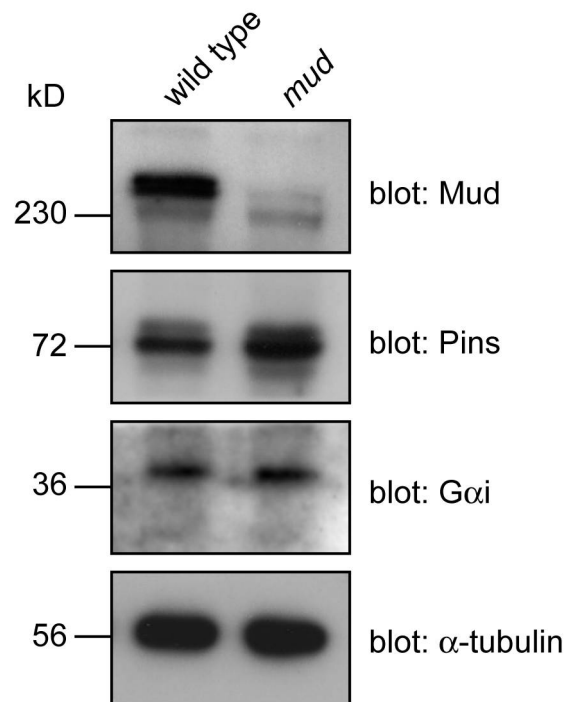


**Figure 9. Wester Blots Showing Protein Expression in Wild-Type and *mud* Mutant Brain Extracts.**

**Figure 10: *pins* Interacts genetically with *mud*.**

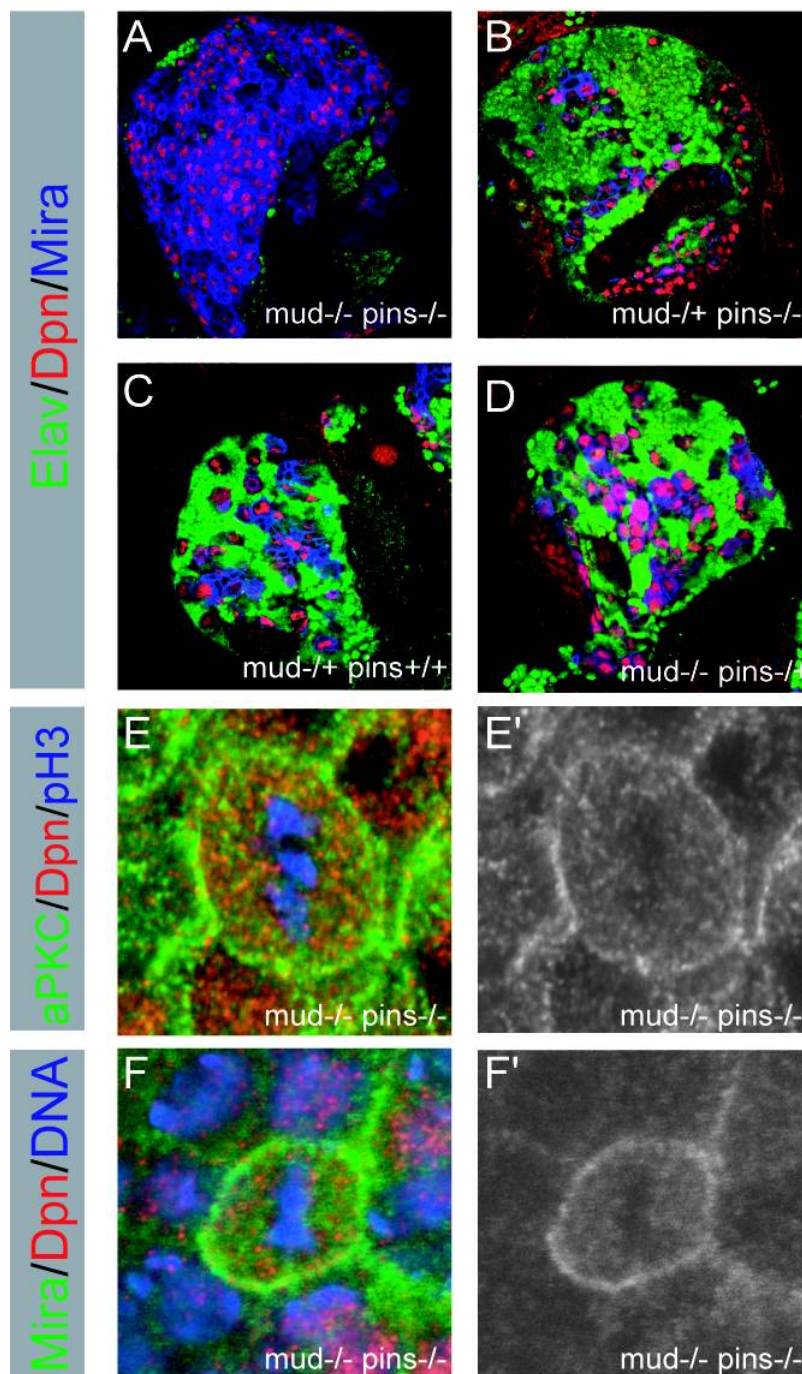


**Figure 10. *pins* Interacts genetically with *mud***

Removal of *pins* in a *mud* mutant background leads to massive overproduction on neuroblasts marked by deadpan (A-D). aPKC and Miranda are delocalized in *pins*, *mud* neuroblasts (E, F).

## **2. Part II: Mei-P26 regulates micro RNAs and cell growth in the *Drosophila* ovarian stem cell lineage**

*Drosophila* neuroblasts <sup>1</sup> and ovarian stem cells <sup>85,86</sup> are well characterized models for stem cell biology. In both cell types, one daughter cell self-renews continuously while the other undergoes a limited number of divisions, stops to proliferate mitotically and differentiates. While neuroblasts segregate the Trim-NHL protein Brat into one of the two daughter cells <sup>66,67,72</sup>, ovarian stem cells are regulated by an extracellular signal from the surrounding stem cell niche. After division, one daughter cell loses niche contact. It undergoes four transit amplifying divisions to form a cyst of 16 interconnected cells which reduce their rate of growth and stop to proliferate mitotically. Here we show that the Trim-NHL protein Mei-P26 <sup>77,78</sup> restricts growth and proliferation in the ovarian stem cell lineage. Mei-P26 expression is low in stem cells but strongly induced in 16 cell cysts. In *mei-P26* mutants transit amplifying cells are larger and proliferate indefinitely leading to the formation of an ovarian tumor. Like *brat*, *mei-P26* regulates nucleolar size and can induce differentiation in *Drosophila* neuroblasts, suggesting that these genes act through the same pathway. We identify Argonaute-1, a component of the RISC complex, as a common binding partner of Brat and Mei-P26 and show that Mei-P26 acts by inhibiting the micro-RNA pathway. Mei-P26 and Brat have a similar domain composition that is also found in other tumor suppressors and might be a defining property of a new family of micro RNA regulators that act specifically in stem cell lineages.

When *Drosophila* germline stem cell divide (Fig. 1a), one daughter cell (the cystoblast) loses niche contact and undergoes four transit-amplifying divisions to create a cyst of 16 cystocytes, which remain connected by the fusome. In each cyst, one cell becomes the oocyte, while the other cells undergo endoreplication to form 15 so-called nurse cells.

Since *brat*<sup>192</sup> mutant germline clones do not show any obvious defects in oogenesis (data not shown), we analyzed the ovarian phenotype of *mei-P26*. Like Brat, Mei-P26 is a TRIM-NHL protein<sup>87</sup> and carries an NHL domain, a coiled coil region and several B-boxes. Weak *mei-P26* mutants have defects in meiosis<sup>78</sup> while stronger alleles cause tumorous overproliferation<sup>77</sup>. *mei-P26* mutant ovaries were stained using the monoclonal antibody mAb1B1<sup>50</sup> which labels the fusome and the spectrosome, a cytoplasmic organelle only present in stem cells and cystoblasts<sup>88</sup> (Fig. 1b-f). Wild type ovaries contain two stem cells near the tip of the germarium while cystoblasts and cysts are separated from the stem cell niche (Fig. 1b). In *mei-P26* mutant ovaries, germaria are filled with individual spectrosome containing cells (19%) and cysts containing varying numbers of cells (<4 in 39%, >4 in 42%, n> 400 cells) connected by a fusome (Fig. 1c,d, Fig. 2a,a'). Nurse cells and oocytes are not formed and fusomes or spectrosomes are maintained at later stages of oogenesis (Fig. 1e,f). In wild type ovaries, the S-phase marker Cyclin E oscillates with the cell cycle in stem cells and mitotically active cysts, is down regulated as cystocytes exit mitotic proliferation and is re-expressed as nurse cells enter endoreplication<sup>52</sup> (Fig. 1g). In *mei-P26* mutant ovaries, however, Cyclin E is highly expressed at all stages of oogenesis (Fig. 1h). Upregulation of Cyclin E occurs even in small *mei-P26* clones (Fig. 2b,c), and is therefore not an indirect consequence of tumor formation. Phospho-Histone H3 (pH3) positive mitotic germline cells are restricted to the anterior tip of the germarium in wild type ovaries (Fig. 1i) but are detected throughout the ovarioles in *mei-P26* mutants (Fig. 1j, Fig. 2a,a'). While all cells in a wild type cyst divide synchronously, *mei-P26* mutant cysts frequently contain both mitotic and interphase cells (data not shown). Thus, *mei-P26* is required for proliferation control and differentiation in the female germline stem cell lineage.

To test stem cell niche signaling, we used a GFP fusion to the *bam* promoter<sup>35</sup>, which is suppressed by Dpp from the niche in stem cells but not in cystocytes (Fig. 1k, Fig. 2d). In *mei-*

*P26* mutants (Fig. 1l, Fig. 2e), *bam* transcription is repressed in niche-contacting cells but upregulated in cystocytes. Since staining for the niche marker Armadillo (Fig. 1m,n) reveals no structural abnormalities and ovarian tumors are also observed when *mei-P26* is removed exclusively from the female germline (Fig. 2f,g), *mei-P26* is not required for sending or receiving the niche signal.

*mei-P26* mutant tumor cells have branched fusomes and express Bam. To further confirm that these cells do not have stem cell identity, we analyzed the expression of Orb. Orb expression starts in all cystocytes between the 8 and 16 cell stage<sup>89</sup> but is restricted to the oocyte during later stages (Fig. 1o). In *mei-P26* mutants, Orb expression is initiated normally (Fig. 1p) and is detected throughout the tumor. However, Orb is never restricted to a single cell suggesting that the oocyte is not specified. Thus, *mei-P26* mutants develop a 'cystocytoma' in which tumor cells express markers for the cystocyte fate. Single spectroscopy containing cells in the tumor might arise from occasional disintegration of fusome-connected cysts, a process that has been described before<sup>58</sup>.

Brat can inhibit cell growth and ribosome biogenesis<sup>68</sup>. *mei-P26* might also regulate cell growth since overexpression from the *eyeless* promoter reduces eye size (Fig. 4a,b), even when cell death is inhibited by co-expressing *p35* (data not shown). To test whether cell growth is differentially regulated in the ovarian stem cell lineage, we quantified the volume of stem cells and cysts after 3D reconstruction (see suppl. methods). Shortly after stem cell division (elongated spectroscopy morphology), stem cells are  $314 \pm 13$  (s.e.m.)  $\mu\text{m}^3$  (n=4) while cystoblasts are  $330 \pm 30 \mu\text{m}^3$  (n=4). Stem cells grow to a maximum of  $600 \mu\text{m}^3$  (average  $437 \pm 21 \mu\text{m}^3$  (n = 19)) and double their volume between each mitotic division (about once per day). To measure cyst volumes mitotic clones were marked by the absence of GFP (Fig. 3a). 3 and 4 day old 16-cell cysts are  $1215 \pm 61 \mu\text{m}^3$  (n=7) and  $1163 \pm 48 \mu\text{m}^3$  (n=7), respectively. Thus, cell growth slows down significantly as cells exit mitotic proliferation. Consistent with this, cystocytes become progressively smaller during transit amplifying divisions (Fig. 3g). dMyc, an important regulator of cell growth, is highly expressed in stem cells and cystoblasts but down regulated in 16-cell

cysts (Fig. 3e). Nucleoli (stained by anti-Fibrillarin), the sites of ribosomal RNA transcription, are large in stem cells but much smaller in 16 cell cysts (Fig. 3c, Fig. 4c). Since ribosome number is thought to control cellular growth in *Drosophila*<sup>90,91</sup>, a reduction in ribosome biogenesis might be responsible for the reduced cell growth at the end of mitotic proliferation.

In *mei-P26* mutants, cellular and nucleolar size are significantly increased and dMyc is highly expressed throughout the tumor (Fig. 3d,f,g, Fig. 4c): The volume of 16 cell cysts is increased to  $3956 \pm 424 \mu\text{m}^3$  (n=4) (Fig. 3b) and cell diameters no longer decrease as cells are displaced from the stem cell niche (Fig. 3g). Thus, *mei-P26* is responsible for the differential regulation of cell growth in the *Drosophila* ovarian stem cell lineage. Like *brat*, it might achieve its function by regulating ribosome biogenesis and controlling the expression of dMyc.

To analyze Mei-P26 expression, we generated a specific antibody (Fig. 4d,e,f). Mei-P26 mRNA and protein levels are low in stem cells but are upregulated in cysts as they decrease growth and exit mitotic proliferation (Fig. 3h,j, Fig. 4e,g,h). This regulation is functionally important since *mei-P26* overexpression in ovaries results in stem cell loss and complete depletion of the female germline (Fig. 5a,b). In *bam* mutant ovaries, Mei-P26 levels remain low suggesting that *mei-P26* is regulated in a Bam-dependent manner (Fig. 3i). *bam* overexpression induces premature differentiation of stem cells in a wild type (Fig. 5d) but not in a *mei-P26* mutant background (Fig. 5e) demonstrating that Mei-P26 is essential for Bam to induce cystocyte differentiation. Consistently, germline stem cells do not differentiate when *pumilio* is removed in a *mei-P26* mutant background (Fig. 4k,l). To test whether Mei-P26 is the only target of Bam, we overexpressed *mei-P26* in a *bam* mutant background (Fig. 5f,g, Fig. 4i,j). *mei-P26* overexpression reduces the size of *bam* mutant cells and the enlarged nucleolus in *bam* mutants (Fig. 4c) but does not rescue the differentiation defects (Fig. 4i,j) observed in these mutants. Thus, *mei-P26* is upregulated by Bam activity in cystocytes and inhibits cell growth and mitotic proliferation.

In the brain, *mei-P26* is weakly expressed in neuroblasts, absent from ganglion mother cells but highly expressed in neurons (Fig. 6a-d). Although *mei-P26* mutants have no obvious defects in neurogenesis, *mei-P26* overexpression can induce premature neuronal differentiation (Fig. 6e,f)

suggesting that *mei-P26* and *brat* might have some common targets. Using mass-spectrometry we identified the RNase Argonaute-1 (Ago1) in anti-Brat immunoprecipitates (Fig. 7a). Brat and Ago1 can be co-immunoprecipitated from *Drosophila* embryos (Fig. 5h) and co-transfection experiments in S2 cells show that Ago1 also binds Mei-P26 and the TRIM-NHL protein Dappled (Fig. 7b). This interaction is functionally significant since Mei-P26 lacking the NHL domain no longer binds Ago1 (Fig. 5i) and fails to block self renewal when overexpressed in ovarian stem cells (Fig. 5c).

Ago1 is a core component of the RISC complex<sup>92</sup> and is important for micro-RNA mediated translational repression and RNA degradation. Micro-RNAs are essential for self renewal in *Drosophila* ovarian stem cells since mutations in *ago-1* (Fig. 8), *dicer-1*<sup>47</sup> or its binding partner *loquacious*<sup>46</sup> result in premature stem cell differentiation. To test whether Mei-P26 regulates micro-RNAs, we measured micro-RNA levels by quantitative RT-PCR. In *mei-P26* mutants most micro-RNAs are significantly upregulated (Fig. 10a,b), while overexpression of *mei-P26* in *bam* mutants broadly reduces micro-RNA levels (Fig. 9a, Fig. 10a). Importantly, the *mei-P26* mutant phenotype can be partially rescued by removing one copy of *loquacious* and thereby reducing micro-RNA levels (Fig. 9b,c, Fig 11a-f) indicating that *mei-P26* acts by inhibiting the micro-RNA pathway in cystocytes.

One of the best characterized *Drosophila* micro-RNAs is *bantam*, a regulator of proliferation and apoptosis<sup>93</sup>. We used a sensor that expresses GFP from the *tubulin* promotor and carries two *bantam* binding sites in the 3' UTR<sup>93</sup>. In wild type ovaries, this sensor is repressed by *bantam* activity in stem cells but derepressed in cystocytes where high levels of Mei-P26 are present (Fig. 9e). In *mei-P26* mutants the sensor is off in all germline cells (Fig. 9g). In contrast, a control sensor lacking micro-RNA binding sites shows high expression in all wild type and mutant cells (Fig. 9d,f). Although *mei-P26* regulates many micro-RNAs, *bantam* seems to be an important target: Even animals heterozygous for a *bantam* null mutation have a reduced number of stem cells ( $1.15 \pm 0.12$  per germarium (n= 32 germaria) compared to  $2.09 \pm 0.05$  (n= 32 germaria) in 14 days old *bantam* heterozygous and wild type flies respectively), suggesting a defect in self-renewal (Fig. 10e,f). To test whether *mei-P26* regulates *bantam* directly, we expressed a luciferase

construct carrying a *bantam* binding site in its 3' UTR in S2 cells. In control cells, the bantam sensor but not a construct lacking the binding site (Fig. 10d) is repressed. Upon cotransfection of *mei-P26* but not *mei-P26* lacking the NHL domain (Fig. 10c) luciferase expression is significantly derepressed indicating that Mei-P26 can repress bantam activity even in S2 cells.

Our data suggest that *brat* and *mei-P26* might act in a similar manner to control proliferation in stem cell lineages. In both mutants, cells that normally stop self renewal increase ribosome biogenesis, grow abnormally large and fail to exit the cell cycle leading to the formation of a tumor. The general upregulation of micro-RNAs in *mei-P26* mutants leaves several possibilities for how these proteins might regulate the micro-RNA pathway. The presence of a RING finger in Mei-P26 suggests a role in protein degradation. The high amounts of Ago1 detected in Mei-P26 immunoprecipitates make it unlikely that Ago1 itself is degraded by Mei-P26. However, another member of the RISC complex might be a degradation target of Mei-P26. Equally likely, Mei-P26 could prevent the incorporation or increase the turnover of micro-RNAs in the RISC complex.

Many human tumors contain cancer stem cells that drive tumor growth and metastasis <sup>3,94</sup>. Although the similarities between *Drosophila* tumors and human cancer are limited, *brat* mutant brains and *mei-P26* mutant ovaries (as well as the other mutant conditions causing stem cell tumors <sup>83,95,96</sup>) provide an invertebrate model for stem cell derived tumor formation. In *mei-P26* mutants, tumors originate from cystocytes, the transit amplifying pool of the ovarian stem cell lineage. In *mei-P26* mutants, these cells re-gain the ability to self-renew: After *bam* overexpression - which leads to premature differentiation of stem cells - the germline is depleted in a wild type but not in a *mei-P26* mutant background. Thus, *mei-P26* tumors arise from growth defects in the transit amplifying compartment of the ovarian stem cell lineage - a mechanism that could occur in human tumors as well.

Our data establish TRIM-NHL proteins as regulators of stem cell proliferation. Vertebrate members of this family exist and are down regulated in human cancer cell lines <sup>97</sup> suggesting that their tumor suppressor function might be conserved in vertebrates as well.



## 2.1. Materials and Methods

### Cytology and Immunofluorescence.

Immunofluorescence experiments in larval brains were carried out as described before <sup>67</sup>. Ovaries were dissected in PBS and fixed for 20 min in a 1:1 mixture of n-heptane and PBS containing 5% PFA. After three washes in PBS containing 0.1% Triton X-100, they were treated as described for brains . For in situ hybridisations, DIG-labelled antisense probes were synthesized from the EST GH01646. For clonal analysis, Flp expression was induced by incubating flies at 37°C for 1 hour. *hs-bam* (Fig. 5 **d,e**) was induced by three consecutive 1 hour incubations at 37°C within one day during development. Overexpression of *mei-P26* in the larval brain was carried out with a temperature sensitive gal80 to circumvent embryonic lethality and expression was induced for 60 hours at 29°C. The following antibodies were used: mouse anti-1B1 (7H9, Developmental Studies Hybridoma Bank (DSHB), 1:1), rabbit anti Ago1 (abcam 1:100), mouse anti-Armadillo (N2 7A1, DSHB, 1:100), rabbit anti brat (1:100), mouse anti-CycE (from H. Richardson, 1:10), guinea pig anti-Deadpan (generous gift from J. Skeath, unpublished, 1:1000), mouse anti-Fibrillarin (Abcam, 1:10), mouse anti-GFP (Roche, 1:100), rabbit anti-GFP (Abcam, 1:100), mouse anti-c-myc (1:100, Santa Cruz Biotechnology), rabbit anti-dMyc (from D. Stein 1:5000), rabbit anti-phosphorylated Histone H3 (Upstate Biotechnology, 1:1000), mouse anti-Prospero (DSHB, 1:10), mouse anti- Orb (4H8, DSHB, 1:10), mouse anti alpha- tubulin (Sigma), rabbit anti-Vasa (gift from P. Lasko, 1:10000) and goat anti-Vasa (Santa Cruz, 1:200). Rhodamine conjugated phalloidine (Alexa) was used 1:1000 and rabbit anti-Mei-P26 (1:300) was raised against the peptide NLKTVLSDDASNSSVLED corresponding to aa 23-40. Samples were mounted in Vectashield containing DAPI (Vector Laboratories) and imaged on a Zeiss LSM 500 confocal microscope equipped with a blue diod laser to visualize DAPI. Images were processed in Adobe Photoshop and Adobe Illustrator.

### **Constructs.**

The *mei-P26* full length, *mei-P26ΔNHL*, *ago1*, *dappled* and *brat* coding sequences were PCR amplified from total cDNA or ESTs with appropriate primers containing attB recombination sites (or with primers containing appropriate restriction sites), sequenced and recombined into pDONR221 (Invitrogen) and thereafter recombined into either tagged or untagged pUASp or pUASt destination vectors (DGRC). For fly transformation the final construct was injected into *Drosophila w<sup>1118</sup>* embryos.

Two copies of a sequence complementary to the bantam miRNA were cloned downstream of the firefly luciferase (FLuc) reporter plasmid (bantam sensor). The plasmid expressing *Renilla* luciferase (RLuc) (gift from E. Izaurralde) served as a transfection control.

### **Biochemistry and S2 cell experiments.**

For ovary lysates 20 ovaries from the respective genotypes were dissected in PBS, proteins were extracted with Laemmli- buffer and run on a 10% SDS-page. S2 cell transfections, immunoprecipitations, silverstaining and mass-spectroscopy were performed essentially as described <sup>5</sup>.

For micro-RNA-assays, S2 cells were simultaneously transfected with actin-Gal4, the firefly luciferase micro-RNA reporter construct, the *Renilla* luciferase transfection control construct and pUASp *mei-P26*, pUASp *mei-P26ΔNHL* or the empty pUASp vector as a control. Dual luciferase assays were performed 24 hours after transfection following the manufacturer s instructions (Promega). For each experiment, transfections were performed in triplicates. Three independent experiments showed comparable results, one of which is shown in Fig. 10.

### **Fly strains.**

We used the following *Drosophila* strains: *ago1<sup>k08121</sup>* (gift from T. Uemura), *bantam<sup>Δ1</sup>*, *mei-P26<sup>fs1</sup>*, *mei-P26<sup>mfs1</sup>*, *bam<sup>Δ86</sup>* (Bloomington), *loqs<sup>sf00791</sup>* (Bloomington), *loqs<sup>KO</sup>* (gift from D. McKearin), *nanos-Gal4::VP16* (gift from Frank Schnorrer), *hs-Bam [11d]* (gift from D.

McKearin), *brat*<sup>192</sup>, *FRT18A P[Ubi-GFP.nls]*, *hs-Flp/CyO* (Bloomington), *yw hsFLP; FRT G13 P[2xGFP.nls]*, *UASP-mei-P26* (generous gift from Scott Hawley, unpublished), *P[BamP-GFP]* (gift from D. McKearin), the *Gal4* lines *OK107* (gift from Liquan Luo) and *1407*, *P[tub-Gal80<sup>ts</sup>]* (Bloomington), *Rho1-GFP trap* (ZCL1957, Fly Trap), *pum*<sup>01688</sup> (Bloomington), *pum*<sup>ET3</sup>. All fly strains were raised on standard food without wet or dry yeast.

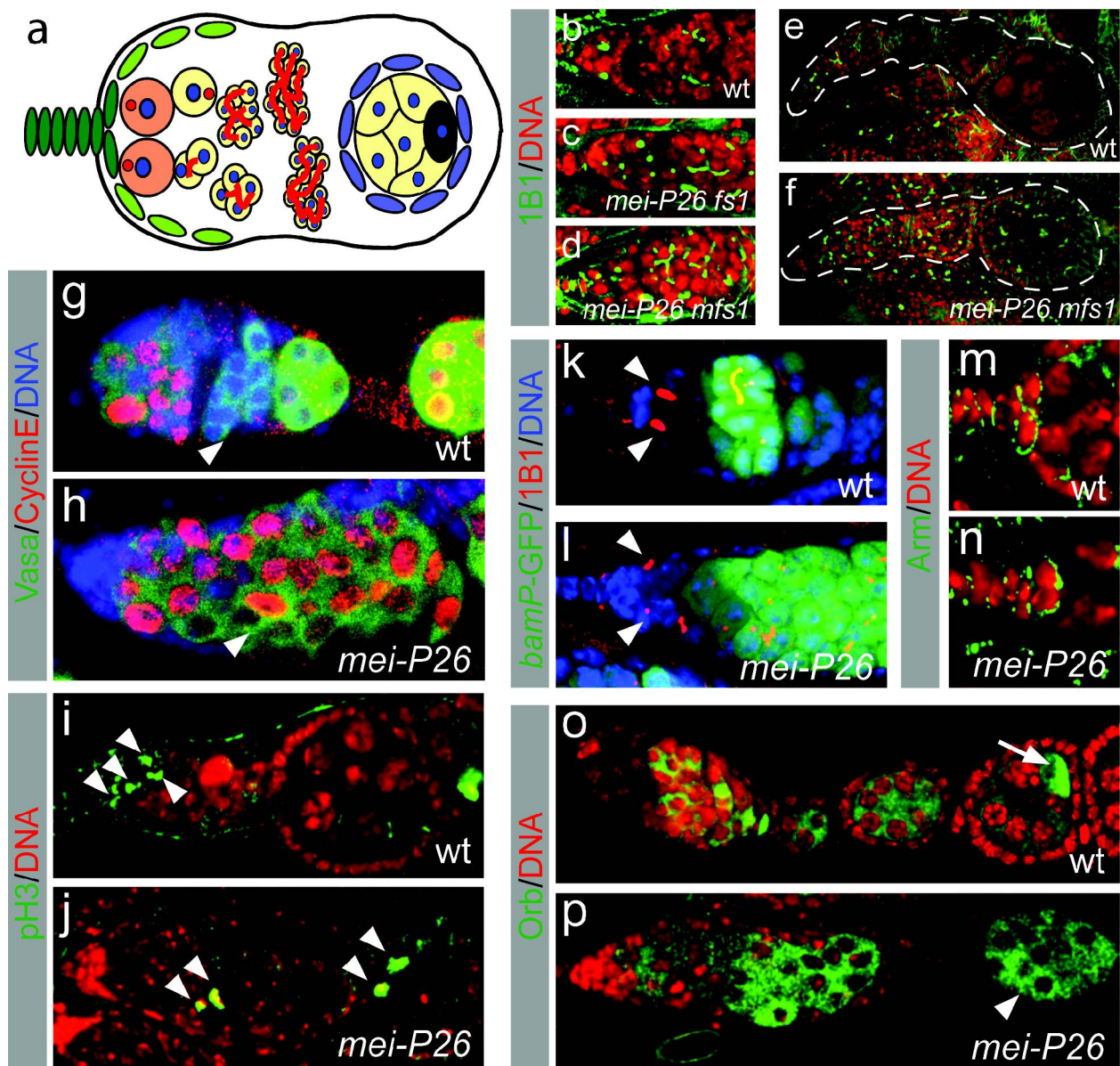
### miRNA Q-PCRs.

Total RNA from ovaries was extracted from the four respective genotypes (*wt*, *mei-P26<sup>mfs1/fs1</sup>*, *bam*<sup>Δ86</sup> and *bam*<sup>Δ86</sup> *nanos-Gal4::VP16 >>pUASp- mei-P26*) using the TRIzol Reagent (Invitrogen). Primer sets designed to amplify mature microRNAs (and sno RNA227 as a control reaction) were obtained from Applied Biosystems. Products were amplified from 10 ng total RNA samples from the respective genotypes with the TaqMan MicroRNA assay using a Quantitative- PCR machine (Applied Biosystems). Wt micro-RNA levels are set to zero in Fig. 10 a.

### Quantification.

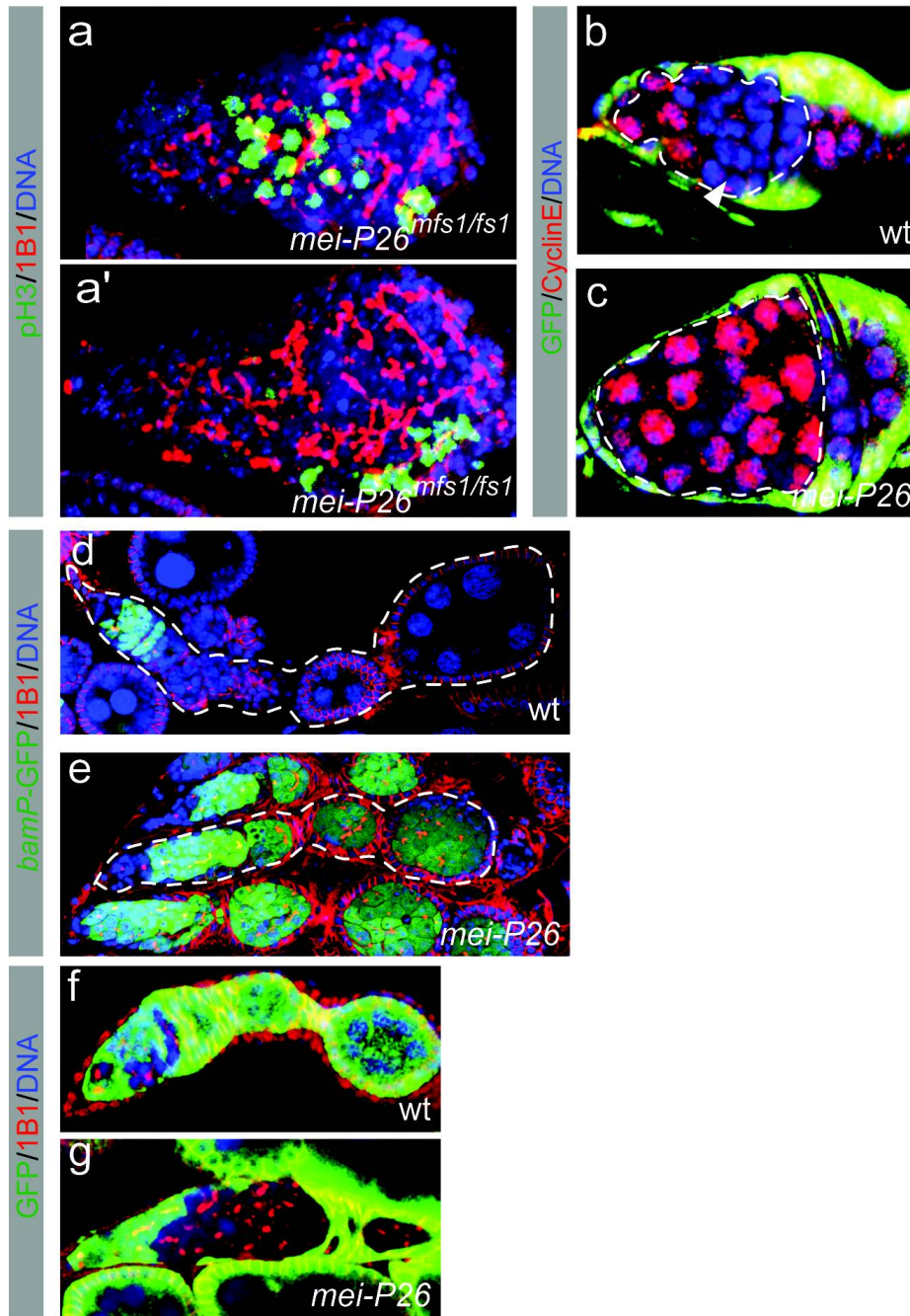
Wt and *mei-P26<sup>mfs1</sup>* flies carrying *P[BamP-GFP]* were stained with mAb1B1 to identify cell types and rhodamine-phalloidine to outline cells. Cell diameters were determined from image stacks of 0.4 μm sections using the measuring tool of LSM software (Zeiss). Cell types were defined as follows: Stem cells: GFP negative, niche contacting single spectrosome containing cells. Cystoblasts: GFP positive single spectrosome containing cells. Cystocytes: 4, 8 or 16 GFP positive cells connected by fusomes. To determine nucleolar : cell size ratio, anti-Fibrillarin and rhodamine phalloidine were used in stainings. For ellipsoid cells, the mean cell diameter was determined (from the longest and shortest cell diameter) and used in the statistics.

**Figure 1: Differentiation and cell cycle defects in *mei-P26* mutant ovaries.**



**Figure 1. Differentiation and cell cycle defects in *mei-P26* mutant ovaries.** (a) Overview of *Drosophila* oogenesis showing cap cells (dark green), escort cells (light green), stem cells (orange), cystoblasts and cystocytes (yellow), follicle cells (blue) and the oocyte (grey). The spectrosome and fusome are red. (b-f) Wild type (wt) (b,e) and *mei-P26* (c,d,f) ovarioles stained with mAb1B1 (green) and for DNA (red). (g,h) Cyclin E (red, green: Vasa, blue: DNA) is downregulated in wt (g, arrowhead) but not in *mei-P26<sup>fs1</sup>* mutant (h, arrowhead) cystocytes. (i,j) Phospho- H3 (green, red: DNA) positive mitotic cells (arrowheads) are restricted to the tip of the ovariole in wild type (i) but found at all stages in *mei-P26<sup>fs1</sup>* ovarioles (j). (k,l) *BamP-GFP* (green, red: mAb1B1, blue: DNA) is not expressed in wt (k) and *mei-P26<sup>fs1</sup>* mutant (l) niche contacting cells (arrowheads). (m,n) Anti-Armadillo (green, red: DNA) shows integrity of wt (m) and *mei-P26<sup>fs1</sup>* (n) mutant cap cells. (o,p) Orb expression is initiated in wt (o) and *mei-P26<sup>fs1</sup>* mutant (p) cystocytes but restricted to the oocyte only in wt (o, arrow) and not in *mei-P26<sup>fs1</sup>/mfs1* mutant (p, arrowhead) egg chambers.

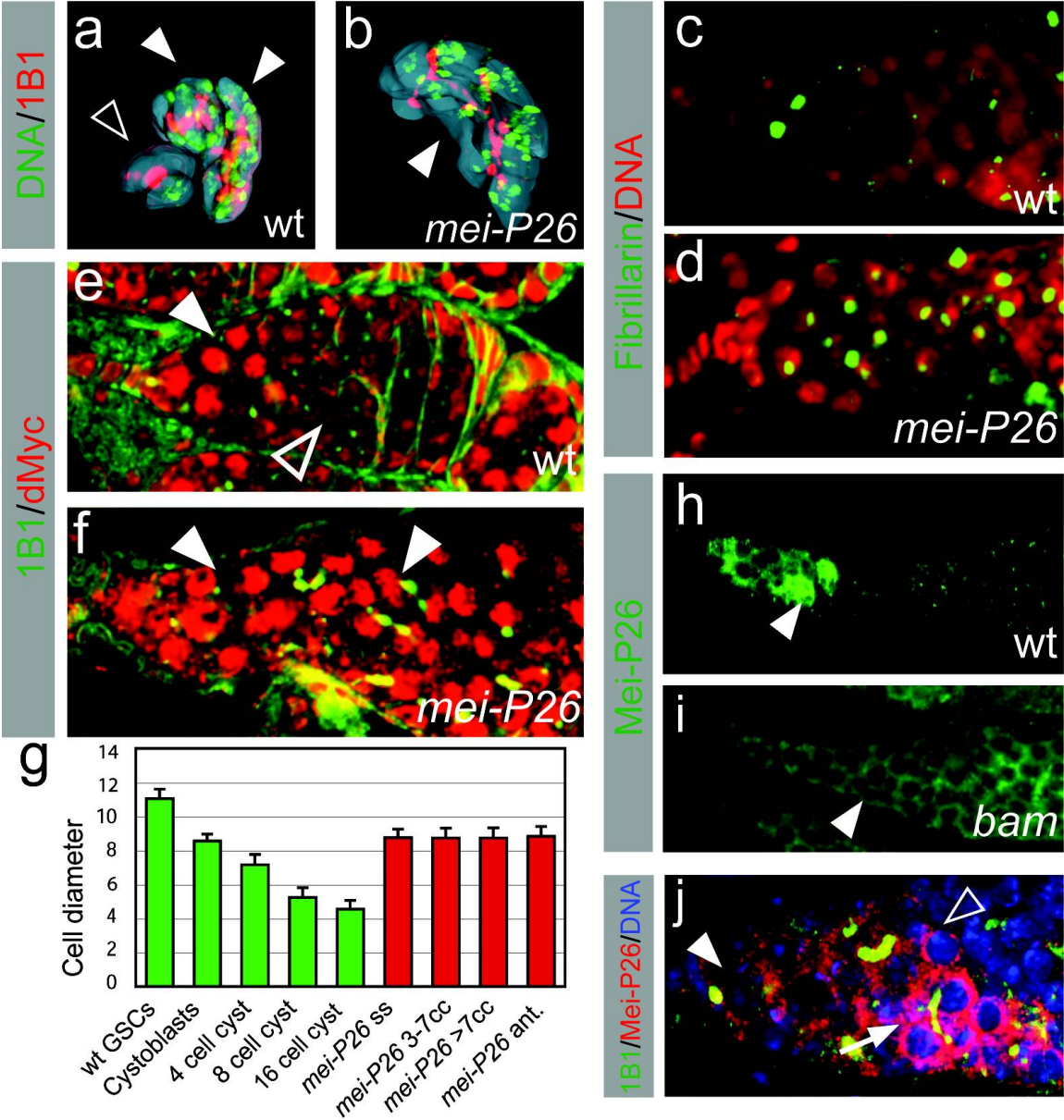
**Figure 2: Cystocytes overproliferate in *mei-P26* mutants.**



**Figure 2: Cystocytes overproliferate in *mei-P26* mutants.** (a,a ) Examples of *mei-P26<sup>mfs1</sup>* mutant cystocytes (connected by a branched fusome) undergoing synchronous mitotic divisions (The images in **a** and **a** are projections form a confocal stack). (b,c) 6 day old negatively marked germline clones showing upregulation of CyclinE (red) in almost all *mei-P26<sup>mfs1</sup>* mutant cells (c) compared to wt (arrowhead in b). (d,e) *BamP-GFP* (green, red: mAb1B1, blue: DNA) is not expressed in wt (d) and *mei-P26<sup>mfs1</sup>* mutant (e) niche contacting cells. During later stages of oogenesis, *BamP-GFP* is downregulated in wild type (d) but not in *mei-P26<sup>mfs1</sup>* (e) mutant ovaries. (f,g) Ten days old *mei-P26<sup>mfs1</sup>* germline clones (g) result in tumorous overproliferation compared to wt (f).



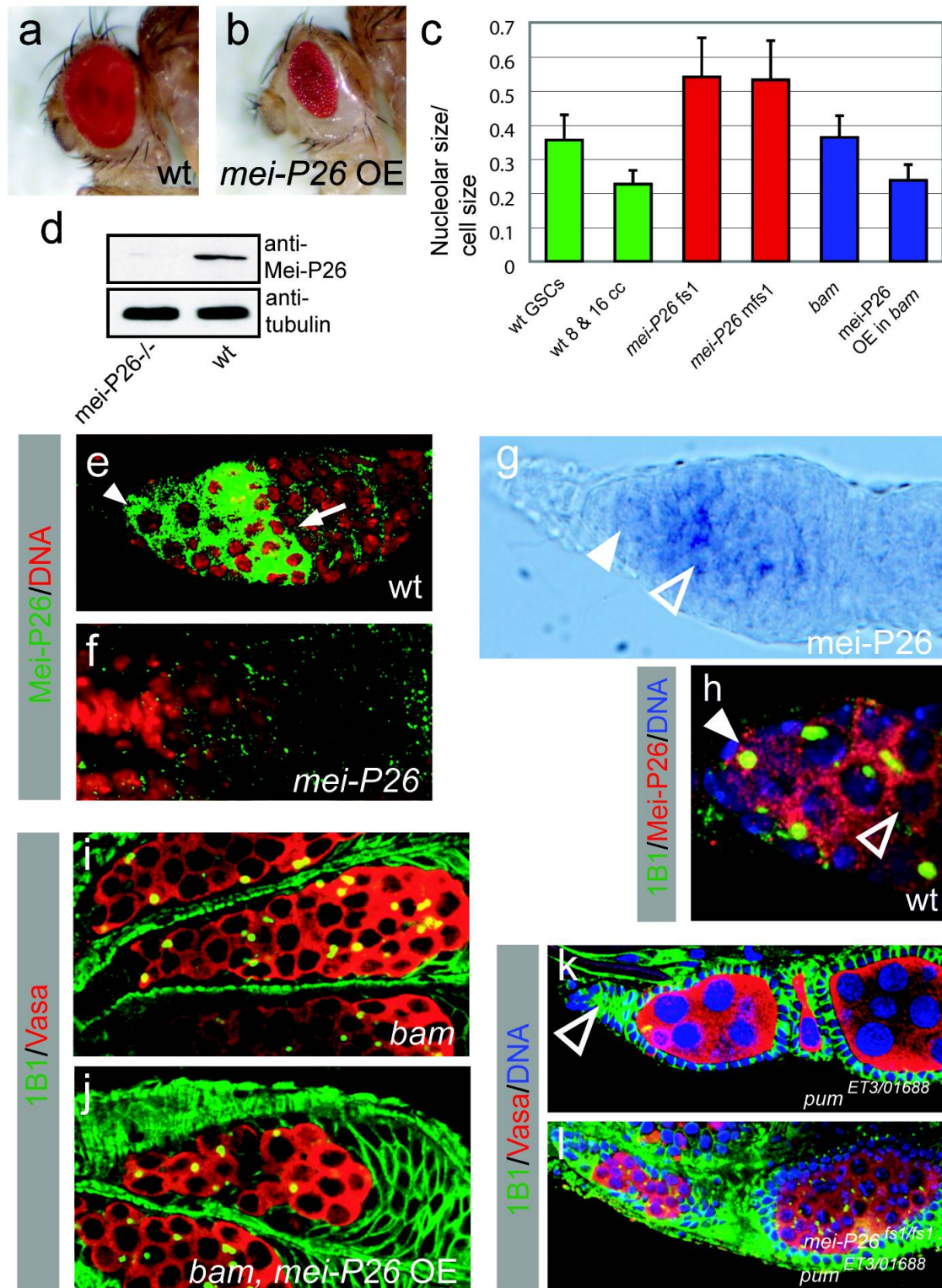
Figure 3: Mei-P26 regulates cell and nucleolar size.





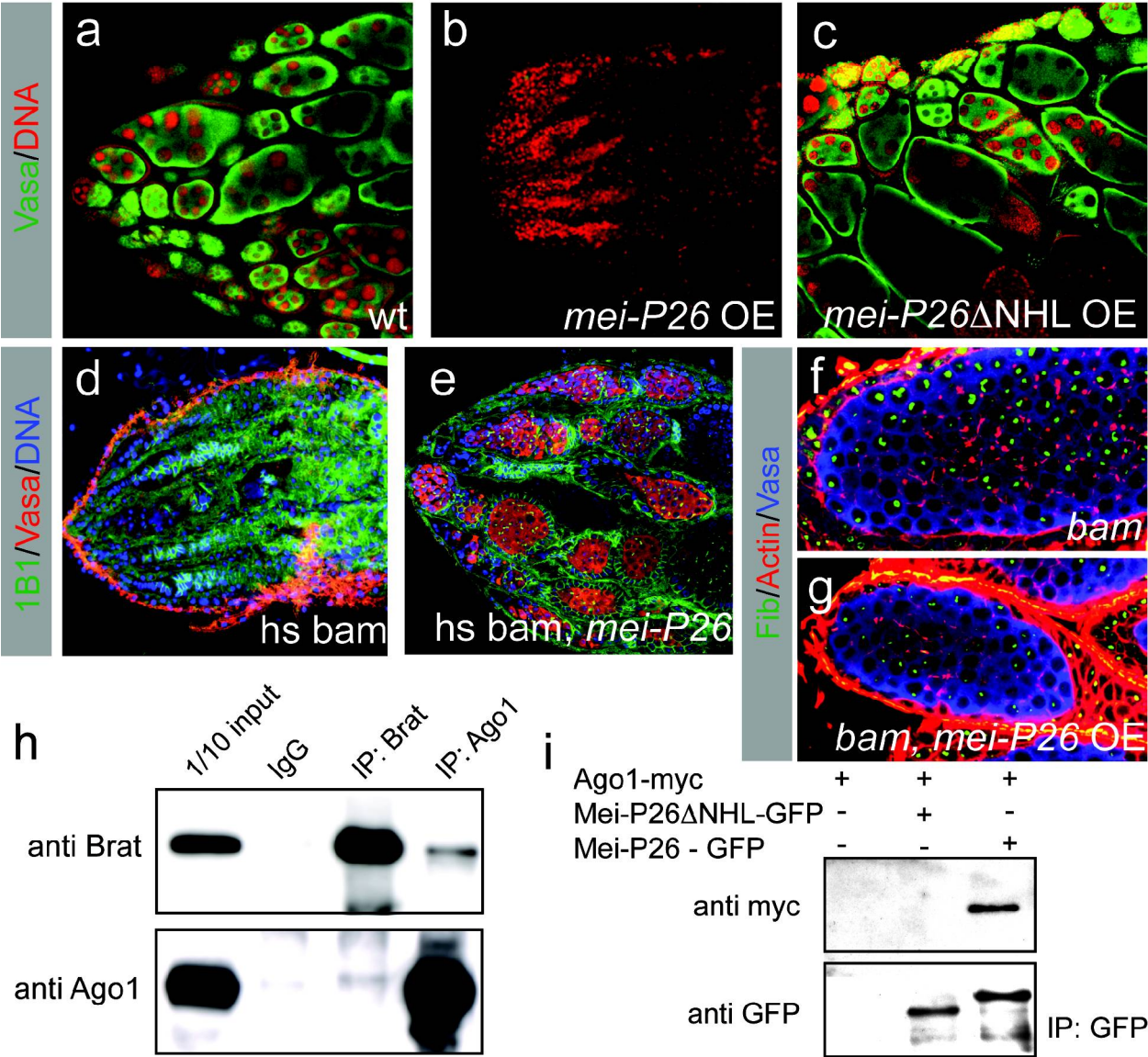
**Figure 3. Mei-P26 regulates cell and nucleolar size.** (a,b) 3D reconstruction of wt 16 cell cysts (closed arrowheads), a wt 8 cell cyst (open arrowhead) (a) and a *mei-P26<sup>fs1</sup>/mfs1* mutant cyst containing 14 cells (b). (c,d) Nucleoli (green: anti-Fibrillarin) in *mei-P26<sup>fs1</sup>* mutant ovaries (d) are larger than in wt (c). (e,f) High levels of dMyc (red, green: mAb1B1) are detected in germline stem cells and early cysts (arrowhead). In postmitotic cysts, dMyc levels are decreased (open arrowhead) and levels increase again as nurse cells undergo endoreplication (e). In *mei-P26<sup>fs1</sup>/mfs1* mutants high levels of dMyc are detected throughout the tumor (arrowheads in f). (g) Diameter in  $\mu\text{m}$  of the indicated cell types in wt and *mei-P26<sup>fs1</sup>/mfs1* mutant ovaries (Abbreviations: Mei-P26 ss = single spectrosome containing cells; Mei-P26 3-7 cc, Mei-P26 >7 cc = cystocytes in *mei-P26<sup>fs1</sup>* mutant cysts containing either 3-7 or > 7 cells; Mei-P26 ant. = anterior niche contacting cells). (Error bars: s.e.m.) (h,i) Mei-P26 expression peaks in early 16 cell cysts in wild type and is not detected at later stages of oogenesis (h). In *bam<sup>Δ86</sup>* mutant ovaries expression is not upregulated (i, compare to wt in h). Arrowheads point at equivalent stages. Note that Mei-P26 staining appears more intense in later stages due to sample thickness and out of focus fluorescence (i). (j, Fig. S2 e,f,h) Germarium close up: Mei-P26 (red,green: mAb1b1 ,blue: DNA) expression is low in stem cells (j, arrowhead), weakly upregulated in 8 cell cysts (open arrowhead) and peaks in 16 cell cystocytes (j, arrow).

**Figure 4: *mei-P26* regulates growth.**



**Figure 4: *mei-P26* regulates growth.** (a,b) *Eyeless* induced *mei-P26* overexpression reduces eye size (b). (c) Ratio of nucleolar and whole cell diameter of the indicated genotypes (Error bars: s.e.m.). Ratio between nucleolar/cell size is  $0.35 \pm 0.01$  (n=14) in wt stem cells and  $0.23 \pm 0.004$  (n=83) in wt 16 cell cysts. The nucleolar to cell size ratio is  $0.54 \pm 0.01$  (n=71) and  $0.52 \pm 0.01$  (n=41) in *mei-P26<sup>fs1</sup>* and *mei-P26<sup>mfs1</sup>* mutant cells, respectively. *mei-P26* overexpression reduces the size of *bam* mutant cells from  $10.1 \pm 0.17 \mu\text{m}$  (*bam*, n=27) to  $7.0 \pm 0.19 \mu\text{m}$  (*bam*, *UASP-meP26*, n=27) and completely rescues the enlarged nucleolus in *bam* mutants (ratio nucleolar/cell size:  $0.36 \pm 0.01$ , n=39) to wild type levels ( $0.24 \pm 0.01$ , n=39). (d) The anti-Mei-P26 antibody recognizes a band of the predicted size on a Western blot of wt but not *mei-P26<sup>mfs1/fs1</sup>* mutant ovary protein extracts. (e,f) Compared to wt (e) the Mei-P26 staining is completely gone in *mei-P26<sup>mfs1</sup>* (f) mutants. Higher levels of Mei-P26 in early 16 cell cysts than in stem cells are detectable in > 85% (n > 200 germaria) (e). (g) In situ hybridisation with a *mei-P26* specific probe reveals low levels of *mei-P26* mRNA in the GSC region (closed arrowhead) and high levels in the more posterior cyst region (open arrowhead). (h) Close up of Mei-P26 staining in a wt germarium revealing increased levels of Mei-P26 in (6 out of 10) 8 cell cysts (open arrowhead) as compared to the stem cell (arrowhead, red: Mei-P26, green: mAb1b1, blue: DNA) (Note that only three of the 8 cells of the cyst are visible in this focal plane). (i,j) *mei-P26* overexpression (from *nanos-Gal4::VP16*) in *bam $\Delta$ 86* does not alter cell fate as revealed by the presence of single spectrosome containing cells and absence of branched fusomes in both genotypes. (k,l) Loss of GSCs in *pum<sup>ET3/01688</sup>* mutants (open arrowhead, red: Vasa, green: mAb1B1, blue: DNA) (k). *mei-P26<sup>fs1</sup>*; *pum<sup>ET3/01688</sup>* double mutants show the *mei-P26* mutant phenotype (l).

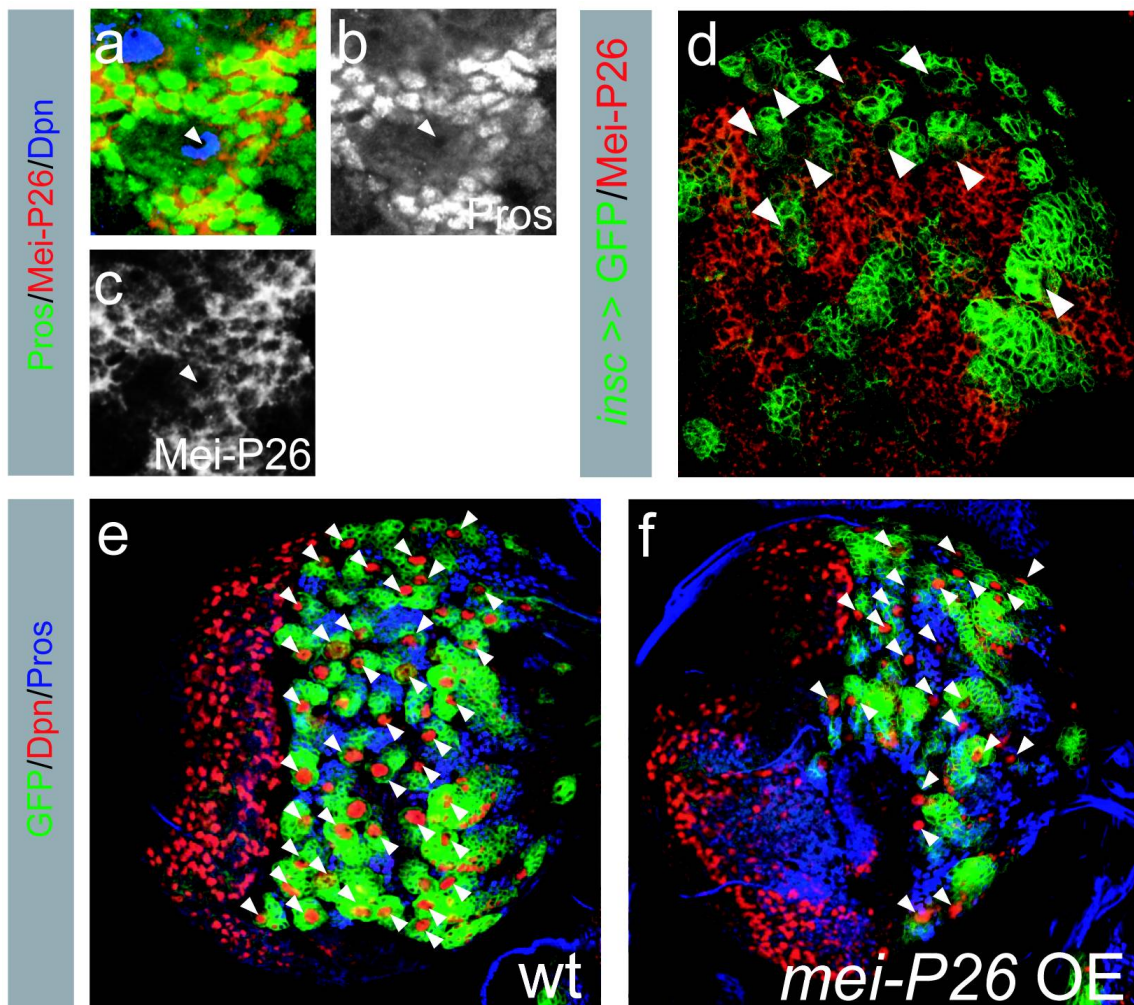
**Figure 5: *Bam* requires the Ago1 binding protein Mei-P26 to induce proper cystocyte differentiation.**



**Figure 5: *Bam* requires the Ago1 binding protein Mei-P26 to induce proper cystocyte differentiation.** (a,b,c) *mei-P26* (b) but not *mei-P26* $\Delta$ NHL (c) overexpression depletes the germline (green: Vasa, red: DNA). (d,e) Transiently induced *bam* overexpression induces stem cell differentiation and depletes the germline (red: Vasa, green: mAb1B1, blue:DNA) in a wt (d) but not *mei-P26*<sup>*fs1/mfs1*</sup> mutant (e) background. (f,g) *mei-P26* overexpression (from *nanos-Gal4::VP16*) in *bam* <sup>$\Delta$ 86</sup> mutants (g) reduces cell and nucleolar size (statistics in Fig. S2c) but does not induce stem cell differentiation (Fig. S2i,j). (h,i Fig. S4b) The NHL domain proteins Brat, Mei-P26 and Dappled interact with Ago1. Reciprocal immunoprecipitations of Brat and Ago1 from *Drosophila* embryo extracts (h). GFP- tagged Mei-P26 but not GFP- tagged Mei-P26 $\Delta$ NHL (i) coimmunoprecipitates myc-tagged Ago1 in S2 cells.

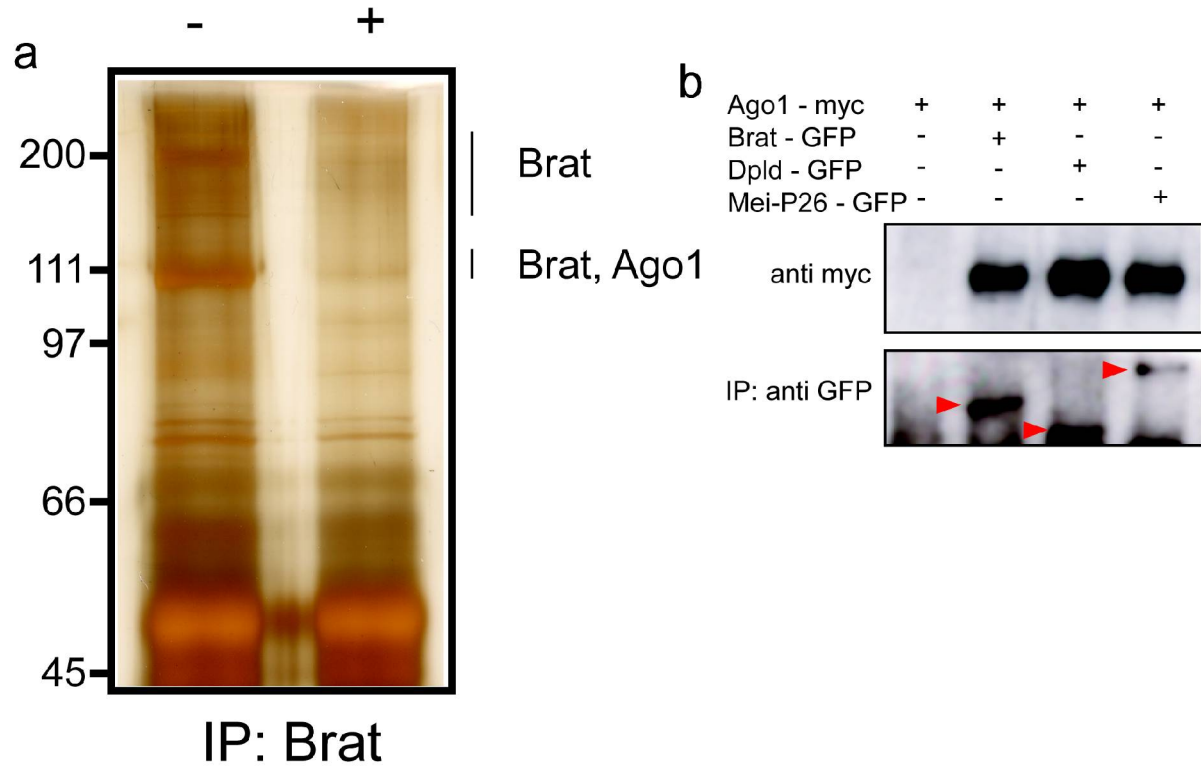


**Figure 6: *mei-P26* is expressed in the larval brain.**



**Figure 6: *mei-P26* is expressed in the larval brain.** (a,b,c) *Mei-P26* expression is low in larval neuroblasts (marked by *deadpan*: blue; arrowheads) undetectable in GMCs and young neurons (cells with low levels of *Prospero* surrounding the neuroblast) and high in differentiated neurons (high levels of *Prospero*). (d) Larval brain overview: *Mei-P26* is weakly expressed in larval neuroblasts and strongly in postmitotic neurons (red: *Mei-P26*, green: 1407 (*inscuteable* promoter) driven *cd8GFP*, arrowheads: neuroblasts). (e,f) Overexpression of *mei-P26* from the *inscuteable* promoter reduces the number of neuroblasts (arrowheads) (f) compared to wt (e) (red: *deadpan*, GFP positive cells >10um: green, marked by arrowheads). Approximately 20 of the 183 central brain neuroblasts are lost when *mei-P26* is overexpressed for 60 hours.

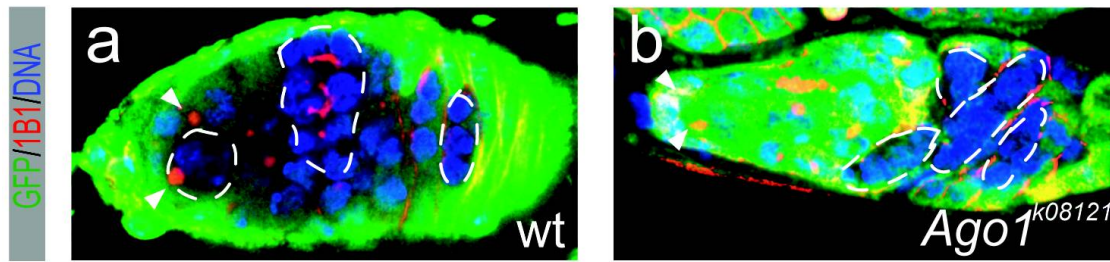
**Figure 7: Trim-NHL proteins interact with Ago1.**





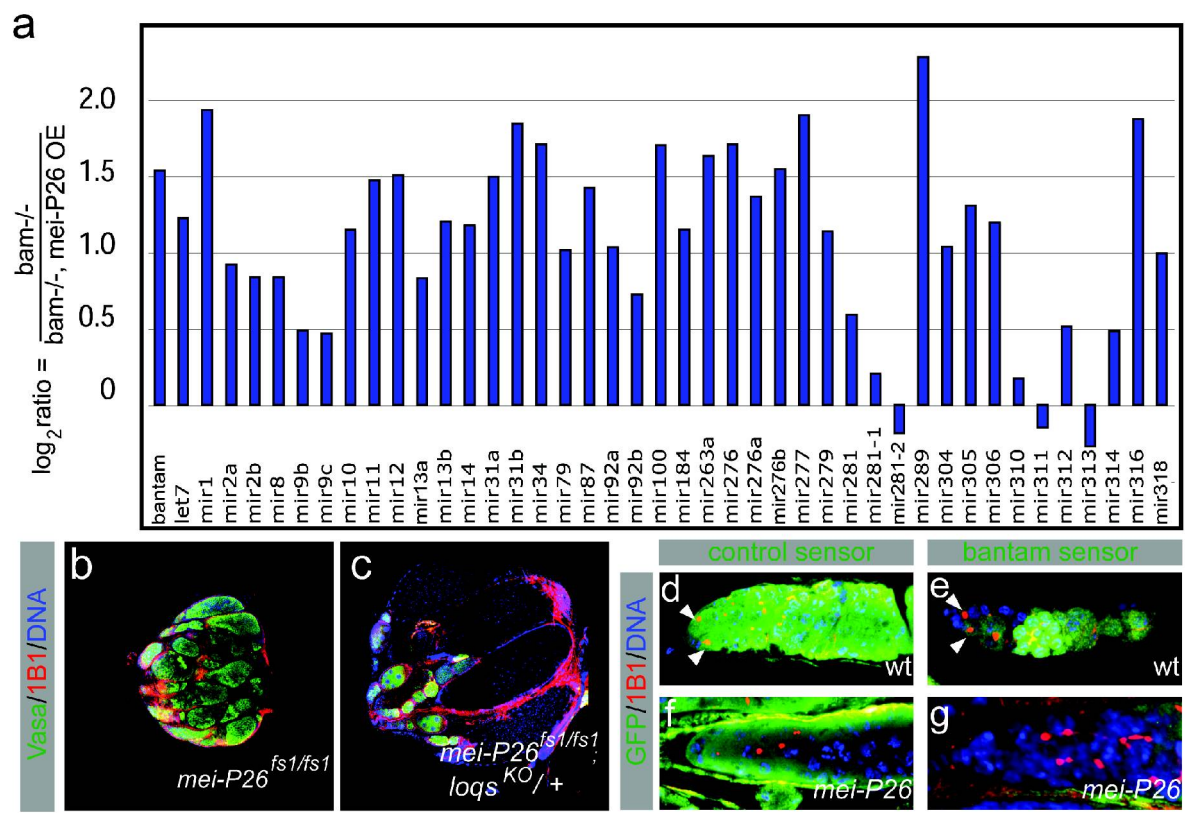
**Figure 7: Trim-NHL proteins interact with Ago1.** Silver stain of immunoprecipitations from *Drosophila* embryos using anti-Brat (-) or anti-Brat blocked by peptide antigen (+). Gel regions (marked by bars) were cut out from individual lanes and analyzed by MS/MS for the presence of specific proteins in the Brat immunoprecipitation only. GFP- tagged Brat, Mei-P26 and Dappled (b) coimmunoprecipitate myc-tagged Ago1 in S2 cells.

**Figure 8: Ago1 is required for germline stem cell maintenance.**



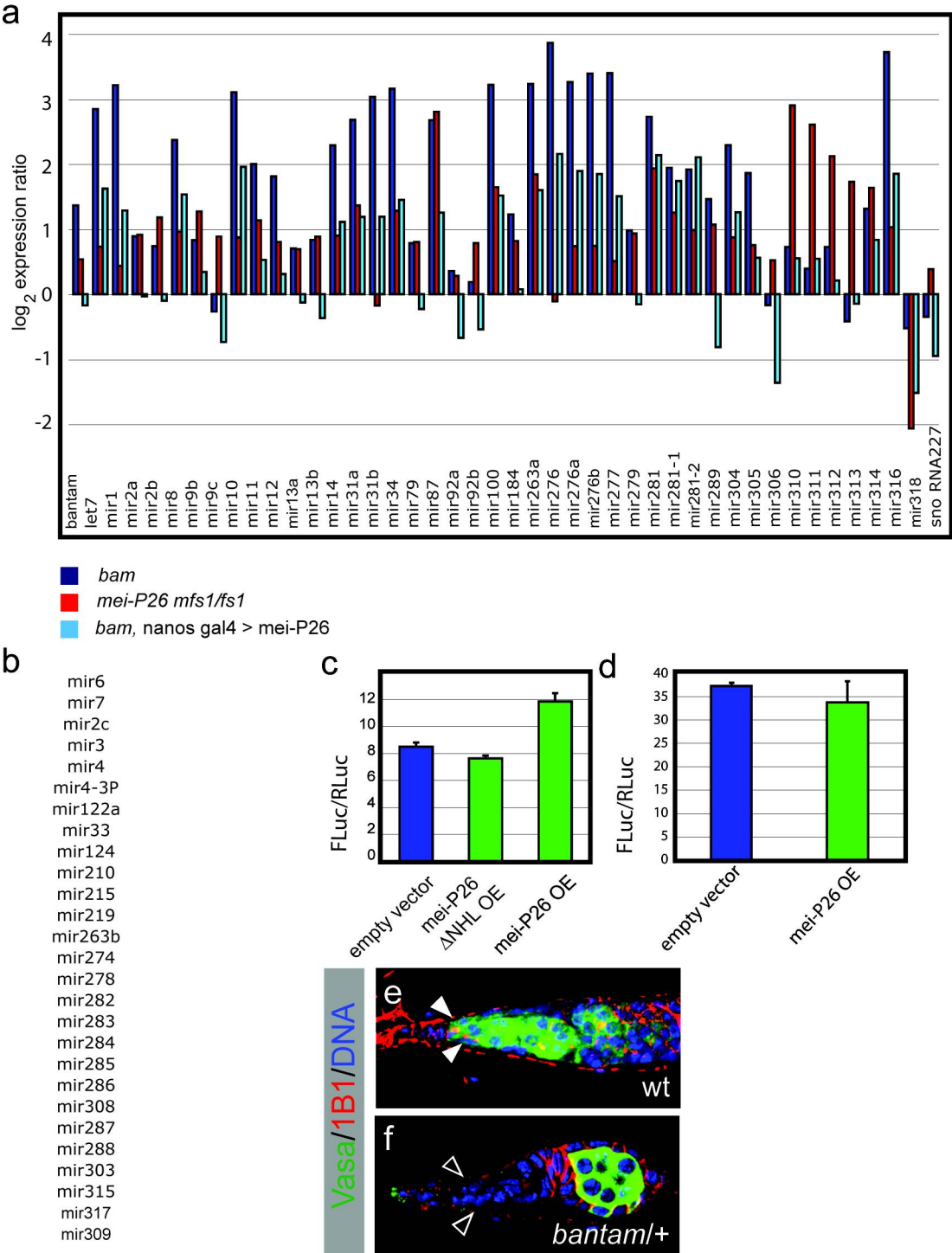
**Figure 8: Ago1 is required for germline stem cell maintenance.** (a,b) *ago1* mutant and control clones (marked by the absence of GFP: green). In wt 85% (n=27 clones) of the GFP negative germline stem cells (arrowheads) (a) are maintained whereas only 20.6% (n= 29 clones) of GFP negative *ago1<sup>k08121</sup>* stem cells (b) are maintained 17 days after clone induction. (Seven days after clone induction 96% (n= 25 clones) of GFP negative wt and 88% (n= 25 clones) of GFP negative *ago1<sup>k08121</sup>* mutant stem cells are maintained.)

**Figure 9: Mei-P26 regulates miRNAs.**



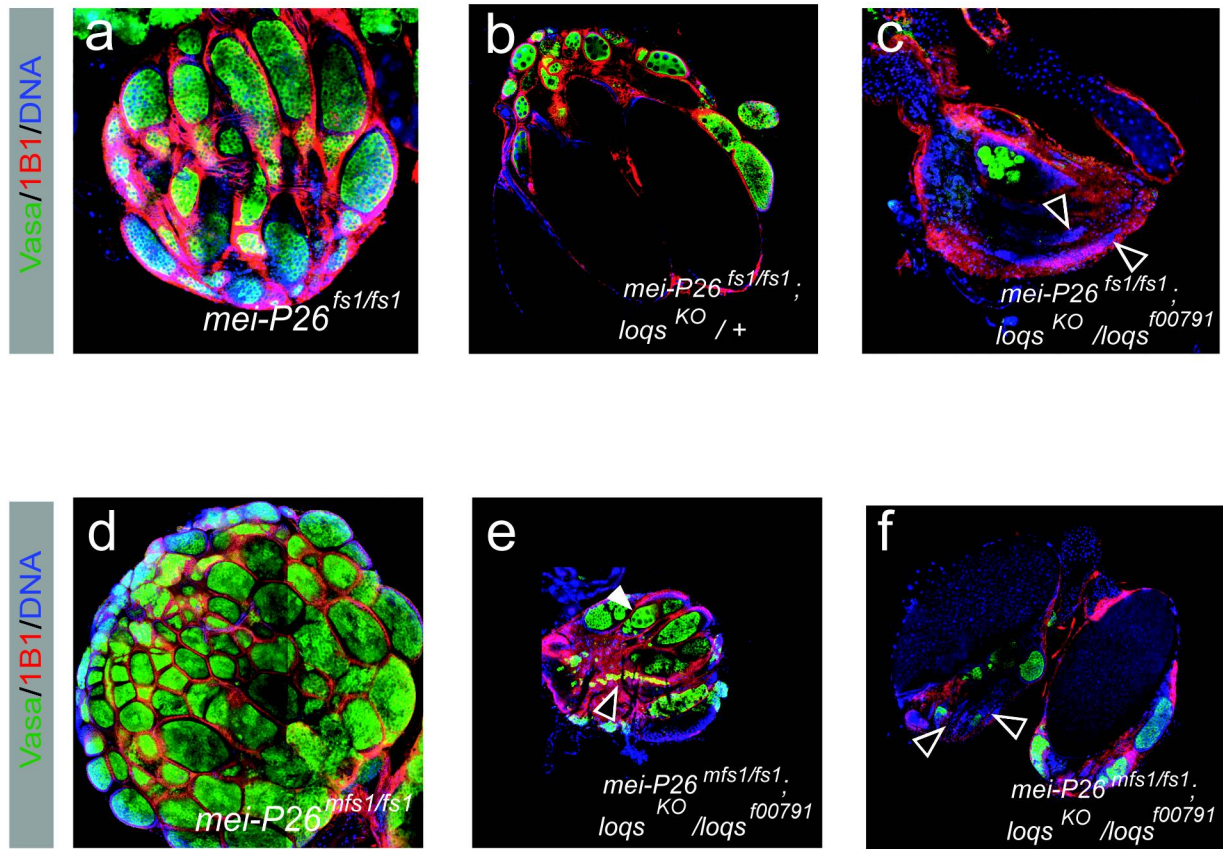
**Figure 9: Mei-P26 regulates miRNAs.** (a) Q-PCR experiment comparing the level of mature micro-RNAs in *bam*<sup>Δ86</sup> and *bam*<sup>Δ86</sup>, *nanos-Gal4::VP16* >> *pUASp-meï-P26*. y axis: log<sub>2</sub> of the expression ratio between the two genotypes. (b,c) Loss of one copy of *loquacious* partially rescues the *mei-P26<sup>fs1</sup>* mutant phenotype (Fig. S6). (d-g) Down-regulation of the bantam sensor reveals bantam miRNA expression in stem cells but not cystocytes (e), whereas the control sensor is uniformly expressed throughout the germline (d). The bantam sensor (g) but not the control sensor (f) is silenced in the germline of *mei-P26<sup>fs1</sup>/mfs1* mutants.

Figure 10: microRNAs are deregulated in germline tumors.



**Figure 10: microRNAs are deregulated in germline tumors.** (a,b) Q-PCR for a set of 71 micro-RNAs on total RNA of, *mei-P26<sup>mfs1/fs1</sup>*, *bam<sup>Δ86</sup>* and *bam<sup>Δ86</sup> nanos-Gal4::VP16 >>pUASp- mei-P26* (a). y axis: log<sub>2</sub> of the expression ratio between the indicated genotypes and wt. (b) List of miRNAs not detected in wt sample. (c) Ectopic expression of *mei-P26* (p< 0.001 (2-tailed) t-test; n=3; Error bars: s.e.m.) but not *mei-P26ΔNHL* down-regulates the endogenously expressed *bantam* micro-RNA (revealed by the upregulation of the bantam sensor) in S2 cells. (d) Ectopic expression of mei-P26 does not regulate the control sensor (lacking a *bantam* binding site) in S2 cells. (e,f) Occasional loss of both germline stem cells in *bantam* heterozygous animals. Closed arrowheads point out stem cells in (e) which are missing in (f) (open arrowheads).

**Figure 11: *loquacious* is required for *mei-P26* loss of function associated tumor growth.**





**Figure 11: *loquacious* is required *mei-P26* loss of function associated tumor growth. (a,b,c)**

Partial rescue of the *mei-P26<sup>fs1</sup>* mutant phenotype by the loss of one copy of *loquacious* (**b**): *mei-P26<sup>fs1</sup>* single mutants: 87% tumorous, 8,8% empty, 1,85% ovarioles containing nurse cells and 2,35% ovarioles containing eggs (n= 540 ovarioles) (**a**); *mei-P26<sup>fs1</sup> ; loqs<sup>KO/+</sup>*: 43% tumorous, 24% empty, 23% ovarioles containing nurse cells, 10% ovarioles containing eggs (n= 513 ovarioles) (**b**). Compared to *mei-P26<sup>fs1</sup>* single mutants, in *mei-P26<sup>fs1</sup>; loqs<sup>KO/f00791</sup>* double mutants a large fraction of ovarioles does not contain germline cells (**c**, germline cells marked by Vasa: green, open arrowheads point to empty ovarioles). (**d,e,f**) *mei-P26<sup>mfs1/fs1</sup>; loqs<sup>KO/f00791</sup>* double mutant ovaries appear much smaller than the ovaries of *mei-P26<sup>mfs1/fs1</sup>* single mutants. Infrequent signs of further differentiation as nurse cells (closed arrowhead in **e**) and eggs (2 in 40 ovaries versus 0 in 40 ovaries in wt) (**f**) can be observed in the double mutants. Closed arrowheads point out empty ovarioles that are frequently observed in the *mei-P26<sup>mfs1/fs1</sup>; loqs<sup>KO/f00791</sup>* double mutants but not in the *mei-P26<sup>mfs1/fs1</sup>* single mutants. (Note that all the images in this figure have been assembled from individual pictures acquired with a 25x objective and are of the same magnification; all genotypes analyzed 4 days after hatching on standard food.)

### III. Discussion

#### 1. Spindle orientation and neurogenesis

The presented data on *mushroom body defect (mud)* during asymmetric cell division and neurogenesis highlight the importance of proper spindle alignment with the axis of cellular polarity in neural stem cells. This alignment assures the correct partitioning of the cell fate determinants into the stem cell daughter cells. *mud* loss of function results in spindle orientation defects and hence defects in the segregation of cell fate determinants. This mis-segregation is accompanied by defects in cell fate specification. The striking defects of spindle misalignment during metaphase are contrasted by a surprisingly low rate of symmetric neuroblast divisions (4%). This discrepancy might however entirely be explained by a phenomenon referred to as telophase rescue <sup>98</sup>. The low rate of symmetric divisions is however sufficient to lead to a substantial increase of the stem cell pool (Illustration 4). Consistently spindle orientation has been shown to regulate the size of another stem cell pool in *Drosophila* as well. The mitotic spindle is always oriented perpendicular to the hub (GSC niche)- germline stem cell interface in the *Drosophila* testes. Mutations as for example in the *Drosophila* homolog of the tumor suppressor gene *apc2*, that disrupt this alignment, result in an increase of the stem cell pool <sup>99</sup>. This increase is due to divisions in which, unlike the wild type situation, both daughter cells remain in contact with the stem cell niche and consequently adopt stem cell fate. Thus proper spindle orientation is essential in extrinsic and intrinsic asymmetric stem cell divisions in *Drosophila* in order to regulate the size of the stem cell pool.

Since *mud* mutant neuroblasts as their wild type counterparts do stop to proliferate in early pupal phases (Ralph Neumüller unpublished data) this expansion of the neuroblast pool leads to hyperplastic over growth without neoplastic transformation *in vivo*. Thus the rare symmetric

stem cell divisions are not sufficient to cause tumorous proliferation and do not impair differentiation capacity of the stem cell progeny cells. It will however be interesting to determine if *mud* mutant third instar larval brain tissue would proliferate in a tumorous manner after transplantation in a wild type host. Several recent studies suggest that defects in stem cell division might precede genomic instability and thus are causative for neoplastic transformation<sup>83,100,101</sup>. These data suggest that improper stem cell divisions are a prerequisite for oncogenic growth. *mud* mutant brains would be an attractive tool to address this hypothesis.

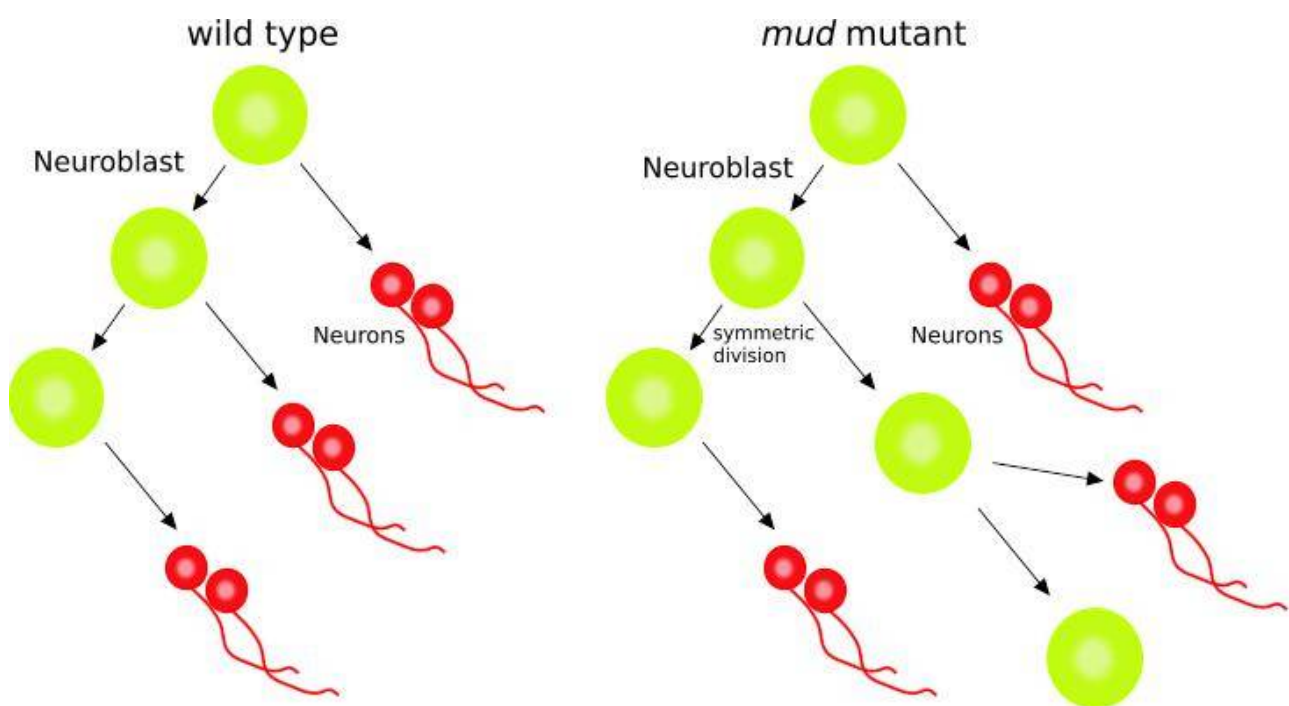


**Illustration 4**

The overproduction of neuroblasts is further accompanied by an excess of neurons. Thus stem cells do not overproliferate at the expense of differentiating cells, but instead, the ectopically generated neuroblasts continue to divide asymmetrically and thus produce ectopic neurons. The fact that only  $\gamma$  neuron axons but no  $\alpha\beta/\alpha'\beta'$  lobes are present in *mud* mutant Mushroom Bodies

further implicates *mushroom body defect* in axon specification and/ or axon growth. In contrast to the asymmetric divisions, the rare symmetric divisions lead to an equal inheritance of both apical and basal proteins into the two daughter cells. It is prodigious that both cells retain neuroblast rather than neuron fate, since both cells inherit half the amount of the cell fate determinants *brat*, *numb* and *prospero*. Since these proteins can inhibit self renewal one would expect that the inheritance of these determinants into both cells would drive them into differentiation. The levels of cell fate determinants in cells generated after a symmetric division might however be too small to do so. Alternatively these cell fate determinants could be inhibited by apical proteins or other factors that need to be excluded from the future ganglion mother cell.

The supernumerary Mushroom body neuroblasts in *mud* mutants further indicate that in these lineages self renewal is restricted to the stem cell by similar manners as in other neuroblast lineages (see introduction). Therefore it is surprising that *brat*, *numb* and *prospero* mutant neuroblasts do not overproliferate (Ralph Neumüller unpublished). These data suggest that asymmetrically segregating determinants act in a redundant manner to control Mushroom Body neuroblast proliferation, since symmetric divisions (*mud* mutant) can increase the stem cell pool whereas the loss of individual cell fate determinants does not result in ectopic neuroblast formation.

Despite these obvious differences in the proliferation pattern of different neuroblast lineages it is unclear why these differences exist. It is however tempting to speculate that the lack of Mushroom Body neuroblast quiescence at first instar larval stages and the delayed cessation of proliferation during pupal stages are required to equip larvae and adults with a critical number of neurons for developmental, behavioral intermediates and adult specific circuits. PAN (DM/ Type II) lineages might conversely amplify neuron production at late larval stages since the generated neurons could be required for adult specific behaviors only. These different proliferation patterns would make it necessary to modify proliferation control in a lineage specific manner.

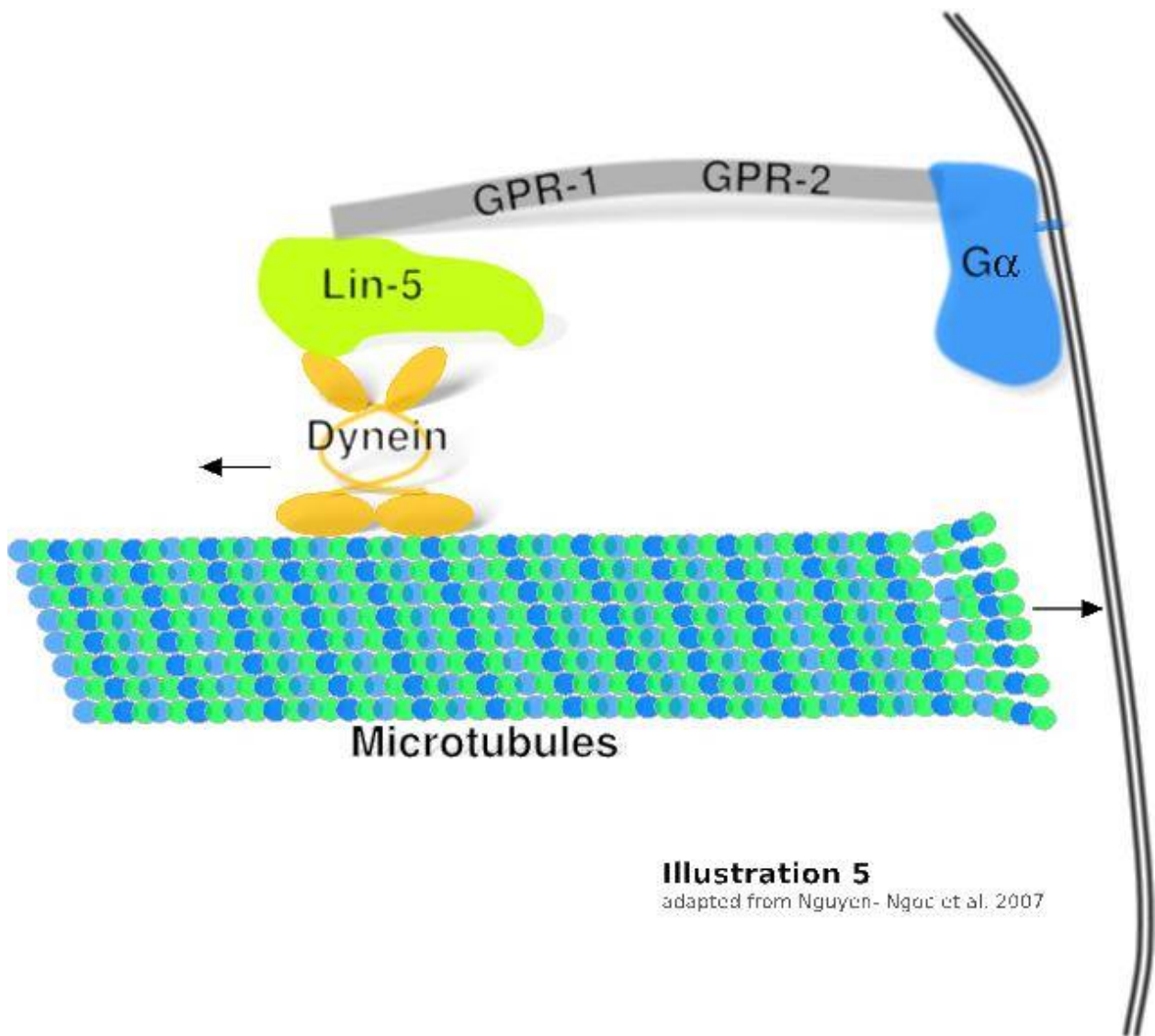


**Illustration 5**  
adapted from Nguyen- Ngoc et al. 2007

On the molecular level Mud (as its vertebrate homolog NuMA) forms a complex with Pins and Gαi. Since Mud can additionally interact with microtubules, Mud can link astral microtubules to the apical cortex and thus ensures alignment of the cell division axis with the axis of polarity. Recent evidence from *C. elegans* further supports this model (Illustration 5) <sup>102,103</sup>. Lin-5, the *C. elegans* homolog of Mud, has been shown to interact with GPR-1/2 and components of the Dynein complex (as Lis-1 and Dyrb-1 (which encodes a dynein light chain)) simultaneously <sup>102</sup>. The Dynein- Lin-5 complex gets recruited to the cell cortex via the binding of Lin-5 to GPR-1/2, which itself can interact with Gα proteins. Since Gα is myristoylated, it serves as a membrane anchor which ensures the correct spatial accumulation of Dynein/ Lin-5/ GPR-1/2 at the cell cortex. Once associated with cortical proteins, Dynein anchors the spindle at this interface and

can further generate pulling forces, since it moves towards the minus end of microtubules while being tethered at the cortex. Even though an association of Mud with components of the Dynein complex has not been demonstrated in *Drosophila*, a similar molecular mechanism might be operational in flies. Consistently it has recently been demonstrated that Lis-1 and dynactin are required for spindle orientation in *Drosophila* larval neuroblasts<sup>104</sup>. Similarly in vertebrates it has been demonstrated that the binding of NuMA to LGN<sup>30</sup> is necessary for the association of LGN with G $\alpha$ i and subsequently the interaction of astral microtubules with the cell cortex. Furthermore NuMA has been implicated in the organization of microtubules into aster like structures. Overall the molecular apparatus that controls spindle orientation in *C. elegans*, *Drosophila* and vertebrates seems to be conserved.

As pointed out above spindle orientation is of central importance in *Drosophila* asymmetric stem cell division during neurogenesis and oogenesis. Given the conservation of the involved molecules in vertebrates it is thus tempting to speculate that as in neuroblasts, spindle orientation might as well play a fundamental role in regulating cell fate decisions in mammalian (neural) stem cell divisions. Similarly it has been proposed that proper spindle orientation is an essential parameter during mammalian neurogenesis<sup>102,103</sup>. Several groups have established a model in which neural precursor cells (neuroepithelial and radial glia cells respectively) orient their axis of division in a temporal pattern which correlates with different phases of stem cell divisions. At early phases during development, neuroepithelial cells mainly undergo symmetric divisions (divisions parallel to the ventricular surface) in order to increase the stem cell pool. By the time neuron production starts and neural precursor cells start to divide asymmetrically, this model proposes that neural precursor cells shift their division axis by 90 degrees and this division perpendicular to the ventricular surface is a prerequisite for the daughter cells to adopt different fates. At the end stages of embryonic neurogenesis, divisions parallel to the ventricular surface become predominant again, but instead of generating two progenitor cells, two differentiating neurons originate from a terminal symmetric division. This conceptually appealing model, that heavily takes the *Drosophila* data of neuroblast division into account, has recently been

substantially challenged<sup>104-106</sup>. Several groups used live imaging and immunohistochemical approaches to re- investigate spindle orientation during development and came to the contradictory conclusion, that spindle orientation does not correlate with cell fate specification during mammalian neurogenesis. Noctor et al. very convincingly demonstrated that both horizontal and vertical divisions can give rise to two cells of the same fate<sup>105</sup>. A different study found that even at the peak of neurogenesis the by far predominant mode of division is actually parallel to the ventricular surface <sup>106</sup>.

These data suggest that cell fate decisions occur independently of spindle orientation. Possibly extracellular instructive signals or intracellular determinants that segregate<sup>84</sup> (uncoupled of spindle orientation) predominantly in either one of the two daughter cells upon mitosis regulate cell fate decisions in the developing mammalian brain.

Loss of function studies of molecules homologous to invertebrate spindle orientation regulators as for example LGN<sup>106</sup> (the *Drosophila* Pins homolog) and Lis1<sup>107</sup> have suggested that these molecules lock the spindle in a horizontal position to ensure divisions parallel to the ventricular surface. The loss of LGN is accompanied with a randomization of mitotic spindle orientation and a subsequent increase in divisions perpendicular to the ventricular surface. This subsequently leads to the formation of an increased number of cells that divide non- apically, the so called 'non surface progenitors'. The spindle orientation defects caused upon loss of Lis1 however result in a dramatic increase in apoptosis during early phases of neurogenesis. These data highlight that proper spindle orientation is important during mammalian neurogenesis, but unlike *Drosophila*, cell fate specification between stem cells and differentiating cells does not rely on spindle orientation. Thus the molecular machinery might have acquired a different functionality under different evolutionary constraints.

A recent interesting hypothesis<sup>108</sup> suggests that in particular the loss of spindle rotation, as observed in *Drosophila*, is an important prerequisite for the relative expansion of brain size in the vertebrate and especially primate lineages. The precise vertical divisions are suggested to be required for symmetric proliferative divisions and hence stem cell pool increase. Slight meanderings from this division mode (by downregulation of spindle locking molecules (as

demonstrated for *Aspm*<sup>109</sup>)) would lead to asymmetric divisions of the neural stem cells. Thus, even though the molecules that regulate spindle orientation in *Drosophila* are conserved, their primary role seems to be anchoring the mitotic spindle horizontally, ensuring precise divisions parallel to the ventricular surface. It will thus be interesting to study the NuMA mutant phenotype in the developing mammalian cortex. As LGN, NuMA could have a role in locking the mitotic spindle of neural precursor cells (perpendicular to apical- basal polarity).

## **2. The role of the Trim-NHL protein Mei-P26 in the ovarian stem cell lineage**

### **2.1. Mei-P26 and growth control**

*brat* and its *C. elegans* homolog *ncl-1* have been suggested to regulate nucleolar size and thus cellular growth<sup>64,110</sup>. Similarly *mei-P26* possesses growth suppressor activity. Five lines of evidence support this conclusion: A) Ectopic expression of *mei-P26* in the eye imaginal disc from the *eyeless* promoter (OK107- *gal4*) significantly reduces the size of the eye. B) Simultaneous overexpression of *p35* (a potent inhibitor of apoptosis) and *mei-P26* with *eyeless gal4* results in only a mild rescue of the small eye phenotype suggesting that *mei-P26* GOF does not induce massive cell death. C) Overexpression of *mei-P26* in a *bam* mutant background significantly reduces the size of the nucleolus without inducing further differentiation. D) *mei-P26* mutant germline cells have significantly enlarged nucleoli and cysts are significantly bigger than their wild type counterparts. E) High levels of *mei-P26* expression in the germline tightly correlate with a reduction of cellular growth of the respective cells. Additionally high levels of *mei-P26* are inversely correlated with the expression level of dMyc and *mei-P26* mutant cells have increased levels of dMyc. Thus deregulation of dMyc could provide a potential explanation for the growth phenotype observed in *mei-P26* mutants. Unlike *brat*, *mei-P26* does contain a



RING domain and could thus regulate dMyc directly as it was recently shown for its vertebrate homolog *trim32*<sup>84</sup>. Since dMyc loss (and gain) of function does not have an obvious phenotype during early steps of oogenesis but affects endoreplication of nurse cells at later stages of oogenesis<sup>111</sup>, deregulation of dMyc doubtlessly can not explain the whole phenotypic range observed in *mei-P26* gain and loss of function experiments. Nonetheless it will be interesting to determine if *mei-P26* does function as an ubiquitin ligase and if dMyc is a relevant target *in vivo*.

The growth repressing potential of both *mei-P26* and *brat* in the differentiating stem cell progeny cells raises the interesting possibilities, that A) germline and neural stem cells need to sustain a high rate of cellular growth in order to be maintained (*mei-P26* overexpression in the brain results in neuroblast loss) and B) that growth rate reduction might be a prerequisite for/ or induces mitotic cell cycle exit. The isolation of two different types of yeast mutants that either affect cell cycle progression without influencing cell growth or mutants in which both processes are impaired simultaneously led to the hypothesis that the rate of cellular growth is the rate limiting step of these two coupled processes<sup>112,113</sup>. Studies in the *Drosophila* imaginal wing disc further support this hypothesis<sup>114</sup>. Thus reducing the rate of cellular growth in the transit amplifying cells in a stem cell lineage might be the trigger to A) divide terminally and differentiate into neurons (*brat*) or B) switch from mitotic proliferation to meiosis and at later stages endoreplication (*mei-P26*). Both stem cell lineages however seem to rely on high growth rates of the respective stem cells.

## **2.2. Mei-P26 and microRNAs**

The biochemical data presented suggest that Ago1 is a common binding partner for Trim-NHL domain proteins. Indeed, reports from both *C. elegans*<sup>115</sup> and mouse<sup>84</sup> suggest that this interaction is evolutionary conserved. As in *Drosophila*, a recent report suggests that this interaction is mediated by the NHL domain which is required for protein function of Brat<sup>65</sup>, Mei-P26 and

Trim32<sup>84</sup> respectively. Interestingly the NHL domain is also required to mediate binding of Brat to the ternary complex consisting of Pumilio, Nanos and *hunchback mRNA*<sup>75</sup>. Thus it is tempting to speculate that the NHL domain might generally be required to mediate interactions between mRNAs that contain specific cis- acting sequences and proteins that recognize these motifs. The fact that the *cyclinB* mRNA is not recruited to the Brat/ Nanos/ Pumilio complex suggests that Brat might act in mediating translational repression in a combinatorial, sequence specific manner. The binding of Brat, Mei-P26 and Trim32 to Ago1 might follow this principle. Trim32 has been shown to associate with a subset of microRNAs only<sup>84</sup> and consistently *mei-P26* does not regulate all microRNAs. It will be of central importance in the future to determine if Mei-P26 is associated with a specific set of microRNAs and if the Ago1/ Trim-NHL Protein complex does contain mRNAs.

Indirect evidence suggests that Mei-P26 inhibits microRNAs: In *mei-P26* mutant ovaries most microRNAs are upregulated and conversely most microRNAs are downregulated upon *mei-P26* overexpression in a *bam* mutant background compared to *bam* mutants alone. Moreover ectopic expression of *mei-P26* can downregulate the levels of the mature microRNA *bantam* in S2 cells. In contrast to these data, *trim32* has been suggested to upregulate the activity of the let-7 microRNA<sup>84</sup>. How could this obvious discrepancy be explained/resolved? A) microRNAs seem to have a fundamentally different impact in stem cell lineages in *Drosophila* and *Vertebrates* respectively<sup>116</sup>. microRNAs possess an instructive function in germline stem cell fate specification. Mutations that impair microRNA function result in stem cell loss whereas *ago1* overexpression from a heat shock inducible promoter increases the stem cell number<sup>48</sup>. Consistently microRNA levels are higher in *bam* mutant ovaries as compared to wild type ovaries. In vertebrates however microRNAs have been suggested to rather promote differentiation. Thus Trim-NHL proteins could have adopted to differentially regulate microRNAs in an evolutionary constrained manner. B) Mei-P26 could regulate microRNAs on two levels: i) the growth inhibitory effect of *mei-P26* could have a negative impact on the transcriptional level and could thereby affect microRNA levels in an indirect manner. Especially the *bantam* microRNA has been shown to be regulated and respond to growth associated signal

transduction pathway output<sup>93,117</sup>. ii) in this scenario Mei-P26 could function in the Ago1 complex on a separate regulatory level. Thus the growth inhibitory effect of *mei-P26* could explain the downregulation of *bantam* in S2 cells. It will therefore be important to conduct further studies to determine if *bantam* is associated with the Mei-P26/Ago1 complex. C) Mei-P26 could increase the turnover of microRNAs or titrate microRNAs towards specific mRNA targets which again could explain all the measurements on mature microRNAs presented. The absence of this high turn over could entail an accumulation of microRNAs in *mei-P26* mutants. D) Both *mei-P26* and *trim32* might regulate different microRNAs differently. Even microRNAs directly associated with the Trim-NHL Ago1 complex might follow different regulations. Some microRNAs being stabilized and others being turned over.

Thus the current literature does not allow to reach a comprehensive mechanistic explanation of how Trim-NHL proteins interact with microRNAs in translational regulation and additional studies are required to address the most central questions: Are microRNAs and target mRNA molecules associated simultaneously in the Trim-NHL/Ago1 complex and are these complexes specific in terms of their targets? Further it will be essential to investigate to what extent the observed biological properties of Trim-NHL proteins are explainable by microRNA regulation. Since *trim32* has been shown to contain a functional RING domain it is tempting to speculate that at least those Trim-NHL domain proteins that contain both a RING and NHL domain are bi-functional proteins.

Regardless of the above mentioned uncertainties about the mechanistic mode of action and the directionality of microRNA regulation, the deregulation of microRNAs significantly contributes to the formation of germline tumors upon *mei-P26* loss. Analysis of a large set of microRNAs in *mei-P26* mutants revealed a upregulation of a large fraction of microRNAs. This deregulation seems to be causative for the *mei-P26* loss of function associated tumor phenotype. Reducing microRNA levels by almost completely removing *loquacious* (using a transheterozygous combination of a null allele and a strong hypomorph) partially rescues the *mei-P26* tumor phenotype. The ovaries of the double mutants are dramatically reduced in size and a large fraction of ovarioles does not contain any germ line cells. This suggests that the tumor cells

require high levels of microRNAs to actively proliferate and to be maintained in the ovaries. The increased frequency of ovarioles containing mature eggs upon the removal of one copy of *loquacious* in a *mei-P26* mutant background, compared to *mei-P26* mutants alone, suggests that the deregulation of microRNAs contributes to the inability of *mei-P26* mutant cells to differentiate beyond the cystocyte stage. Thus microRNAs might be involved in cell fate decisions in the ovarian stem cell lineage. Consistently a parallel study could reveal that *ago1*, *bam* double mutants show signs of cystocyte differentiation and forced *ago1* expression results in tumorous germaria (although at a low frequency) resembling *mei-P26* mutant tumors<sup>48</sup>. Thus microRNA deregulation seems to be necessary and surprisingly even sufficient for germline tumor formation.

It will be interesting to determine which microRNAs (individual or in a combinatorial manner) contribute to cell fate specification and proliferation. A good candidate is the *bantam* microRNA. The above shown data suggest that *bantam* loss of function results in germline stem cell self renewal defects. A parallel study also demonstrated the requirement of *bantam* in germline stem cell maintenance and was able to show that *bantam* possesses a cell autonomous function in germline stem cells<sup>118</sup>. *bantam* has been shown to promote growth and proliferation in the wing imaginal disc<sup>93,117</sup> and it is thus likely that growth defects of *bantam* mutant germline stem cells are the underlying defect of *bantam* loss of function associated germline stem cell loss. Since *bantam* levels are increased in various tumor mutants (*bam*, *brat* (Natascha Bushati and Jörg Betschinger personal communication) and *mei-P26*) as compared to wild type, *bantam* could promote growth and proliferation in various contexts.

The binding of Brat to Ago1 further suggests that microRNAs might also possess a function in neural stem cell lineages. It will be a challenging task in the future to determine if microRNAs are involved in neurogenesis and neural stem cell derived tumor formation in *Drosophila*.

### 3. Concluding remarks

Despite the apparent differences in regulation of stem cell proliferation in the *Drosophila* germline and central nervous system, these two systems show surprising similarities and parallels. The proper orientation of the mitotic spindle is required in both stem cell lineages to ensure the correct cell fate specification of stem cells and daughter cells respectively. Faulty aligned mitotic spindles lead to an expansion of the stem cell pool in both lineages albeit through a different mechanism: Whereas correct spindle orientation in *Drosophila* germline stem cell is required for ensuring niche detachment of the daughter cell, the neuroblast uses spindle orientation to partition cell fate determinants unequally between the two daughters.

Additionally these two lineages use related molecules (*brat* and *mei-P26* respectively) to restrict self renewal capacity to the stem cells only. Both proteins are inhibitors of cell growth and proliferation. It is interesting to notice that as *mei-P26*, *brat* mutant tumors arise from transit amplifying cells that regain the ability to self- renew and proliferate mitotically. Thus as proper spindle orientation both stem cell lineages need to restrict growth and proliferation capacity to the stem cell only and seem to use similar molecular mechanisms. These similarities raise the interesting possibility that other stem cell lineages in the fly might be regulated by similar processes as well and the high degree of conservation of *Drosophila* genes suggests that homologous vertebrate proteins fulfill the same functions in mammalian stem cell lineages.

These data qualify *Drosophila* as a valuable and genetically accessible model to study stem cell derived tumor formation.

## IV. References

1. Doe CQ Neural stem cells: balancing self-renewal with differentiation. *Development* **135**, 1575-1587(2008).
2. Knoblich JA Mechanisms of asymmetric stem cell division. *Cell* **132(4)**, 583-97(2008).
3. Clarke MF and Fuller M Stem cells and cancer: two faces of eve. *Cell* **124(6)**, 1111-5(2006).
4. Bonnet D and Dick JE Human acute myeloid leukemia is organized as a hierarchy that originates from a primitive hematopoietic cell. *Nature Medicine* **3(7)**, 730-7(1997).
5. Singh SK, Clarke ID, Terasaki M, Bonn VE, Hawkins C, Squire J, Dirks PB. Identification of a cancer stem cell in human brain tumors. *Cancer Res* **63(18)**, 5821-8(2003).
6. Al-Hajj M, Wicha MS, Benito-Hernandez A, Morrison SJ, Clarke MF. Prospective identification of tumorigenic breast cancer cells. *Proc Natl Acad Sci U S A* **100(7)**, 3547-9(2003).
7. O'Brien CA, Pollett A, Gallinger S, Dick JE. A human colon cancer cell capable of initiating tumour growth in immunodeficient mice. *Nature* **445(7123)**, 106-10(2007).
8. Borst P and Elferink RO. Mammalian ABC transporters in health and disease. *Annu Rev Biochem.* **71**, 537-92(2002).
9. Xie T and Spradling AC. A Niche Maintaining Germ Line Stem Cells in the Drosophila Ovary. *Science* **290(5490)**, 328-30(2000).
10. Ito K and Hotta Y. Proliferation pattern of postembryonic neuroblasts in the brain of Drosophila melanogaster. *Dev Biol.* **149(1)**, 134-48(1992).
11. Bello BC, Izergina N, Caussinus E, Reichert H. Amplification of neural stem cell proliferation by intermediate progenitor cells in Drosophila brain development. *Neural Develop.* **3:5**, (2008).
12. Boone JQ, Doe CQ. Identification of Drosophila type II neuroblast lineages containing transit amplifying ganglion mother cells. *Dev Neurobiol.* **68(9)**, 1185-95(2008).
13. Bowman SK, Rolland V, Betschinger J, Kinsey KA, Emery G, Knoblich JA. The tumor suppressors Brat and Numb regulate transit-amplifying neuroblast lineages in Drosophila. *Dev Cell* **14(4)**, 535-46(2008).
14. Betschinger J, Knoblich JA. Dare to be different: asymmetric cell division in Drosophila, C. elegans and vertebrates. *Curr Biol.* **14(16)**, 674-85(2004).
15. Kemphues KJ, Priess JR, Morton DG, Cheng NS. Identification of genes required for cytoplasmic localization in early C. elegans embryos. *Cell* **52(3)**, 311-20(1988).
16. Kuchinke U, Grawe F, Knust E. Control of spindle orientation in Drosophila by the Par-3-related PDZ-domain protein Bazooka. *Curr Biol.* **8(25)**, 1357(1998).
17. Wodarz A, Ramrath A, Grimm A, Knust E. Drosophila atypical protein kinase C associates with Bazooka and controls polarity of epithelia and neuroblasts. *J Cell Biol.* **150(6)**, 1361-74(2000).

18. Petronczki M, Knoblich JA. DmPAR-6 directs epithelial polarity and asymmetric cell division of neuroblasts in *Drosophila*. *Nat Cell Biol.* **3(1)**, 43-9(2001).
19. Schober M, Schaefer M, Knoblich JA. Bazooka recruits Inscuteable to orient asymmetric cell divisions in *Drosophila* neuroblasts. *Nature* **402(6761)**, 548-51(1999).
20. Betschinger J, Mechtler K, Knoblich JA. The Par complex directs asymmetric cell division by phosphorylating the cytoskeletal protein Lgl. *Nature* **422(6929)**, 326-30(2003).
21. Wirtz-Peitz F, Nishimura T, Knoblich JA. Aurora-A Initiates the Asymmetric Localization of Numb by Phosphorylating the Par complex. *Cell* in press(2008).
22. Smith CA, Lau KM, Rahmani Z, Dho SE, Brothers G, She YM, Berry DM, Bonneil E, Thibault P, Schweisguth F, Le Borgne R, McGlade CJ. aPKC-mediated phosphorylation regulates asymmetric membrane localization of the cell fate determinant Numb. *EMBO J.* **26(2)**, 468-80(2007).
23. Erben V, Waldhuber M, Langer D, Fetka I, Jansen RP, Petritsch C. Asymmetric localization of the adaptor protein Miranda in neuroblasts is achieved by diffusion and sequential interaction of Myosin II and VI. *J Cell Sci.* **121(Pt9)**, 1403-14(2008).
24. Slack C, Overton PM, Tuxworth RI, Chia W. Asymmetric localisation of Miranda and its cargo proteins during neuroblast division requires the anaphase-promoting complex/cyclosome. *Development* **134(21)**, 3781-7(2007).
25. Barros CS, Phelps CB, Brand AH. *Drosophila* nonmuscle myosin II promotes the asymmetric segregation of cell fate determinants by cortical exclusion rather than active transport. *Dev Cell* **5(6)**, 829-40(2003).
26. Gonzalez C. Spindle orientation, asymmetric division and tumour suppression in *Drosophila* stem cells. *Nat Rev Genet.* **8(6)**, 462-72(2007).
27. Bellaiche Y, Gotta M. Heterotrimeric G proteins and regulation of size asymmetry during cell division. *Curr Opin Cell Biol.* **17(6)**, 658-63(2005).
28. Kraut R, Chia W, Jan LY, Jan YN, Knoblich JA. Role of inscuteable in orienting asymmetric cell divisions in *Drosophila*. *Nature* **383(6595)**, 50-5(1996).
29. Yu F, Morin X, Cai Y, Yang X, Chia W. Analysis of partner of inscuteable, a novel player of *Drosophila* asymmetric divisions, reveals two distinct steps in inscuteable apical localization. *Cell* **100(4)**, 399-409(2000).
30. Du Q, Macara IG. Mammalian Pins is a conformational switch that links NuMA to heterotrimeric G proteins. *Cell* **119(4)**, 503-16(2004).
31. Hampoelz B, Knoblich JA. Heterotrimeric G proteins: new tricks for an old dog. *Cell* **119(4)**, 453-6(2004).
32. Xie T, Spradling AC. decapentaplegic is essential for the maintenance and division of germline stem cells in the *Drosophila* ovary. *Cell* **94(2)**, 251-60(1998).
33. Chen D, McKearin D. Dpp signaling silences bam transcription directly to establish asymmetric divisions of germline stem cells. *Curr Biol.* **13(20)**, 1786-91(2003).
34. Wong MD, Jin Z, Xie T. Molecular mechanisms of germline stem cell regulation. *Annu Rev Genet.* **39**, 173-95(2005).

35. Chen D, McKearin DM. A discrete transcriptional silencer in the bam gene determines asymmetric division of the Drosophila germline stem cell. *Development* **130(6)**, 1159-70(2003).
36. Lavoie CA, Ohlstein B, McKearin DM. Localization and Function of Bam Protein Require the benign gonial cell neoplasm Gene Product. *Dev Biol.* **212(2)**, 405-13(1999).
37. Ohlstein B, Lavoie CA, Vef O, Gateff E, McKearin DM. The Drosophila cystoblast differentiation factor, benign gonial cell neoplasm, is related to DExH-box proteins and interacts genetically with bag-of-marbles. *Genetics* **155(4)**, 1809-19(2000).
38. Szakmary A, Cox DN, Wang Z, Lin H. Regulatory relationship among piwi, pumilio, and bag-of-marbles in Drosophila germline stem cell self-renewal and differentiation. *Curr Biol.* **15(2)**, 171-8(2005).
39. Chen D, McKearin D. Gene circuitry controlling a stem cell niche. *Curr Biol.* **15(2)**, 179-84(2005).
40. Lin H, Spradling AC. A novel group of pumilio mutations affects the asymmetric division of germline stem cells in the Drosophila ovary. *Development* **124(12)**, 2463-76(1997).
41. Forbes A, Lehmann R. Nanos and Pumilio have critical roles in the development and function of Drosophila germline stem cells. *Development* **125(4)**, 679-90(1998).
42. Parisi M, Lin H. The Drosophila pumilio gene encodes two functional protein isoforms that play multiple roles in germline development, gonadogenesis, oogenesis and embryogenesis. *Genetics* **153(1)**, 235-50(1999).
43. Wang Z, Lin H. Nanos maintains germline stem cell self-renewal by preventing differentiation. *Science* **303(5666)**, 2016-9(2004).
44. McKearin DM, Spradling AC. bag-of-marbles: a Drosophila gene required to initiate both male and female gametogenesis. *Genes Dev.* **4(12B)**, 2242-51(1990).
45. McKearin D, Ohlstein B. A role for the Drosophila bag-of-marbles protein in the differentiation of cystoblasts from germline stem cells. *Development* **121(9)**, 2937-47(1995).
46. Park JK, Liu X, Strauss TJ, McKearin DM, Liu Q. The miRNA pathway intrinsically controls self-renewal of Drosophila germline stem cells. *Curr Biol.* **17(6)**, 533-8(2007).
47. Jin Z, Xie T. Dcr-1 maintains Drosophila ovarian stem cells. *Curr Biol.* **17(6)**, 539-44(2007).
48. Yang L, Chen D, Duan R, Xia L, Wang J, Qurashi A, Jin P, Chen D. Argonaute 1 regulates the fate of germline stem cells in Drosophila. *Development* **134(23)**, 4265-72(2007).
49. Hatfield SD, Shcherbata HR, Fischer KA, Nakahara K, Carthew RW, Ruohola-Baker H. Stem cell division is regulated by the microRNA pathway. *Nature* **435(7044)**, 974-8(2005).
50. Zaccai M, Lipshitz HD. Differential distributions of two adducin-like protein isoforms in the Drosophila ovary and early embryo. *Zygote* **4(2)**, 159-66(1996).
51. Lin H, Spradling AC. Fusome asymmetry and oocyte determination in Drosophila. *Dev Genet.* **16(1)**, 6-12(1995).
52. Ohlmeyer JT and Schüpbach T. Encore facilitates SCF-Ubiquitin-proteasome-dependent proteolysis during Drosophila oogenesis. *Development* **130(25)**, 6339-49(2003).
53. Yan N, Macdonald PM. Genetic interactions of Drosophila melanogaster arrest reveal roles



- for translational repressor Bruno in accumulation of Gurken and activity of Delta. *Genetics* **168**(3), 1433-42(2004).
54. Parisi MJ, Deng W, Wang Z, Lin H. The arrest gene is required for germline cyst formation during *Drosophila* oogenesis. *Genesis* **29**(4), 196-209(2001).
  55. Wang Z, Lin H. Sex-lethal is a target of Bruno-mediated translational repression in promoting the differentiation of stem cell progeny during *Drosophila* oogenesis. *Dev Biol.* **302**(1), 160-8(2007).
  56. Narbonne-Reveau K, Besse F, Lamour-Isnard C, Busson D, Pret AM. fused regulates germline cyst mitosis and differentiation during *Drosophila* oogenesis. *Mech Dev.* **123**(3), 197-209(2006).
  57. Kim-Ha J, Kim J, Kim YJ. Requirement of RBP9, a *Drosophila* Hu homolog, for regulation of cystocyte differentiation and oocyte determination during oogenesis. *Mol Cell Biol.* **19**(4), 2505-14(1999).
  58. Kai T, Spradling A. Differentiating germ cells can revert into functional stem cells in *Drosophila melanogaster* ovaries. *Nature* **428**(6982), 564-9(2004).
  59. Nisole S, Stoye JP, Saïb A. TRIM family proteins: retroviral restriction and antiviral defence. *Nat Rev Microbiol.* **3**(10), 799-808(2005).
  60. Meroni G, Diez-Roux G. TRIM/RBCC, a novel class of 'single protein RING finger' E3 ubiquitin ligases. *Bioessays* **27**(11), 1147-57(2005).
  61. Torok M, Etkin LD. Two B or not two B? Overview of the rapidly expanding B-box family of proteins. *Differentiation* **67**(3), 63-71(2001).
  62. Slack FJ, Ruvkun G. A novel repeat domain that is often associated with RING finger and B-box motifs. *Trends Biochem Sci.* **23**(12), 474-5(1998).
  63. Hyenne V, Desrosiers M, Labbé JC. *C. elegans* Brat homologs regulate PAR protein-dependent polarity and asymmetric cell division. *Dev Biol.* (2008).
  64. Frank DJ, Roth MB. ncl-1 is required for the regulation of cell size and ribosomal RNA synthesis in *Caenorhabditis elegans*. *J Cell Biol.* **140**(6), 1321-9(1998).
  65. Arama E, Dickman D, Kimchie Z, Shearn A, Lev Z. Mutations in the beta-propeller domain of the *Drosophila* brain tumor (brat) protein induce neoplasm in the larval brain. *Oncogene* **19**(33), 3706-16(2000).
  66. Bello B, Reichert H, Hirth F. The brain tumor gene negatively regulates neural progenitor cell proliferation in the larval central brain of *Drosophila*. *Development* **133**(14), 2639-48(2006).
  67. Betschinger J, Mechtler K, Knoblich JA. Asymmetric segregation of the tumor suppressor brat regulates self-renewal in *Drosophila* neural stem cells. *Cell* **124**(6), 1241-53(2006).
  68. Frank DJ, Edgar BA, Roth MB. The *Drosophila melanogaster* gene brain tumor negatively regulates cell growth and ribosomal RNA synthesis. *Development* 399-407(2002).
  69. Glasscock E, Singhanian A, Tanouye MA. The mei-P26 gene encodes a RING finger B-box coiled-coil-NHL protein that regulates seizure susceptibility in *Drosophila*. *Genetics* **170**(4), 1677-89(2005).

70. Gateff E. Malignant neoplasms of genetic origin in *Drosophila melanogaster*. *Science* **200(4349)**, 1448-59(1978).
71. Löer B, Bauer R, Bornheim R, Grell J, Kremmer E, Kolanus W, Hoch M. The NHL-domain protein Wech is crucial for the integrin-cytoskeleton link. *Nat Cell Biol.* **10(4)**, 422-8(2008).
72. Lee CY, Wilkinson BD, Siegrist SE, Wharton RP, Doe CQ. Brat is a Miranda cargo protein that promotes neuronal differentiation and inhibits neuroblast self-renewal. *Dev Cell.* **10(4)**, 441-9(2006).
73. Loop T, Leemans R, Stiefel U, Hermida L, Egger B, Xie F, Primig M, Certa U, Fischbach KF, Reichert H, Hirth F. Transcriptional signature of an adult brain tumor in *Drosophila*. *BMC Genomics* **5(1)**, 24(2004).
74. Rodriguez A, Zhou Z, Tang ML, Meller S, Chen J, Bellen H, Kimbrell DA. Identification of immune system and response genes, and novel mutations causing melanotic tumor formation in *Drosophila melanogaster*. *Genetics* **143(2)**, 929-40(1996).
75. Sonoda J, Wharton RP. *Drosophila* Brain Tumor is a translational repressor. *Genes Dev.* **15(6)**, 762-73(2001).
76. O'Farrell F, Esfahani SS, Engström Y, Kylsten P. Regulation of the *Drosophila* lin-41 homologue dappled by let-7 reveals conservation of a regulatory mechanism within the LIN-41 subclade. *Dev Dyn.* **237(1)**, 196-208(2008).
77. Page SL, McKim KS, Deneen B, Van Hook TL, Hawley RS. Genetic studies of mei-P26 reveal a link between the processes that control germ cell proliferation in both sexes and those that control meiotic exchange in *Drosophila*. *Genetics* **155(4)**, 1757-72(2000).
78. Sekelsky JJ, McKim KS, Messina L, French RL, Hurley WD, Arbel T, Chin GM, Deneen B, Force SJ, Hari KL, Jang JK, Laurençon AC, Madden LD, Matthies HJ, Milliken DB, Page SL, Ring AD, Wayson SM, Zimmerman CC, Hawley RS. Identification of novel *Drosophila* meiotic genes recovered in a P-element screen. *Genetics* **152(2)**, 529-42(1999).
79. Frosk P, Weiler T, Nylen E, Sudha T, Greenberg CR, Morgan K, Fujiwara TM, Wrogemann K. Limb-girdle muscular dystrophy type 2H associated with mutation in TRIM32, a putative E3-ubiquitin-ligase gene. *Am J Hum Genet.* **70(3)**, 663-72(2002).
80. Horn EJ, Albor A, Liu Y, El-Hizawi S, Vanderbeek GE, Babcock M, Bowden GT, Hennings H, Lozano G, Weinberg WC, Kulesz-Martin M. RING protein Trim32 associated with skin carcinogenesis has anti-apoptotic and E3-ubiquitin ligase properties. *Carcinogenesis* **25(2)**, 157-67(2004).
81. Wright, T.R., Bewley, G.C., Sherald, A.F. The genetics of dopa decarboxylase in *Drosophila melanogaster*. II. Isolation and characterization of dopa-decarboxylase-deficient mutants and their relationship to the alpha-methyl-dopa-hypersensitive mutants. *Genetics* **84**, 287-310(1976).
82. Gateff E. Tumor suppressor and overgrowth suppressor genes of *Drosophila melanogaster*: developmental aspects. *Int J Dev Biol.* **38(4)**, 565-90(1994).
83. Caussinus E, Gonzalez C. Induction of tumor growth by altered stem-cell asymmetric division in *Drosophila melanogaster*. *Nat Genet.* **37(10)**, 1125-9(2005).

84. Schwamborn J, Berezikov E, Knoblich JA. The Asymmetrically Segregating Protein TRIM32 Prevents Self-renewal in Neural Progenitor Cells by Degrading c-Myc and Activating Micro-RNAs. *submitted* (2008).
85. Gilboa L, Lehmann R. How different is Venus from Mars? The genetics of germ-line stem cells in *Drosophila* females and males. *Development* **131(20)**, 4895-905(2004).
86. Fuller MT, Spradling AC. Male and female *Drosophila* germline stem cells: two versions of immortality. *Science* **316(5823)**, 402-4(2007).
87. Reymond A, Meroni G, Fantozzi A, Merla G, Cairo S, Luzi L, Riganelli D, Zanaria E, Messali S, Cainarca S, Guffanti A, Minucci S, Pelicci PG, Ballabio A. The tripartite motif family identifies cell compartments. *EMBO J.* **20(9)**, 2140-51(2001).
88. Lin H, Yue L, Spradling AC. The *Drosophila* fusome, a germline-specific organelle, contains membrane skeletal proteins and functions in cyst formation. *Development* **120(4)**, 947-56(1994).
89. Lantz V, Chang JS, Horabin JJ, Bopp D, Schedl P. The *Drosophila* orb RNA-binding protein is required for the formation of the egg chamber and establishment of polarity. *Genes Dev.* **8(5)**, 598-613(1994).
90. Grewal SS, Li L, Orian A, Eisenman RN, Edgar BA. Myc-dependent regulation of ribosomal RNA synthesis during *Drosophila* development. *Nat Cell Biol.* **7(3)**, 295-302(2005).
91. Rudra D, Warner JR. What better measure than ribosome synthesis? *Genes Dev.* **18(20)**, 2431-6(2004).
92. Tolia NH, Joshua-Tor L. Slicer and the argonautes. *Nat Chem Biol.* **3(1)**, 36-43(2007).
93. Brennecke J, Hipfner DR, Stark A, Russell RB, Cohen SM. bantam encodes a developmentally regulated microRNA that controls cell proliferation and regulates the proapoptotic gene *hid* in *Drosophila*. *Cell* **113(1)**, 25-36(2003).
94. Reya T, Morrison SJ, Clarke MF, Weissman IL. Stem cells, cancer, and cancer stem cells. *Nature* **414(6859)**, 105-11(2001).
95. Lee CY, Andersen RO, Cabernard C, Manning L, Tran KD, Lanskey MJ, Bashirullah A, Doe CQ. *Drosophila* Aurora-A kinase inhibits neuroblast self-renewal by regulating aPKC/Numb cortical polarity and spindle orientation. *Genes Dev.* **20(24)**, 3464-74(2006).
96. Wang H, Somers GW, Bashirullah A, Heberlein U, Yu F, Chia W. Aurora-A acts as a tumor suppressor and regulates self-renewal of *Drosophila* neuroblasts. *Genes Dev.* **20(24)**, 3453-63(2006).
97. Ross DT, Scherf U, Eisen MB, Perou CM, Rees C, Spellman P, Iyer V, Jeffrey SS, Van de Rijn M, Waltham M, Pergamenschikov A, Lee JC, Lashkari D, Shalon D, Myers TG, Weinstein JN, Botstein D, Brown PO. Systematic variation in gene expression patterns in human cancer cell lines. *Nat Genet.* **24(3)**, 227-35(2000).
98. Wang H, Cai Y, Chia W, Yang X. *Drosophila* homologs of mammalian TNF/TNFR-related molecules regulate segregation of Miranda/Prospero in neuroblasts. *EMBO J.* **25(24)**, 5783-93(2006).
99. Yamashita YM, Jones DL, Fuller MT. Orientation of asymmetric stem cell division by the

- APC tumor suppressor and centrosome. *Science* **301(5639)**, 1547(2003).
100. Basto R, Brunk K, Vinadogrova T, Peel N, Franz A, Khodjakov A, Raff JW. Centrosome amplification can initiate tumorigenesis in flies. *Cell* **133(6)**, 1032-42(2008).
  101. Castellanos E, Dominguez P, Gonzalez C. Centrosome Dysfunction in Drosophila Neural Stem Cells Causes Tumors that Are Not Due to Genome Instability. *Curr Biol.* **18(16)**, 1209-14(2008).
  102. Chenn A, McConnell SK. Cleavage orientation and the asymmetric inheritance of Notch1 immunoreactivity in mammalian neurogenesis. *Cell* **82(4)**, 631-41(1995).
  103. Haydar TF, Ang E Jr, Rakic P. Mitotic spindle rotation and mode of cell division in the developing telencephalon. *Proc Natl Acad Sci U S A* **100(5)**, 2890-5(2003).
  104. Morin X, Jaouen F, Durbec P. Control of planar divisions by the G-protein regulator LGN maintains progenitors in the chick neuroepithelium. *Nat Neurosci.* **10(11)**, 1440-8(2007).
  105. Noctor SC, Martínez-Cerdeño V, Kriegstein AR. Distinct behaviors of neural stem and progenitor cells underlie cortical neurogenesis. *J Comp Neurol.* **508(1)**, 28-44(2008).
  106. Konno D, Shioi G, Shitamukai A, Mori A, Kiyonari H, Miyata T, Matsuzaki F. Neuroepithelial progenitors undergo LGN-dependent planar divisions to maintain self-renewability during mammalian neurogenesis. *Nat Cell Biol.* **10(1)**, 93-101(2008).
  107. Yingling J, Youn YH, Darling D, Toyo-Oka K, Pramparo T, Hirotsune S, Wynshaw-Boris A. Neuroepithelial stem cell proliferation requires LIS1 for precise spindle orientation and symmetric division. *Cell* **132(3)**, 474-86(2008).
  108. Fish JL, Dehay C, Kennedy H, Huttner WB. Making bigger brains-the evolution of neural-progenitor-cell division. *J Cell Sci.* **121(Pt17)**, 2783-93(2008).
  109. Fish JL, Kosodo Y, Enard W, Pääbo S, Huttner WB. Aspm specifically maintains symmetric proliferative divisions of neuroepithelial cells. *Proc Natl Acad Sci U S A* **103(27)**, 10438-43(2006).
  110. Frank DJ, Edgar BA, Roth MB. The Drosophila melanogaster gene brain tumor negatively regulates cell growth and ribosomal RNA synthesis. *Development* **129(2)**, 399-407(2002).
  111. Maines JZ, Stevens LM, Tong X, Stein D. Drosophila dMyc is required for ovary cell growth and endoreplication. *Development* **131(4)**, 775-86(2004).
  112. Nurse P, Thuriaux P, Nasmyth K. Genetic control of the cell division cycle in the fission yeast *Schizosaccharomyces pombe*. *Mol Gen Genet.* **146(2)**, 167-78(1976).
  113. Hartwell LH. Genetic control of the cell division cycle in yeast. II. Genes controlling DNA replication and its initiation. *J Mol Biol.* **59(1)**, 183-94(1971).
  114. Neufeld TP, de la Cruz AF, Johnston LA, Edgar BA. Coordination of growth and cell division in the Drosophila wing. *Cell* **93(7)**, 1183-93(1998).
  115. Hammel C, Ambros V NHL-2, a predicted E3 ubiquitin ligase, functions with the let-7 family microRNAs in hbl-1 regulation. *Wormbase Abstract (International Worm Meeting)* (2007).
  116. Hatfield S, Ruohola-Baker H. microRNA and stem cell function. *Cell Tissue Res.* **331(1)**, 57-66(2008).

117. Thompson BJ, Cohen SM. The Hippo pathway regulates the bantam microRNA to control cell proliferation and apoptosis in *Drosophila*. *Cell* **126(4)**, 767-74(2006).
118. Shcherbata HR, Ward EJ, Fischer KA, Yu JY, Reynolds SH, Chen CH, Xu P, Hay BA, Ruohola-Baker H. Stage-specific differences in the requirements for germline stem cell maintenance in the *Drosophila* ovary. *Cell Stem Cell*. **1(6)**, 698-709(2007).

## **V. Contributions**

### **Thesis**

The introduction and discussion were written by the author. The results sections Part I and Part II were taken from the two papers: Bowman SK, Neumüller RA et al. (2006) and Neumüller RA et al. (2008).

The contribution of the authors in these two studies is as follows:

### **Mushroom Body Defect project**

Maria Novatschkova contributed Figure 1 and Figure S1. Quansheng Du contributed Figure 3B and 3C. Sarah Bowman contributed Figure 2, Figure 3A and Figure 5 (Figure 5 with the help of the author). The author conducted the experiments in Figure 4, Figure 6 and parts of the experiments in Figure 5. Jürgen Knoblich and Sarah Bowman wrote the manuscript with the help of the author in the spindle orientation and proliferation sections.

### **Mei-P26 project**

Jürgen Knoblich and the author designed the study. The author performed the oogenesis experiments. Jörg Betschinger and Karl Mechtler contributed biochemical data (Fig. 7). Anja Fischer contributed the S2 luciferase assay (Fig. 10c,d). Ingrid Pörnbacher assisted in the experiment in Fig. 5f,g and performed experiments in the larval brain (Fig. 6). Stephen Cohen and Natascha Bushati designed the miRNA qPCR experiment which was performed by Natascha Bushati (Fig. 8a, 10a,b). Jürgen Knoblich wrote the paper with the help of the author (Figure legends).

## VI. Acknowledgments

During the time at IMP/IMBA I had the privilege to work in an extraordinarily exciting and stimulating environment. Besides inspiring scientific discussions and debates, I truly enjoyed the helpful atmosphere at the campus as well as the ease of establishing ties with a lot of people.

Foremost I would like to thank Jürgen Knoblich for allowing me to enter his lab and supervising my work. In particular I would like to thank him for always having an open door, his enthusiasm and enduring support. I would further like to thank Jürgen for the always constructive and very helpful critique of my work and ideas and for guiding me through the time of my PhD at IMBA.

Many thanks to Constance Richter, Jörg Betschinger and Andrea Hutterer for all the fun we had during the time here. For constantly challenging my views and encouraging me during the sometimes demanding phases of the neuroblast screen.

Big thanks to Sarah Bowman for the fantastic collaboration on *mud* and all the discussions that accompanied and stimulated our experimental work so much.

A lot of thanks to all members of the Knoblich laboratory for the great atmosphere and the helpfulness of all. For their enthusiasm and dedication towards discussions and debates about all matters of life. My flyroom, bench and table soccer companions know what I am talking about!!

Thanks to my PhD committee Dr. Barry Dickson and Prof. Roland Foisner for evaluating my work and progress during my PhD.

Special thanks to Stefan Kuthan for recovering my thesis by fixing my computer.

Thousand thanks to the sunshine in my life: Mia and Lisi!

## VII. Publications

### 2008

Ralph A. Neumüller, Joerg Betschinger, Anja Fischer, Natascha Bushati, Ingrid Poernbacher, Karl Mechtler, Stephen M. Cohen & Juergen A. Knoblich (2008). Mei-P26 regulates microRNAs and cell growth in the *Drosophila* ovarian stem cell lineage. Nature. 454, 241-245

Wolfgang Benetka, Norbert Mehlmer, Sebastian Maurer-Stroh, Michaela Sammer, Manfred Koranda, Ralph Neumüller, Jörg Betschinger, Jürgen Knoblich, Markus Teige, Frank Eisenhaber. (2008) Prediction and reality: Experimental testing of predicted myristoylation targets involved in asymmetric cell division and calcium signalling. Cell Cycle. 7(23). 3709-19. Epub 2008 Dec 13.

### 2007

Viktoria Nizhynska, Ralph Neumueller and Ruth Herbst (2007). Phosphoinositide 3-kinase acts through RAC and Cdc42 during agrin-induced acetylcholine receptor clustering. Developmental Neurobiology. 67/8, 1047-1058

### 2006

Sarah K. Bowman #, Ralph A. Neumüller #, Maria Novatchkova, Quansheng Du and Juergen A. Knoblich (2006). The Drosophila NuMA Homolog Mud Regulates Spindle Orientation in Asymmetric Cell Division. Developmental Cell. 10, 731-742. (# equal contribution)



## VIII. CURRICULUM VITAE

### Personal Data

Name: Ralph Alexander Neumüller

Date of Birth: 24.04.1980

Place of Birth: Linz

Nationality: Austrian

### Education

Jul 2005- present: PhD thesis at the Institute of Molecular Biotechnology (IMBA) in the laboratory of Dr. Jürgen Knoblich

Apr 2003- Jan 2005: Diploma thesis at the Brain Research Institute Vienna in the laboratory of Dr. Ruth Herbst

2002- 2005: University of Vienna: Anthropology (Human genetics, Neurobiology)

1999- 2002: University of Vienna: General Biology

1998-1999: Civil service at the Diakonissen Hospital Linz

1991- 1998: Secondary school 'Bundesrealgymnasium Auhof'

1987- 1991: Primary school in Altenberg bei Linz